The composite mini element : a mixed FEM for the Stokes equations on complicated domains

Peterseim, Daniel

The Composite Mini Element

A Mixed FEM for the Stokes Equations on Complicated Domains

Dissertation
zur
Erlangung der naturwissenschaftlichen Doktorwürde
(Dr. sc. nat.)
vorgelegt der
Mathematisch-naturwissenschaftlichen Fakultät
der
Universität Zürich
von

Daniel Peterseim
aus Deutschland

Promotionskomitee
Prof. Dr. Stefan A. Sauter (Vorsitz)
Prof. Dr. Michel Chipot

Zürich, 2007

Begutachtet von
Prof. Dr. Rüdiger Verfürth

Abstract

The finite element method nowadays is one of the most powerful tools in the numerical solution of partial differential equations and therefore in the simulation of many physical processes, for instance, in the field of fluid dynamics. In this thesis we discuss the efficient computation of the viscous fluid flows, so called Stokes flows, with two different types of boundary conditions: the Dirichlet and the slip boundary condition. We introduce a new finite element method for the mixed discretization of the corresponding differential equations.

The basis of every finite element method is the subdivision, for instance a triangulation, of the physical domain. The approximation quality is determined by the maximal meshwidth of the triangulation, while the computational effort is determined by its number of elements. If the physical domain is very complicated, i.e. its boundary contains a huge number of geometric details, then the minimal number of triangles, that are necessary to resolve the domain, can be affected critically. In this case, the computational effort can be too large to solve it even on state-of-the-art computers.

In contrast to that, our approach decouples the minimal dimension of the approximation space, and therefore the numerical effort, from the domain geometry by adapting the shape of the finite element functions to the needs of the complex geometry and the imposed boundary condition. This approach allows low-dimensional approximations even for problems with complicated geometric details.

This new nonconforming mixed method for the Stokes equation, the composite mini element, is analyzed in detail in two as well as three dimensions. We prove its linear (optimal order) convergence and its stability. In addition, it turns out that the method can be viewed as a coarse scale generalization of the classical mini element approach, i.e. it reduces the computational effort while the approximation quality depends on the (coarse) mesh width in the usual way.

Zusammenfassung

Die Finite Elemente Methode ist heute eines der wichtigsten Werkzeuge zur numerischen Lösung partieller Differentialgleichungen. Sie ermöglicht die Simulation zahlreicher physikalischer Prozesse, z.B. im Bereich der Fluiddynamik. In der vorliegenden Arbeit werden wir die effiziente Berechnung viskoser Flüssigkeitsströmungen, sogenannter Stokesscher Strömungen, diskutieren. Wir werden dabei auf zwei verschiedene Typen von Randbedingungen eingehen, die Haft- und die Gleitrandbedingung. Wir stellen eine neue Finite Elemente Methode für die gemischte Diskretisierung der modellierenden Differentialgleichung vor.

Grundlage einer jeden Finite Elemente Methode ist die Zerlegung (z.B. Triangulierung) des zugrunde liegenden Gebiets. Die Approximationsgüte wird dabei von der maximalen Maschenweite bestimmt. Der Rechenaufwand hingegen hängt von der Anzahl der Gitterelemente ab. Diese kann, selbst für grosse Maschenweiten, sehr gross sein, wenn das physikalische Gebiet kompliziert ist, d.h. wenn der Gebietsrand eine grosse Anzahl geometrischer Details besitzt, die durch das Gitter aufgelöst werden müssen. Der resultierende Rechenaufwand könnte dann sogar die Kapazität neuester Computertechnologie übersteigen.

Im Gegensatz dazu entkoppelt unser Ansatz die minimale Dimension des Approximationsraumes, und somit den numerischen Aufwand, von der Gebietsgeometrie. Die Ansatzfunktionen werden dabei den Bedürfnissen der komplexen Geometrie und der Randbedingung angepasst. Dieser Zugang erlaubt kostengünstige Approximationen trotz einer Vielzahl geometrischer Details.

Diese neue, nichtkonforme, gemischte Finite Elemente Methode für die Stokes Gleichungen, das sogenannte Composite Mini Element, wird detailliert analysiert, in zwei, wie auch in drei Raumdimensionen. Wir werden lineare (optimale) Konvergenz und Stabilität nachweisen. Weiterhin wird sich heraus stellen, dass die Methode als Grobgitter-Verallgemeinerung des klassischen Mini Elements angesehen werden kann, d.h. es reduziert den Rechenaufwand bei vergleichbarer Approximationsgüte.

Danksagung

Dank gebührt vielen Menschen, die auf ganz unterschiedlichen Ebenen massgeblich zur Erstellung und zum Gelingen der vorliegenden Arbeit beigetragen haben. Ich danke meiner Familie, die mir auf meinem Weg stets zur Seite gestanden hat. Besonderer Dank richtet sich dabei an meine Eltern, ohne deren aufopferungsvolle Unterstützung das alles nicht möglich gewesen wäre.

Für die Schaffung der finanziellen und strukturellen Rahmenbedingungen danke ich Herrn Prof. Sauter. Ihm gilt auch der Dank für die wissenschaftliche Betreuung der Dissertation, die immer sehr gut organisiert und zielstrebig war; die zügige Fertigstellung der Arbeit belegt dies. Ich danke Lehel Banjai für die finalen Korrekturen und Anregungen, ferner allen Compmath-Mitabeitern, die mich in meiner Zeit hier in Zürich begleitet haben.

Und nicht zuletzt, danke Claudia, danke für deinen Beistand in allen Lebenslagen und danke für all die Liebe, die du mir schenkst.

Zürich, den 5. April 2007 Daniel Peterseim

Table of Contents

1 Introduction **1**

2 Stokes Problems **5**

2.1 The Stokes Equations 5

2.1.1 Boundary Conditions 6

2.1.2 The Abstract Variational Problem 6

2.1.3 The Abstract Operator Problem 8

2.1.4 Weak Solutions of the Stokes Problem 8

2.1.5 A Different Variational Formulation - Handling of the Pressure Constraint . 11

2.2 Finite Element Approximation 12

2.2.1 Abstract Approximation 13

2.2.2 Finite Element Approximation of the Stokes Problem 15

2.2.3 Notes on the Resolution Condition 17

3 Composite Mini Elements **21**

3.1 Two Scale Grids 21

3.2 Extension Operators 25

3.2.1 Scalar Operators 26

3.2.2 Vector Valued Operators 28

3.3 The Composite Mini Element for Dirichlet Condition 30

3.4 The Composite Mini Element for Slip Condition 31

3.5 CME and Matrix Compression 32

4 Convergence Analysis **35**

4.1 Interpolation and Extrapolation Estimates 35

4.2 Approximability 40

4.2.1 The CME Velocity Space for Dirichlet Boundary 40

4.2.2 The CME Velocity Space for Slip Boundary 46

4.2.3 The CME Pressure Space 48

4.3 Stability and Convergence 49

5 Numerical Experiments **59**
5.1 Model Problems 59
5.2 Parameter Tests 64
5.3 Convergence 66
5.3.1 The Dirichlet Model Problem 68
5.3.2 The Slip Model Problem 70

6 Conclusions **75**

Bibliography **78**

Glossary

$\langle \cdot, \cdot \rangle$	Euclidean inner product in $\mathbb{R}^d$	6
$\left\|\cdot\right\|_{m,\Omega}$	Norm in $\mathrm{H}^m(\Omega)$	8
$\left\|\cdot\right\|_{m,p,\Omega}$	Norm in $\mathrm{W}_p^m(\Omega)$	8
$\left\|\cdot\right\|_{m,\Omega}$	Seminorm in $\mathrm{H}^m(\Omega)$	8
$\left\|\cdot\right\|_{m,p,\Omega}$	Seminorm in $\mathrm{W}_p^m(\Omega)$	8
$\mathfrak{a}$	Continous bilinear form on $\mathbf{H}^1(\Omega) \times \mathbf{H}^1(\Omega)$	9
α_{D}	Coercivity constant of $\mathfrak{a}$ with respect to $\mathbf{H}^1_{\mathrm{D}}(\Omega)$	9
α_{s}	Coercivity constant of $\mathfrak{a}$ with respect to $\mathbf{H}^1_{\mathrm{s}}(\Omega)$	10
$\mathfrak{b}$	Continous bilinear form on $\mathbf{H}^1(\Omega) \times \mathrm{L}^2(\Omega)$	9
β^{CME}	Inf-sup constant of the composite mini element space	50
β^{mini}	Inf-sup constant of the classical mini element space	16
$B_{\mathcal{T}}$, $\mathbf{B}_{\mathcal{T}}$	Space of bubble functions (vector fields) with respect to the triangulation $\mathcal{T}$	16
$\mathfrak{c}$	Continous bilinear form on $\mathbb{R} \times \mathrm{L}^2(\Omega)$	11
C_{dist}, C_{size}	Moderate constants describing the position of a simplex in relation to another one	36
$C_{\mathcal{E}^{\mathrm{p}}_{\mathsf{H}}}$	Continuity constant of the extension operator $\mathcal{E}^{\mathrm{p}}_{\mathsf{H}}$	49
C_{ext}	Continuity constant of the operator $\mathfrak{E}$	35
C_{F}	Constant of the Friedrichs inequality	9
C_{int}	Moderate constant appearing in the approximation error of the nodal interpolation	35
$C_{\boldsymbol{\nu}}$	Moderate constant describing the smoothness of Ω	46
C_{qint}	Moderate constant appearing in the approximation error of the quasi interpolation operator $\Pi_{\mathcal{T}_{\mathsf{H}}}$	39

C_{reg}	Moderate constant describing the dependence between the regularity of a Stokes flow and the outer force density	10, 11
$C_1^{\mathcal{T}}, C_2^{\mathcal{T}}$	Moderate constants describing the quality of the refined grid $\mathcal{T}_{\mathsf{H},\mathsf{h}}$	24
$C_3^{\mathcal{T}}$	Moderate constant describing the relative boundary length of Ω	52
$\mathbf{D}$	Deformation tensor (symmetric gradient)	6
d	Dimension, $d \in \{2, 3\}$	5
$\boldsymbol{\mathcal{E}}^{\mathrm{CME_D}}, \boldsymbol{\mathcal{E}}^{\mathrm{CME_s}}$	Extension operators defining the composite mini element spaces	30
$\boldsymbol{\mathcal{E}}^{\mathrm{D}}_{\mathsf{H},\mathsf{h}}$	Vector valued extension operator taking Dirichlet boundary condition into account	28
$\mathcal{E}_{\mathsf{H},\mathsf{h}}, \mathcal{E}_{\mathsf{H}}, \mathcal{E}^{\mathrm{p}}_{\mathsf{H}}$	Scalar extension operators	26, 27
$\mathcal{E}^{D}_{\mathsf{H},\mathsf{h}}$	Scalar extension operator taking zero boundary conditions into account	26
$\boldsymbol{\mathcal{E}}_{\mathsf{H},\mathsf{h}}$	Vector valued extension operator	29
$\tilde{\mathcal{E}}^{\mathrm{p}}_{\mathsf{H}}$	Scalar extension operator taking zero mean value into account	50
$\boldsymbol{\mathcal{E}}^{\mathrm{s}}_{\mathsf{H},\mathsf{h}}$	Vector valued extension operator taking slip boundary condition into account	29
$\mathfrak{E}$	Stein [1970] extension of Sobolev functions	35
$\boldsymbol{\mathcal{E}}^{\mathbf{0}}$	Zero extension	30
Γ	Boundary of the domain Ω	6
H	Maximal mesh width of a triangulation (coarse scale)	21
$\mathrm{H}^m(\Omega), \mathbf{H}^m(\Omega)$	Sobolev space of L^2-functions (vector fields) with weak derivatives up to order $m \in \mathbb{N} \cup \{0\}$ in $\mathrm{L}^2(\Omega)$	8
h	Mesh width of a triangulation close to the boundary (fine scale)	21
$\mathbf{H}^1_{\mathrm{D}}(\Omega)$	Space of $\mathbf{H}^1(\Omega)$-vector fields with zero traces	8
$\mathbf{H}^1_{\mathrm{s}}(\Omega)$	Space of $\mathbf{H}^1(\Omega)$-vector fields with zero normal traces	10
$\mathbf{I}$	Identity matrix in $\mathbb{R}^d$	6
$\mathcal{I}_{\mathrm{T}}, \mathcal{I}_{\mathcal{T}}$	Piecewise affine nodal interpolation operator with respect to a simplex T or a triangulation $\mathcal{T}$	35
$\mathrm{L}^2_0(\Omega)$	Space of $\mathrm{L}^2(\Omega)$-functions with mean value zero	8
$\mathrm{M}^{\mathrm{CME}}_{\mathsf{H}}$	Pressure part of the composite mini element space	31
$\mathrm{M}^{\mathrm{mini}}_{\mathsf{H}}$	Pressure part of the classical mini element space	16

$\boldsymbol{\nu}$	Outer normal of the domain Ω	6
Ω	Bounded connected Lipschitz domain in $\mathbb{R}^d$	5
Ω_{H}, $\Omega_{\mathsf{H,h}}$	Polygonal approximations of Ω	21, 22
ω_T	Set of neighbors of a simplex T in a triangulation	39
$\tilde{\omega}_T$	Set of simplices that are neighbors of T in a triangulation or neighbors of neighbors of T	48
$\Pi_{\mathcal{T}_{\mathsf{H}}}$	Quasi interpolation operator with respect to the triangulation $\mathcal{T}_{\mathsf{H}}$	38
$\mathbb{P}_1$	Space of polynomials with degree smaller or equal than 1	36
ρ	Regularity constant of the triangulations $\mathcal{T}_{\mathsf{H}}$ and $\mathcal{T}_{\mathsf{H,h}}$	24
ρ_t	Regularity constant of a simplex t	24
$\boldsymbol{\sigma}$	Stress tensor	6
$S_{\mathcal{T}}$, $\mathbf{S}_{\mathcal{T}}$	Space of continuous piecewise affine functions (vector fields) with respect to the triangulation $\mathcal{T}$	15
$\mathcal{T}_{\mathsf{H,h}}^{\mathrm{dof}}$, $\mathcal{T}_{\mathsf{H,h}}^{\Gamma}$	Subsets of $\mathcal{T}_{\mathsf{H,h}}$	22
$\mathcal{T}_{\mathsf{H}}^{\mathrm{dof}}$, $\mathcal{T}_{\mathsf{H}}^{\Gamma}$	Subsets of $\mathcal{T}_{\mathsf{H}}$	23
$\mathcal{T}_{\mathsf{H,h}}$	Two scale triangulation of $\Omega_{\mathsf{H,h}}$	21
$\mathcal{T}_{\mathsf{H}}$	Triangulation of Ω_{H}	22
$\Theta_{\mathsf{H,h}}^{\mathrm{dof}}$, $\Theta_{\mathsf{H,h}}^{\Gamma}$	Subsets of $\Theta_{\mathsf{H,h}}$	22
$\Theta_{\mathsf{H,h}}$	Set of vertices of $\mathcal{T}_{\mathsf{H,h}}$	22
$\mathcal{T}^{\mathrm{T}}$	Set of slave simplices of a simplex T	23
T_t	Closest inner simplex of a simplex t	23
$\hat{\mathcal{T}}^{\mathrm{T}}$	Subset (the interior) of $\mathcal{T}^{\mathrm{T}}$	23
$T_{\mathbf{x}}$	Closest inner simplex of a node $\mathbf{x}$	23
$V(T)$	Set of vertices of a simplex T	24
$\mathrm{W}_p^m(\Omega)$	Sobolev space of L^p-functions with weak derivatives up to order $m \in \mathbb{N} \cup \{0\}$ in $\mathrm{L}^p(\Omega)$, $p \in \mathbb{N} \cup \{\infty\}$	8
$\mathbf{x}^{\Gamma}$	A closest boundary point of $\mathbf{x}$	23
$\mathbf{X}_{\mathsf{H,h}}^{\mathrm{CME_D}}$	Velocity part of the composite mini element space for Dirichlet boundary	31

$\mathbf{X}_{\mathsf{H},\mathsf{h}}^{\mathrm{CME_s}}$	Velocity part of the composite mini element space for slip boundary	31
$\mathbf{X}_{\mathsf{H}}^{\mathrm{mini_D}}$	Velocity part of the classical mini element space, Dirichlet boundary condition	16
$\mathbf{X}_{\mathsf{H}}^{\mathrm{mini_s}}$	Velocity part of the classical mini element space, slip boundary condition	17

1

Introduction

A small example will show what it is all about: We want to compute the motion of a viscous incompressible fluid, a so called Stokes flow, by a finite element method in the bounded domain of Figure 1.1a. It is a slight perturbation of the unit square. The lower boundary was replaced by a sinus wave with frequency 100 and amplitude 0.001. The solution is given in the plot on the right showing the flow direction by arrows and the absolute velocity by the gray intensity. For the numerical approximation we have to triangulate the domain, which is only possible in an approximative way. Then we use piecewise polynomials with respect to the triangulation to approximate the solution. This results in a system of linear equations determining the coefficients which characterize the approximation. The number of equations will thereby be about five times the number of nodes in the triangulation, if we use a standard finite element for Stokes flows, the

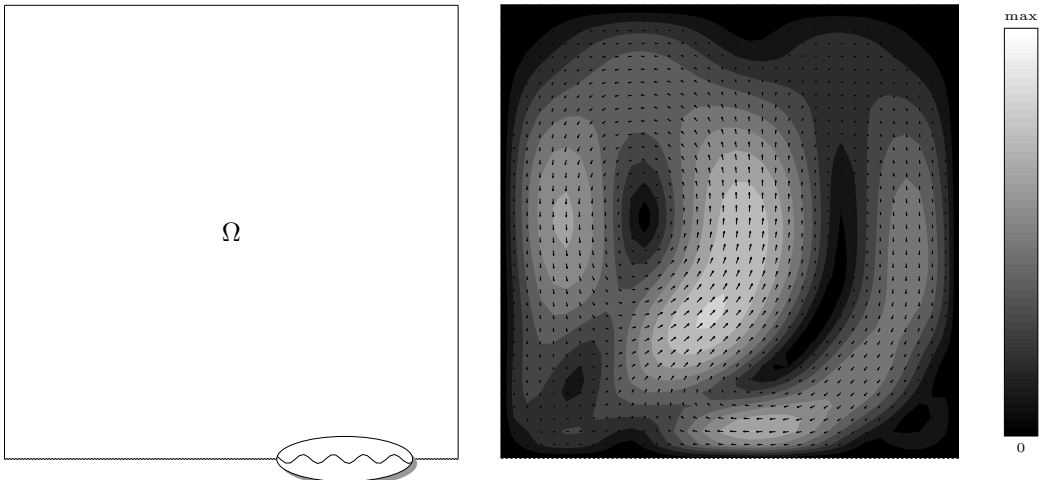

(a) Perturbation of the unit square.

(b) Velocity field with arrows (direction) and gray scale (absolute velocity).

Figure 1.1: Stokes flow on the domain Ω. The outer force causing this flow is precised in (5.1). The fluid is allowed to slip over the oscillating part of the boundary.

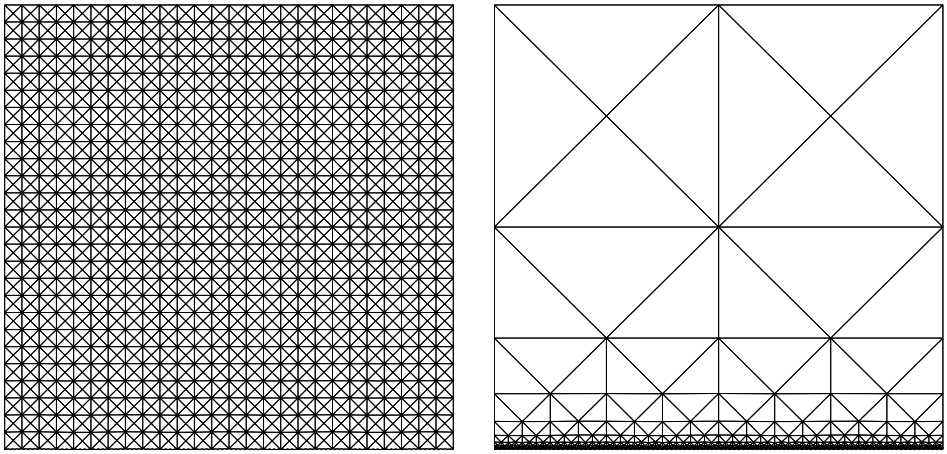

Figure 1.2: Two possible triangulations of the domain Ω from Figure 1.1a.

mini element. Now suppose one's computer is able to solve such a system up to 10000 unknowns, for reasons of limited memory or time. For example, a time limit can be reached quickly if solving this problem is only a sub step in a larger problem like a time dependent simulation. If this is the case one would have about 2000 nodes that can be distributed in the domain; the question arises how to do this distribution of degrees of freedom. Of course, we are not completely free in choosing the distribution, since for the success of the finite element method the triangles have to be of good shape (diameter^2 $\approx$ area). There are two ways that come into mind. The first is a uniform distribution. From the point of view of approximation theory this is a very good choice, since the error depends on the maximal mesh width which is minimized in this case. But the details of the domain boundary cannot be resolved by such a grid. The second possibility is to start resolving the boundary, which costs almost half of the nodes. Only very few nodes are left for the approximation inside the domain. The two grids could look like the ones depicted in Figure 1.2. Unfortunately, both triangulations lead to very poor approximations of the solutions as shown in Figure 1.3. The uniform approach fails close to the boundary since the rough boundary affects the flow critically. This behavior can be captured by the boundary concentrated grid but away from the boundary it is useless. Usually, the problem is solved by using a grid which combines the uniform node distribution in the domain with boundary adaption. This leads to a very good approximation (see Figure 1.4) but it exceeds the limits of the machine, since the resulting system dimension is 25000, which is more than twice the maximal capacity. One may now argue that there are better approaches, for instance an adaptive method. Provided the error estimator is able to handle errors due to domain approximation, it might lead to more optimal grids then those depicted in Figure 1.2. However, if the boundary needs to be resolved as in Figure 1.4, the estimator will, sooner or later, force to put more and more nodes close to the boundary and the limits of the computer will be reached before the approximation error is as small as the error that arises from using the full grid of Figure 1.4.

In this thesis we will present a new finite element, which we call the *composite mini element*,

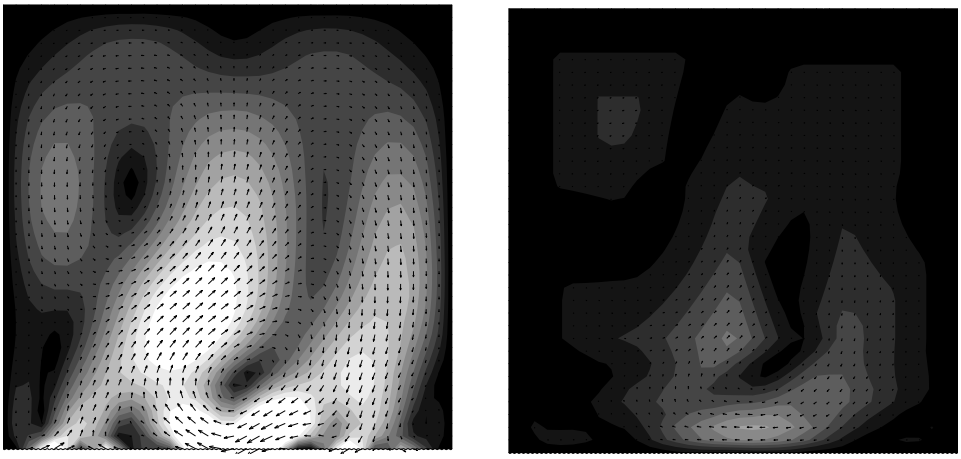

Figure 1.3: Finite element approximations of the Stokes flow from Figure 1.1b with respect to the grid from Figure 1.2.

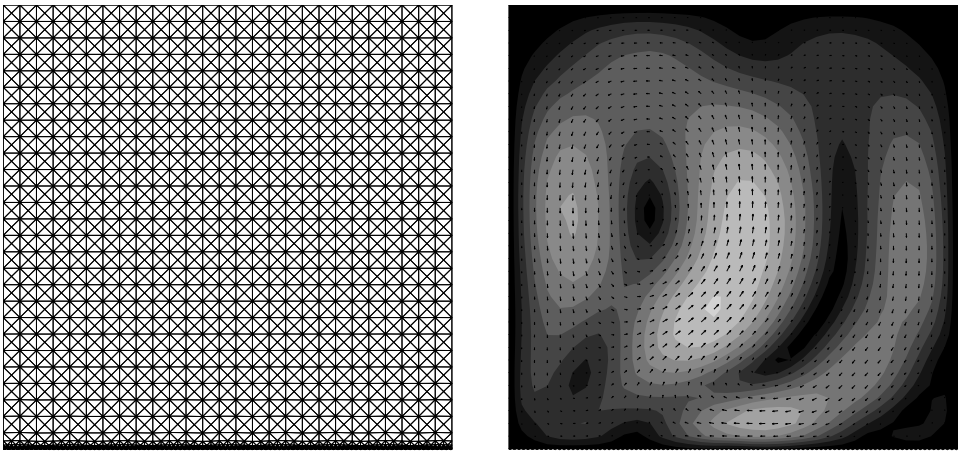

Figure 1.4: Resolving grid and its corresponding finite element approximation of the Stokes flow from Figure 1.1b.

for this class of problems, i.e. the computation of Stokes flows on complicated domains. It is able to produce the approximation quality of Figure 1.4 by solving a system which is in order and structure comparable to the uniform approach.

More generally we introduce a finite element method for the approximation of Stokes flows on bounded domains containing a huge number of geometric details. We emphasize that there is no restriction to periodic cases, which excludes the straight-forward use of analytic homogenization techniques. As seen before these complicated domains need to be resolved by the grid in order to guarantee a certain approximation quality, which increases the computational effort, because the system dimension is, even on coarse levels, determined by the number of geometric details. Our method will decouple the approximation space dimension from the domain complexity by adapting the *shape* of the element functions. They will be composited by finite element functions

of much finer triangulations. The idea goes back to Hackbusch and Sauter [1997] who introduced composite finite elements (CFE) the Neumann problem and especially to [Rech et al., 2006] where the concept of CFE was adapted to the use for Dirichlet problems for the Poisson equation. Here, we go a few steps further by generalizing the ideas to the Stokes equation in mixed form with Dirichlet as well as slip boundary conditions. Thereby we have to meet new challenges, which lie in the slip boundary condition, the additional pressure variable, which forces to reduce regularity assumptions and the discrete stability of mixed finite elements in the sense of Ladyshenskaja, Babuška, and Brezzi (infsup condition). In contrast to [Rech et al., 2006] we also give a complete three dimensional analysis. We will recall some theoretical aspects of the Stokes Problem and its numerical approximation, especially the mini element as a standard method. It will be the starting point for the definition of the composite mini element introduced in Chapter 3. A detailed convergence analysis will follow in Chapter 4. Finally, numerical experiments will support the theoretical results, namely the linear (optimal order) convergence of the method. We emphasize that in this thesis, we develop concepts that can also be carried over to other finite elements for the Stokes equations as well as to different types of partial differential equations.

2

Stokes Problems

In this chapter, we will give a brief introduction to the theory of the Stokes problem and its finite element approximation. We start by presenting the equations and two suitable boundary conditions before the framework of abstract mixed variational problems will be used to answer questions of existence and uniqueness of solutions. Afterward we will describe a way to approximate solutions. In this context we will present an abstract convergence theorem that is the basis of the finite element analysis of the subsequent chapters. Furthermore, a standard finite element for the approximation of the Stokes problem, the *mini element*, will be introduced. We will focus on the problems of this method arising from the complicated physical domain.

2.1 The Stokes Equations

The motion of a viscous incompressible fluid in a bounded, connected Lipschitz domain $\Omega \subseteq \mathbb{R}^d$, $d \in \{2, 3\}$, can be described by a velocity field $\mathbf{u} : \Omega \times \mathbb{R} \to \mathbb{R}^d$ fulfilling the *incompressible Navier-Stokes equations*

$$\begin{aligned} \partial_t \mathbf{u} + (\mathbf{u} \cdot \nabla)\, \mathbf{u} - \mu \Delta \mathbf{u} + \nabla p &= \mathbf{f} \\ \operatorname{div} \mathbf{u} &= 0, \end{aligned} \tag{2.1}$$

where $\mathbf{f} : \Omega \to \mathbb{R}^d$ is a force density and $\mu \in \mathbb{R}_{>0}$ is the so called dynamic viscosity of the fluid. The function $p : \Omega \to \mathbb{R}^d$ describes the pressure of the fluid in the domain. Problem (2.1) is a nonlinear partial differential equation. In numerical solution algorithms the problem is typically reduced to a sequence of simpler problems, namely the *stationary incompressible Navier-Stokes equations*

$$\begin{aligned} (\mathbf{u} \cdot \nabla)\, \mathbf{u} - \mu \Delta \mathbf{u} + \nabla p &= \mathbf{f} \\ \operatorname{div} \mathbf{u} &= 0 \end{aligned} \tag{2.2}$$

or the *Stokes equations*

$$\begin{aligned} -\Delta \mathbf{u} + \nabla p &= \mathbf{f} \\ \operatorname{div} \mathbf{u} &= 0. \end{aligned} \tag{2.3}$$

In comparison to the non stationary case (2.1), the time derivative is neglected in (2.2). If we linearize the latter in $\mathbf{u} = \mathbf{0}$ and scale the viscosity μ to 1, we finally get the linear partial differential

equation (2.3). Being able to solve the Stokes equations efficiently is a main building block of the simulation of viscous fluid motion and from now on we will concentrate on this.

2.1.1 Boundary Conditions

The differential equations have to be equipped with a suitable boundary condition. In his original paper Navier [1827] had proposed a general class of boundary conditions including for instance the assumption that the liquid adheres to the solid boundary $\Gamma := \partial\Omega$. This condition is very popular and seems to be the right choice in case of small fluid velocities. It is known as *no-slip* or *Dirichlet* boundary condition and reads:

$$\mathbf{u} = \mathbf{0} \quad \text{on } \Gamma. \tag{2.4}$$

A different important special type of Navier's condition is the *slip* boundary condition:

$$\langle \mathbf{u}, \boldsymbol{\nu} \rangle = 0 \quad \text{on } \Gamma \tag{2.5}$$

$$\boldsymbol{\sigma}_{\boldsymbol{\nu}} - \langle \boldsymbol{\nu}, \boldsymbol{\sigma}_{\boldsymbol{\nu}} \rangle \, \boldsymbol{\nu} = \mathbf{0} \quad \text{on } \Gamma. \tag{2.6}$$

Thereby

$$\boldsymbol{\sigma} = \boldsymbol{\sigma}(\mathbf{u}, p) := 2\mathbf{D}\mathbf{u} - p\mathbf{I}$$

is the *stress tensor* and

$$\mathbf{D}\mathbf{u} := \tfrac{1}{2}\left(\nabla\mathbf{u} + (\nabla\mathbf{u})^{\mathsf{T}}\right)$$

the *deformation tensor*. $\mathbf{I}$ denotes the $d \times d$ identity matrix, $\nabla\mathbf{u}$ the Jacobi matrix of $\mathbf{u}$ and $\langle \cdot, \cdot \rangle$ the Euclidean inner product which has to interpreted pointwise if the arguments are vector valued functions. The outer domain normal[1] is denoted by $\boldsymbol{\nu}$. Whenever a vector is subscripted by a normal vector $\boldsymbol{\nu}$, we mean its normal component[2].

In contrast to (2.4), the slip condition (2.5) allows tangential velocities at the domain boundary, but inflow or outflow are forbidden. The slip boundary conditions (2.5) seem to be more realistic in case of high fluid velocities.

Both conditions could be generalized by replacing the zero right-hand sides by certain given functions. But those inhomogeneous problems could easily be reduced to the homogeneous ones by standard techniques. Further, for the sake of simplicity, we will not consider mixed boundary conditions but restrict either to the pure Dirichlet problem or to slip boundary conditions overall.

2.1.2 The Abstract Variational Problem

As in the case of the scalar Poisson equation $\Delta u = f$, the Stokes problem (2.3) not always possesses *classical solutions* even for continuous and therefore natural outer forces $\mathbf{f}$. We have to derive a weak setting to overcome this difficulty. That is why we will introduce the framework of

[1] In the case of the slip boundary condition Ω is required to be of class C^1 so that an outer normal always exists.

[2] For $\mathbf{y} \in \mathbb{R}^d$ we define its normal components $\mathbf{y}_{\boldsymbol{\nu}} = \langle \mathbf{y}, \boldsymbol{\nu} \rangle \, \boldsymbol{\nu}$.

mixed variational problems (see [Girault and Raviart, 1979]) which is suitable to handle the Stokes problems.

Let X and M be real Hilbert spaces,

$$\mathfrak{a} : \mathrm{X} \times \mathrm{X} \to \mathbb{R} \quad \text{and} \quad \mathfrak{b} : \mathrm{X} \times \mathrm{M} \to \mathbb{R}$$

be continuous bilinear forms with norms

$$\|\mathfrak{a}\| := \sup_{0 \neq u, v \in \mathrm{X}} \frac{\mathfrak{a}(u,v)}{\|u\|_{\mathrm{X}} \|v\|_{\mathrm{X}}} \quad \text{and} \quad \|\mathfrak{b}\| := \sup_{\substack{0 \neq v \in \mathrm{X} \\ 0 \neq p \in \mathrm{M}}} \frac{\mathfrak{b}(v,p)}{\|v\|_{\mathrm{X}} \|p\|_{\mathrm{M}}}.$$

Let X' and M' be the corresponding dual spaces and $\langle \cdot, \cdot \rangle_{\mathrm{X}}$ be the duality pairing between X and X'. Given $f \in \mathrm{X}'$ we consider the following mixed variational problem: *Find* $(u,p) \in X \times M$ *such that*

$$\begin{aligned} \mathfrak{a}(u,v) + \mathfrak{b}(v,p) &= \langle f, v \rangle_{\mathrm{X}} \quad \forall v \in \mathrm{X}, \\ \mathfrak{b}(u,q) &= 0 \qquad\quad \forall q \in \mathrm{M}. \end{aligned} \tag{2.7}$$

By defining the set of functions which satisfy the second equation

$$\mathrm{V} := \{ v \in \mathrm{X} \mid \mathfrak{b}(v,q) = 0 \ \forall q \in \mathrm{M} \}$$

the problem can be reduced (cf. [Girault and Raviart, 1979]) to: *Find an element* $u \in V$ *such that*

$$\mathfrak{a}(u,v) = \langle f, v \rangle_{\mathrm{X}} \quad \forall v \in \mathrm{V}. \tag{2.8}$$

In this literature, (2.7) and (2.8) are proved to be equivalent under the hypothesis that $\mathfrak{b}$ fulfills the following inf-sup condition[3]:

$$\inf_{0 \neq p \in \mathrm{M}} \sup_{0 \neq u \in \mathrm{X}} \frac{\mathfrak{b}(u,p)}{\|u\|_{\mathrm{X}} \|p\|_{\mathrm{M}}} \geq \beta > 0. \tag{2.9}$$

This allows to apply the Lax-Milgram Theorem to (2.8) which tells us that the coercivity of $\mathfrak{a}$ on V ensures unique solvability.

Theorem 2.1 (Girault and Raviart [1979], Theorem 4.1)
Let X and M be real Hilbert spaces, $\mathfrak{a} : X \times X \to \mathbb{R}$ *and* $\mathfrak{b} : X \times M \to \mathbb{R}$ *be continuous bilinear forms with the following properties:*

1. $\mathfrak{a}$ *is coercive on X, i.e. there is a constant* $\alpha > 0$ *such that*

$$\mathfrak{a}(u,u) \geq \alpha \|u\|_X^2 \qquad \forall u \in X.$$

2. $\mathfrak{b}$ *fulfills the inf-sup condition (2.9).*

Then the general mixed variational problem (2.7) has a unique solution $(u,p) \in X \times M$ *and*

$$\|u\|_X + \|p\|_M \leq C \|f\|_{X'},$$

where C *is a constant depending only on* α, β *and* $\|a\|$. □

[3] It is also known as Ladyshenskaja-Babuška-Brezzi (LBB) condition.

We emphasize that the abstract theory can also be applied to the more general variational problem

$$\begin{aligned} \mathfrak{a}(u,v) + \mathfrak{b}(v,p) &= \langle f, v\rangle_{\mathrm{X}} \quad \forall v \in \mathrm{X}, \\ \mathfrak{b}(u,q) &= \langle g, q\rangle_{\mathrm{M}} \quad \forall q \in \mathrm{M} \end{aligned} \tag{2.10}$$

with non-vanishing divergence. Existence and uniqueness of solutions can be proved under the same assumptions as in Theorem 2.1, provided $g \in \mathrm{M}'$. The solution depends continuously on the right-hand side, i.e.

$$\|u\|_{\mathrm{X}} + \|p\|_{\mathrm{M}} \leq C^*\big(\|f\|_{\mathrm{X}'} + \|g\|_{\mathrm{M}'}\big). \tag{2.11}$$

This generalization will be employed in the stability proof of our method.

2.1.3 The Abstract Operator Problem

Before we apply Theorem 2.1 to the Stokes problems we want to point out that the abstract variational problem can be formulated equivalently as a linear operator equation on $\mathrm{X} \times \mathrm{M}$. We define the two linear operators $\mathfrak{A} : \mathrm{X} \to \mathrm{X}'$ and $\mathfrak{B} : \mathrm{M} \to \mathrm{X}'$ by

$$\langle u, \mathfrak{A}v\rangle_{\mathrm{X}} := \mathfrak{a}(u,v), \quad u, v \in \mathrm{X}, \tag{2.12}$$

$$\langle u, \mathfrak{B}p\rangle_{\mathrm{X}} := \mathfrak{b}(u,p), \quad u \in \mathrm{X}, p \in \mathrm{M}. \tag{2.13}$$

With this notation, problem (2.1.2) can be rewritten as follows

$$\begin{bmatrix} \mathfrak{A} & \mathfrak{B} \\ \mathfrak{B}^* & \mathfrak{o} \end{bmatrix} \begin{bmatrix} u \\ p \end{bmatrix} = \begin{bmatrix} f \\ 0 \end{bmatrix}, \tag{2.14}$$

where $\mathfrak{B}^* : \mathrm{X} \to \mathrm{M}'$ is the dual operator to $\mathfrak{B}$, i.e.

$$\langle u, \mathfrak{B}p\rangle_{\mathrm{X}} = \langle \mathfrak{B}^* u, p\rangle_{\mathrm{M}} = \mathfrak{b}(u,p), \quad u \in \mathrm{X}, p \in \mathrm{M}.$$

If $\mathrm{X} \times \mathrm{M}$ is finite dimensional equation (2.14) can be formulated as a system of linear equations in the coefficients of suitable basis representations of u and p.

2.1.4 Weak Solutions of the Stokes Problem

In the theory of elliptic partial differential equation, X and M, typically, are appropriate Sobolev spaces. We will use the standard notation. By $\mathrm{W}_p^m(\Omega)$ we denote the Sobolev space of L^p-functions with weak derivatives up to order $m \in \mathbb{N} \cup \{0\}$ in $\mathrm{L}^p(\Omega)$, $p \in \mathbb{N} \cup \{\infty\}$. In the special case $p = 2$, these spaces become Hilbert spaces and are denoted by $\mathrm{H}^m(\Omega)$. We will write

$$\begin{aligned} &\|\cdot\|_{m,p,\Omega} && \text{for the norm in } \mathrm{W}_p^m(\Omega), \\ &|\cdot|_{m,p,\Omega} && \text{for the seminorm in } \mathrm{W}_p^m(\Omega), \\ &\|\cdot\|_{m,\Omega} && \text{for the norm in } \mathrm{H}^m(\Omega), \\ &|\cdot|_{m,\Omega} && \text{for the seminorm in } \mathrm{H}^m(\Omega) \\ \text{and} \quad &\langle\cdot,\cdot\rangle_{m,\Omega} && \text{for the scalar product in } \mathrm{H}^m(\Omega). \end{aligned}$$

We will use bold letters for the function spaces if their elements are vector valued.

Weak Solution for Dirichlet Boundary Condition

The Sobolev space which contains the Dirichlet boundary condition is given by

$$\mathbf{H}^1_{\mathrm{D}}(\Omega) := \left\{\mathbf{u} \in \mathbf{H}^1(\Omega) : \mathbf{u}|_\Gamma = \mathbf{0} \quad \text{in the sense of traces}\right\}^4$$

while the associated pressure space is

$$\mathrm{L}^2_0(\Omega) := \left\{p \in \mathrm{L}^2(\Omega) : \int_\Omega p = 0\right\}.$$

If the right-hand side $\mathbf{f} \in \mathbf{L}^2(\Omega)$is given, then the weak formulation of (2.3) with Dirichlet boundary condition is given by *seeking a pair* $(\mathbf{u}, p) \in \mathbf{H}^1_{\mathrm{D}}(\Omega) \times L^2_0(\Omega)$ *such that*

$$\begin{array}{lll} \mathfrak{a}(\mathbf{u},\mathbf{v}) + \mathfrak{b}(\mathbf{v},p) = \langle \mathbf{f},\mathbf{v}\rangle_{0,\Omega} & \forall \mathbf{v} \in \mathbf{H}^1_{\mathrm{D}}(\Omega)\,, \\ \mathfrak{b}(\mathbf{u},q) \qquad\qquad = 0 & \forall q \in \mathrm{L}^2_0(\Omega)\,, \end{array} \tag{2.15}$$

where the bilinear forms are defined in the following way:

$$\begin{aligned} &\mathfrak{a} : \mathbf{H}^1(\Omega) \times \mathbf{H}^1(\Omega) \to \mathbb{R}, \quad \mathfrak{a}(\mathbf{u},\mathbf{v}) := 2\int_\Omega (\mathbf{D}\mathbf{u}) : (\mathbf{D}\mathbf{v})\,, \\ &\mathfrak{b} : \mathbf{H}^1(\Omega) \times \mathrm{L}^2(\Omega) \to \mathbb{R}, \quad \mathfrak{b}(\mathbf{v},q) := -\int_\Omega q \operatorname{div}\mathbf{v}. \end{aligned} \tag{2.16}$$

The fact that $\mathfrak{a}$ and $\mathfrak{b}$ in (2.16) are defined on larger spaces $\mathbf{H}^1(\Omega)$ and $\mathrm{L}^2(\Omega)$ will be useful later. Due to the Cauchy-Schwarz inequality both bilinear forms are continuous on the unconstrained spaces and their norms are $\|\mathfrak{a}\| = 1$ and $\|\mathfrak{b}\| = \sqrt{d}$. The space V from Section 2.1.2 is in our setting the subspace of *divergence free* functions

$$\mathbf{V}_{\mathrm{D}} := \{\mathbf{u} \in \mathbf{H}^1_{\mathrm{D}}(\Omega) \mid \operatorname{div}\mathbf{u} = 0\}. \tag{2.17}$$

For $\mathbf{u} \in \mathbf{H}^1_{\mathrm{D}}(\Omega)$ integration by parts leads to the identity

$$2\mathfrak{a}(\mathbf{u},\mathbf{v}) = \int_\Omega \nabla\mathbf{u} : \nabla\mathbf{v} + \int_\Omega \operatorname{div}\mathbf{u} \operatorname{div}\mathbf{v}.$$

Since the second term on the right-hand side is non-negative whenever $\mathbf{u} = \mathbf{v}$ we get

$$\mathfrak{a}(\mathbf{u},\mathbf{u}) \geq \tfrac{1}{2}\big|\mathbf{u}\big|_{1,\Omega} \quad \forall \mathbf{u} \in \mathbf{H}^1_{\mathrm{D}}(\Omega)\,,$$

which allows to employ the *Friedrichs* inequality

$$\big|\mathbf{u}\big|_{1,\Omega} \geq C_{\mathrm{F}}\big\|\mathbf{u}\big\|_{0,\Omega} \quad \forall \mathbf{u} \in \mathbf{H}^1_{\mathrm{D}}(\Omega)\,, \quad C_{\mathrm{F}} = C(\operatorname{diam}(\Omega)),$$

to prove the coercivity of $\mathfrak{a}$, not only on $\mathbf{V}_{\mathrm{D}}$ but even on $\mathbf{H}^1_{\mathrm{D}}(\Omega)$:

$$\mathfrak{a}(\mathbf{u},\mathbf{u}) \geq \alpha_{\mathrm{D}}\big\|\mathbf{u}\big\|^2_{1,\Omega} \quad \forall \mathbf{u} \in \mathbf{H}^1_{\mathrm{D}}(\Omega)\,, \quad \alpha_{\mathrm{D}} := \tfrac{1+C_{\mathrm{F}}^2}{4}. \tag{2.18}$$

The previous inequality is also known as *Korn*'s inequality (cf. [Duvaut and Lions, 1976] and [Nitsche, 1981]).

[4] It is often denoted by H^1_0 in the literature.

The inf-sup condition (2.9) can be proved using the fact that the divergence operator is an isomorphism from $\mathbf{V}_{\mathrm{D}}$ onto $\mathrm{L}^2_0(\Omega)$ ([Girault and Raviart, 1979, Lemma 3.2]).

By Theorem 2.1, the weak Stokes problem (2.15) is uniquely solvable. Under additional assumptions on the smoothness of the boundary the solution has additional regularity (cf. [Temam, 1984]).

Theorem 2.2 (Existence and uniqueness for Dirichlet boundary)

1. *Problem (2.15) has a unique solution.*
2. *If* $(\mathbf{u},p)\in\big(\mathbf{H}^1_{\mathrm{D}}(\Omega)\times L^2_0(\Omega)\big)\cap\big(\mathbf{H}^2(\Omega)\times H^1(\Omega)\big)$ *is a solution of (2.15) then there is a constant* $C_{\mathrm{reg}}>0$ *such that*
$$\|\mathbf{u}\|_{2,\Omega}+\|p\|_{1,\Omega}\le C_{\mathrm{reg}}\|\mathbf{f}\|_{0,\Omega}. \tag{2.19}$$
3. *If* Γ *is of class* C^2 *then (2.15) has a unique solution* $(\mathbf{u},p)\in\big(\mathbf{H}^2(\Omega)\times H^1(\Omega)\big)$. □

Weak Solution for Slip Boundary Condition

The analysis is more complicated in the case of slip boundary, where the appropriate velocity space is

$$\mathbf{H}^1_{\mathrm{s}}(\Omega):=\big\{\mathbf{u}\in\mathbf{H}^1(\Omega):\ \langle\mathbf{u},\boldsymbol{\nu}\rangle|_\Gamma=0\quad\text{in the sense of traces}\big\}.$$

It contains the essential slip boundary condition. The associated pressure space remains $\mathrm{L}^2_0(\Omega)$. For a given right-hand side $\mathbf{f}\in\mathbf{L}^2(\Omega)\supseteq\mathbf{H}^1_{\mathrm{s}}(\Omega)'$ the weak formulation of (2.3) with slip boundary condition is given by *seeking a pair* $(\mathbf{u},p)\in\mathbf{H}^1_{\mathrm{s}}(\Omega)\times L^2_0(\Omega)$ *such that*

$$\begin{aligned}\mathfrak{a}(\mathbf{u},\mathbf{v})+\mathfrak{b}(\mathbf{v},p)&=\int_\Omega\langle\mathbf{f},\mathbf{v}\rangle\quad&\forall\mathbf{v}\in\mathbf{H}^1_{\mathrm{s}}(\Omega),\\ \mathfrak{b}(\mathbf{u},q)&=0&\forall q\in\mathrm{L}^2_0(\Omega).\end{aligned}\tag{2.20}$$

The bilinear forms $\mathfrak{a}$ and $\mathfrak{b}$ are defined as in (2.16). Corresponding to (2.17) we define

$$\mathbf{V}_{\mathrm{s}}:=\{\mathbf{u}\in\mathbf{H}^1_{\mathrm{s}}(\Omega)\ \mid\ \operatorname{div}\mathbf{u}=0\}.$$

But this time we are running into trouble since the set of admissible functions is intersected by the nontrivial kernel of the bilinear form $\mathfrak{a}$ which is equal to the set of *rigid body motions* $\mathcal{R}$:

$$\mathcal{R}:=\{\mathbf{A}\mathbf{x}+\mathbf{b}\mid\mathbf{A}\in\mathbb{R}^{d\times d}\text{ skew symmetric},\mathbf{b}\in\mathbb{R}^d\}=\{\mathbf{v}\in\mathbf{H}^1(\Omega)\mid\mathfrak{a}(\mathbf{v},\mathbf{v})=0\}.\tag{2.21}$$

If $\Omega\subseteq\mathbb{R}^3$ is a region obtained by revolution around the vector $\xi=(\xi_1,\xi_2,\xi_3)^T\in\mathbb{R}^3$, then the linear skew symmetric mapping

$$\mathbf{x}\mapsto\begin{bmatrix}0&-\xi_3&\xi_2\\ \xi_3&0&-\xi_1\\ -\xi_2&\xi_1&0\end{bmatrix}\mathbf{x}$$

is in $\mathbf{V}_{\mathrm{s}}$. A similar problem occurs in $\mathbb{R}^2$, if Ω is rotational symmetric to the origin, i.e. Ω is a disk or an annulus. Here, the linear skew symmetric mapping

$$\mathbf{x}\mapsto\begin{bmatrix}0&-1\\ 1&0\end{bmatrix}\mathbf{x}$$

is an element of $\mathbf{V}_{\mathrm{s}}$. So we cannot expect coercivity on $\mathbf{V}_{\mathrm{s}}$ or $\mathbf{H}^1_{\mathrm{s}}(\Omega)$ if Ω has rotational symmetries. In such cases we must use the quotient space $\mathbf{H}^1_{\mathrm{s}}(\Omega)/\mathcal{R}$. To avoid these technicalities we exclude the critical cases by assuming Ω not to have rotational symmetries whenever the slip boundary condition is concerned. Under this hypothesis, the bilinear form $\mathfrak{a}$ has been proved to be coercive on the space $\mathbf{H}^1_{\mathrm{s}}(\Omega)$ (cf. [Solonnikov and Ščadilov, 1973], Lemma 4):

$$\mathfrak{a}(\mathbf{u},\mathbf{u}) \geq \alpha_{\mathrm{s}} \big\|\mathbf{u}\big\|^2_{1,\Omega} \quad \forall \mathbf{u} \in \mathbf{H}^1_{\mathrm{s}}(\Omega)\,. \tag{2.22}$$

Since the proof of (2.22) was made by contradiction, the constant α_{s} is not explicitly known, but it depends at least on C_{F} and the curvature of the domain boundary Γ.

As a final remark on the coercivity of $\mathfrak{a}$ we want to mention that it can be shown ([Duvaut and Lions, 1976]) that inequality (2.22) remains true if $\mathbf{H}^1_{\mathrm{s}}(\Omega)$ is replaced by an arbitrary subspace $\mathbf{U} \subseteq \mathbf{H}^1(\Omega)$ intersecting $\mathcal{R}$ only in the zero element, i.e. $\mathbf{U} \cap \mathcal{R} = \{\mathbf{0}\}$:

$$\mathfrak{a}(\mathbf{u},\mathbf{u}) \geq \alpha \big\|\mathbf{u}\big\|^2_{1,\Omega} \quad \forall \mathbf{u} \in \mathbf{U}. \tag{2.23}$$

Later, we will use this argument to prove the coercivity on our finite element spaces.

The inf-sup condition also holds in the slip case, since once it is true for the space $\mathbf{H}^1_{\mathrm{D}}(\Omega)$ it is also true for every linear space containing $\mathbf{H}^1_{\mathrm{D}}(\Omega)$, so for $\mathbf{H}^1_{\mathrm{s}}(\Omega)$ or even the whole space $\mathbf{H}^1(\Omega)$. This implies that the weak Stokes problem (2.20) is uniquely solvable, except for some geometries with special symmetries. As for Dirichlet boundary, additional regularity can be shown (cf. [Solonnikov and Ščadilov, 1973]).

Theorem 2.3 (Existence and uniqueness for slip boundary)

1. *Problem (2.20) always has a solution. If Ω has no rotational symmetries then it is unique.*
2. *If $(\mathbf{u},p) \in \big(\mathbf{H}^1_{\mathrm{s}}(\Omega) \times L^2_0(\Omega)\big) \cap \big(\mathbf{H}^2(\Omega) \times H^1(\Omega)\big)$ is a solution of (2.20) then there is a constant $C_{\mathrm{reg}} > 0$ such that*
$$\big\|\mathbf{u}\big\|_{2,\Omega} + \big\|p\big\|_{1,\Omega} \leq C_{\mathrm{reg}} \big\|\mathbf{f}\big\|_{0,\Omega}. \tag{2.24}$$
3. *If Γ is of class C^3 then the solution $(\mathbf{u},p)$ is in $\in \big(\mathbf{H}^2(\Omega) \times H^1(\Omega)\big)$.* □

2.1.5 A Different Variational Formulation - Handling of the Pressure Constraint

In both cases, it is possible to remove the mean value condition from the pressure space and to incorporate it into the variational equation. The space of pressure test functions will then be $\mathrm{L}^2(\Omega)$ and only the solution will be forced to have mean value zero. This will be very helpful for computations since it allows the use of the standard locally supported basis functions. By introducing the Lagrange multiplier $\lambda \in \mathbb{R}$ we get the following extended mixed problem for Dirichlet boundary condition: *Find* $(\mathbf{u},p,\lambda) \in \mathbf{H}^1_{\mathrm{D}}(\Omega) \times L^2(\Omega) \times \mathbb{R}$ *such that*

$$\begin{array}{lllll} \mathfrak{a}(\mathbf{u},\mathbf{v}) & + \ \mathfrak{b}(\mathbf{v},p) & & = \langle \mathbf{f},\mathbf{v}\rangle_{0,\Omega} & \forall \mathbf{v} \in \mathbf{H}^1_{\mathrm{D}}(\Omega)\,, \\ \mathfrak{b}(\mathbf{u},q) & & + \ \mathfrak{c}(\lambda,q) = 0 & & \forall q \in \mathrm{L}^2(\Omega)\,, \\ & \mathfrak{c}(1,p) & & = 0, & \end{array} \tag{2.25}$$

where the bilinear form $\mathfrak{c}$ is defined as follows:

$$\mathfrak{c} : \mathbb{R} \times \mathrm{L}^2(\Omega) \to \mathbb{R}, \qquad (\lambda, q) \mapsto \lambda \cdot \int_\Omega q.$$

In the slip case the extended problem reads: *Find* $(\mathbf{u}, p, \lambda) \in \mathbf{H}^1_{\mathrm{s}}(\Omega) \times L^2(\Omega) \times \mathbb{R}$ *such that*

$$\begin{aligned} \mathfrak{a}(\mathbf{u}, \mathbf{v}) \;+\; \mathfrak{b}(\mathbf{v}, p) &= \int_\Omega \langle \mathbf{f}, \mathbf{v} \rangle \quad \forall \mathbf{v} \in \mathbf{H}^1_{\mathrm{s}}(\Omega)\,, \\ \mathfrak{b}(\mathbf{u}, q) \;+\; \mathfrak{c}(\lambda, q) &= 0 \qquad\qquad \forall q \in \mathrm{L}^2(\Omega)\,, \\ \mathfrak{c}(1, p) &= 0. \end{aligned} \tag{2.26}$$

The extended problems are equivalent to the problems (2.15) and (2.20). The key to this is the fact that

$$\mathrm{L}^2(\Omega) = \mathrm{L}^2_0(\Omega) \oplus \mathbb{R}.$$

If $(\mathbf{u}, p)$ is a solution to (2.15) then $\mathfrak{c}(1, p) = 0$ and the second equation of (2.25) is fulfilled for $q \in \mathrm{L}^2_0(\Omega)$. Due to Gauss' Theorem and the zero boundary condition it is also fulfilled for a constant q. On the other hand, if $(\mathbf{u}, p, \lambda)$ is a solution of (2.25), the insertion of a constant q in the second equation forces λ to be zero, the insertion of $q \in \mathrm{L}^2_0(\Omega)$ forces $(\mathbf{u}, p)$ to satisfy (2.15). The arguments apply to the slip problems as well.

Corresponding operator formulations can be given using the linear operators defined in (2.12) for the spaces $\mathrm{X} = \mathbf{H}^1_{\mathrm{D}}(\Omega)$ resp. $\mathrm{X} = \mathbf{H}^1_{\mathrm{s}}(\Omega)$ and $\mathrm{M} = \mathrm{L}^2(\Omega)$. Additionally we define the linear functional

$$\mathfrak{C} : \mathrm{L}^2(\Omega) \to \mathbb{R}, \qquad q \mapsto \int_\Omega q,$$

which leads to the operator equation

$$\begin{bmatrix} \mathfrak{A} & \mathfrak{B} & \mathbf{0} \\ \mathfrak{B}^* & \mathbf{0} & \mathfrak{C} \\ \mathbf{0} & \mathfrak{C}^* & 0 \end{bmatrix} \begin{bmatrix} \mathbf{u} \\ p \\ \lambda \end{bmatrix} = \begin{bmatrix} \mathbf{f} \\ \mathbf{0} \\ 0 \end{bmatrix}. \tag{2.27}$$

2.2 Finite Element Approximation

The knowledge of existence of solutions of partial differential equations does not imply that we know how to find them. Analytic solutions to the differential equations are only known in very special situations. So we need to approximate them. Probably the most popular method to do this is the *Finite Element Method*. In [Girault and Raviart, 1979] the basic techniques for a finite element approximation of mixed variational problems were developed. We will give a brief introduction before we present the *mini element* as a standard finite element method for the approximation of the Stokes equation.

2.2.1 Abstract Approximation

First we recall the abstract mixed variational problem from Section 2.1.2: *Find* $(u, p) \in X \times M$ *such that*

$$\begin{aligned} \mathfrak{a}(u, v) + \mathfrak{b}(v, p) &= \langle f, v\rangle_X \quad \forall v \in X, \\ \mathfrak{b}(u, q) &= 0 \qquad\quad \forall q \in M, \end{aligned} \tag{2.28}$$

where X and M are real Hilbert spaces, $\mathfrak{a} : X \times X \to \mathbb{R}$ and $\mathfrak{b} : X \times M \to \mathbb{R}$ are continuous bilinear forms and $f \in X'$ is given.

We want to approximate the solution by a *Galerkin* method, so we formulate related problems in finite dimensional spaces X_H and M_H, where $H > 0$ is the discretization parameter. If $X_H \subseteq X$ and $M_H \subseteq M$ then the resulting method is called *conforming*. If not, the method is *nonconforming* and a general theory can be found in [Brezzi and Fortin, 1991]. In what follows we will mainly get involved in nonconformity arising from violating boundary conditions. Therefore we present a basic theory that includes only this type of nonconformity.

Let $\mathfrak{X}$ be a real Hilbert space including both, the continuous space X and the discrete spaces X_H, and let M_H be a subspace of M, i.e.

$$X \subseteq \mathfrak{X} \supseteq X_H, \quad M_H \subseteq M \quad \forall H > 0.$$

If the bilinear forms can be extended to $\mathfrak{X}$ the discrete Problem for $f \in \mathfrak{X}'$ reads: *Find* $(u_H, p_H) \in X_H \times M_H$ *such that*

$$\begin{aligned} \mathfrak{a}(u_H, v_H) + \mathfrak{b}(v_H, p_H) &= \langle f, v_H\rangle_{X_H} \quad \forall v_H \in X_H, \\ \mathfrak{b}(u_H, q_H) &= 0 \qquad\quad \forall q_H \in M_H. \end{aligned} \tag{2.29}$$

Theorem 2.1 implies existence and uniqueness if $\mathfrak{a}$ is coercive on

$$V_H := \{v_H \in X_H \mid \mathfrak{b}(v_H, q_H) = 0 \ \ \forall q_H \in M_H\}$$

and $\mathfrak{b}$ fulfills an inf-sup condition. Note that neither condition can be inherited by its continuous counter part since in general, $X_H \not\subseteq X$ and $V_H \not\subseteq V$.

Theorem 2.4 (Abstract mixed approximation, [Brezzi and Fortin, 1991])
Let $\mathfrak{X}$ *and* M *be real Hilbert spaces containing families of subspaces* $\{X_H\}_{H>0}$ *and* $\{M_H\}_{H>0}$. *Let* $\mathfrak{a} : \mathfrak{X} \times \mathfrak{X} \to \mathbb{R}$ *and* $\mathfrak{b} : \mathfrak{X} \times M \to \mathbb{R}$ *be continuous bilinear forms with the following properties:*

1. $\mathfrak{a}$ *is uniformly coercive on* $\{X_H\}_{H>0}$, *i.e. there is a constant* $\tilde{\alpha} > 0$ *such that*

$$\mathfrak{a}(u, u) > \tilde{\alpha}\|u\|_{\mathfrak{X}}^2 \qquad \forall u_H \in \bigcup_{H>0} X_H.$$

2. $\mathfrak{b}$ *fulfills the discrete inf-sup condition, i.e. there is a constant* $\tilde{\beta} > 0$ *which does not depend on* H *such that*

$$\inf_{0\neq p_H \in M_H} \sup_{0\neq u_H \in X_H} \frac{\mathfrak{b}(u_H, p_H)}{\|p_H\|_M \|u_H\|_{\mathfrak{X}}} \geq \tilde{\beta} > 0 \quad \forall H > 0. \tag{2.30}$$

Then the discrete mixed variational problem (2.29) has a unique solution $(u_\mathsf{H}, p_\mathsf{H}) \in X_\mathsf{H} \times M_\mathsf{H}$. *If* (u, p) *is the solution of the continuous problem (2.28) then we have the following error estimates:*

$$\|u - u_\mathsf{H}\|_\mathfrak{X} \leq \left(1 + \frac{\|\mathfrak{a}\|}{\tilde{\alpha}}\right)\left(1 + \frac{\|\mathfrak{b}\|}{\tilde{\beta}}\right) \inf_{v_\mathsf{H} \in X_\mathsf{H}} \|u - v_\mathsf{H}\|_\mathfrak{X} + \frac{\|\mathfrak{b}\|}{\tilde{\beta}} \inf_{q_\mathsf{H} \in M_\mathsf{H}} \|p - q_\mathsf{H}\|_M + \frac{1}{\tilde{\alpha}} K_\mathsf{H},$$
$$\|p - p_\mathsf{H}\|_M \leq \frac{\|\mathfrak{a}\|}{\tilde{\beta}} \|u - u_\mathsf{H}\|_\mathfrak{X} + \left(1 + \frac{\|\mathfrak{b}\|}{\tilde{\beta}}\right) \inf_{q_\mathsf{H} \in M_\mathsf{H}} \|p - q_\mathsf{H}\|_M + \frac{1}{\tilde{\beta}} K_\mathsf{H},$$

where

$$K_\mathsf{H} := \sup_{0 \neq v_\mathsf{H} \in X_\mathsf{H}} \frac{\left|\mathfrak{a}(u, v_\mathsf{H}) + \mathfrak{b}(v_\mathsf{H}, p) - \langle f, v_\mathsf{H} \rangle_\mathfrak{X}\right|}{\|v_\mathsf{H}\|_\mathfrak{X}} \tag{2.31}$$

denotes the error due to the nonconformity in the method. □

As a consequence of this theorem the approximations $(u_\mathsf{H}, p_\mathsf{H})$ converge to the continuous solution (u, p) if the distance between (u, p) and the discrete spaces as well as the nonconformity K_H tend to zero as H tends to zero.

As on the continuous level, an operator formulation of (2.29) can be derived. Since the space is finite dimensional the operators have matrix representations. Therefore we introduce a basis in the discrete spaces to define a linear equation as in (2.27). Let the discrete space be given by

$$\mathrm{X}_\mathsf{H} := \operatorname{span}\{v_i\}_{i=1}^{\dim \mathrm{X}_\mathsf{H}}, \quad \mathrm{M}_\mathsf{H} := \operatorname{span}\{q_i\}_{i=1}^{\dim \mathrm{M}_\mathsf{H}},$$

where v_i and q_i are suitable basis functions. If we additionally use the basis representations

$$u(\mathbf{x}) = \sum_{i=1}^{\dim \mathrm{X}_\mathsf{H}} u_i v_i(\mathbf{x}) \quad \text{and} \quad p(\mathbf{x}) = \sum_{i=1}^{\dim \mathrm{M}_\mathsf{H}} p_i q_i(\mathbf{x})$$

we can rewrite (2.29) as a system of linear equations in the unknown coefficients $\mathbf{u} := (u_i)_{i=1}^{\dim \mathrm{X}_\mathsf{H}}$ and $\mathbf{p} := (p_i)_{i=1}^{\dim \mathrm{M}_\mathsf{H}}$ and the multiplier λ:

$$\underbrace{\begin{bmatrix} \mathbf{A} & \mathbf{B} & \mathbf{0} \\ \mathbf{B}^T & \mathbf{0} & \mathbf{C} \\ \mathbf{0} & \mathbf{C}^T & 0 \end{bmatrix}}_{\mathbf{M}} \begin{bmatrix} \mathbf{u} \\ \mathbf{p} \\ \lambda \end{bmatrix} = \begin{bmatrix} \mathbf{f} \\ \mathbf{0} \\ 0 \end{bmatrix}. \tag{2.32}$$

Thereby

$$\begin{array}{lllll} \mathbf{A} & = & \big(a_{i,j}\big)_{i,j} & = & \big(\mathfrak{a}(v_i, v_j)\big)_{i,j} \quad \in \mathbb{R}^{\dim \mathrm{X}_\mathsf{H} \times \dim \mathrm{X}_\mathsf{H}}, \\ \mathbf{B} & = & \big(b_{i,j}\big)_{i,j} & = & \big(\mathfrak{b}(v_i, q_j)\big)_{i,j} \quad \in \mathbb{R}^{\dim \mathrm{X}_\mathsf{H} \times \dim \mathrm{M}_\mathsf{H}}, \\ \mathbf{C} & = & (c_i)_i & = & \big(\int_\Omega q_i)\big)_i \quad \in \mathbb{R}^{\dim \mathrm{M}_\mathsf{H} \times 1}, \\ \mathbf{f} & = & \big(f_i\big)_i & = & \big(\int_\Omega \langle f, v_i \rangle\big)_i \quad \in \mathbb{R}^{\dim \mathrm{X}_\mathsf{H}}. \end{array}$$

So finally, the Stokes problem is reduced to solve a system of linear equations which has a unique solution under the assumptions of Theorem 2.4. The key to an efficient numerical solution of (2.32) is the sparsity of the system matrix $\mathbf{M}$. A finite element discretization typically leads to such a sparse structure.

2.2.2 Finite Element Approximation of the Stokes Problem

In the finite element method, we choose the discrete approximation spaces from the previous section to be piecewise polynomial. The advantage is that the basis functions are supported only locally which leads to a sparse linear system, i.e. the number of nonzero entries is of order $\dim \mathsf{X}_\mathsf{H} + \dim \mathsf{M}_\mathsf{H}$. To define spline spaces we need to introduce a family of subdivisions of the domain, e.g., into a finite number of simplices. Obviously, this is only possible if Ω is a polyhedron. If not, Ω needs to be approximated by polyhedral domains Ω_H. Let $\mathcal{T}_\mathsf{H} := \{T_i : 1 \le i \le n\}$ be a subdivision of Ω_H consisting of (closed) simplices such that

$$\overline{\Omega_\mathsf{H}} = \bigcup_{T \in \mathcal{T}_\mathsf{H}} T \quad \text{and} \quad \mathsf{H} := \max_{T \in \mathcal{T}_\mathsf{H}} \operatorname{diam}(T), \tag{2.33}$$

where any two different simplices are either disjoint or share exactly either one face or one side or one vertex. We will refer to H as the discretization parameter and to Θ_H as the set of vertices. The subset of boundary vertices is denoted by Θ_H^Γ. We require

$$\Theta_\mathsf{H}^\Gamma \subseteq \Gamma = \partial\Omega,$$

which helps avoiding effects like the Babuška paradox (cf. [Babuška, 1963]). $\{\mathcal{T}_\mathsf{H}\}_{\mathsf{H}>0}$ is assumed to be shape-regular, i. e. there exists $\rho > 0$ such that

$$\rho_T := \frac{\operatorname{diam}(B_T)}{\operatorname{diam}(T)} \ge \rho \qquad \forall T \in \mathcal{T}_\mathsf{H}, \quad \forall \mathsf{H} > 0, \tag{2.34}$$

where B_T denotes the largest ball contained in T (cf. [Brenner and Scott, 1994]). ρ_T is called the regularity constant of a simplex T.

With the help of such triangulations finite element spaces on the domains Ω_H can be defined. The approximation of non-polygonal/non-polyhedral domains by triangulations introduces some additional error. The convergence analysis has to be modified since the solution and their approximations are defined on different domains. The abstract theory presented before does not cover this case of nonconformity. In most textbooks on finite elements the problem is shifted to the modeling process by supposing Ω is polyhedral. Another way to circumvent the problem is to impose a resolution condition on the subdivisions $\mathcal{T}_\mathsf{H}$, i.e. a condition which controls the error arising from polyhedral approximations. In both cases the minimal space dimension may be affected. The number of unknowns is of order $\sharp\Theta_\mathsf{H}$. Obviously, it is bounded from below by the quotient $\sqrt{|\Omega|}/\mathsf{H}$. But additionally, the number of corners (for a polyhedral domain) or a resolution condition will force to put a large number of grid points on the boundary. This number depends on the size and number of geometrical details and bounds the minimal space dimension from below. We will give a detailed description of such resolution conditions at the end of this chapter.

For the time being, let us introduce an example of a finite element for the Stokes equations. We will give a version for the Dirichlet condition, and one for slip boundary condition.

The Mini Element (Dirichlet Boundary Condition)

The *Mini Element* (cf. [Brezzi and Fortin, 1991]) is a prototype of a finite element method for the Stokes problem. The velocity components and the pressure are approximated by continuous piecewise affine functions, i.e. by suitable elements of the space

$$S_{\mathcal{T}_\mathsf{H}} := \left\{ v \in C^0\left(\overline{\Omega_\mathsf{H}}\right) \mid \forall T \in \mathcal{T}_\mathsf{H} : v|_T \in \mathbb{P}_1 \right\}. \tag{2.35}$$

We know that the set of hat functions on $\mathcal{T}_\mathsf{H}$

$$\Lambda_{\mathcal{T}_\mathsf{H}} := \{\lambda_\mathbf{y} \mid \mathbf{y} \in \Theta_\mathsf{H}\} \subseteq S_{\mathcal{T}_\mathsf{H}}, \quad \text{where } \lambda_\mathbf{y}(\mathbf{x}) = \begin{cases} 1, & \text{if } \mathbf{x} = \mathbf{y} \\ 0, & \text{if } \mathbf{x} \neq \mathbf{y} \end{cases}, \quad \mathbf{x} \in \Theta_\mathsf{H}, \tag{2.36}$$

forms a basis of $S_{\mathcal{T}_\mathsf{H}}$. In order to fulfill the inf-sup condition the velocity space must be enriched by simplex bubble functions given by

$$\psi_T := (d+1)^{d+1} \prod_{\mathbf{y} \in V(T)} \lambda_\mathbf{y},$$

where $V(T)$ denotes the set of vertices of T. The bubbles are collected in the space

$$B_{\mathcal{T}_\mathsf{H}} := \operatorname{span}\{\psi_T : T \in \mathcal{T}_\mathsf{H}\} \tag{2.37}$$

and the mini element space on $\mathcal{T}_\mathsf{H}$ is defined by

$$\mathbf{X}^{\mathrm{mini}}_{\mathcal{T}_\mathsf{H}} \times \mathrm{M}^{\mathrm{mini}}_{\mathcal{T}_\mathsf{H}} := \left(\mathbf{S}_{\mathcal{T}_\mathsf{H}} \oplus \mathbf{B}_{\mathcal{T}_\mathsf{H}}\right) \times S_{\mathcal{T}_\mathsf{H}}, \tag{2.38}$$

where bold letters mark vector valued spaces. The Dirichlet boundary condition can now be imposed pointwise on the boundary vertices by removing those hat functions which correspond to boundary vertices. The resulting space is

$$\mathbf{X}^{\mathrm{mini_D}}_\mathsf{H} \times \mathrm{M}^{\mathrm{mini}}_\mathsf{H} := \Big(\underbrace{\left\{\mathbf{v} \in \mathbf{S}_{\mathcal{T}_\mathsf{H}} \mid \mathbf{v}(\mathbf{x}) = 0 \ \forall \mathbf{x} \in \Theta^\Gamma_\mathsf{H}\right\}}_{\left\{\mathbf{v} \in \mathbf{S}_{\mathcal{T}_\mathsf{H}} \mid \mathbf{v}|_{\partial\Omega} = 0\right\}} \oplus \mathbf{B}_{\mathcal{T}_\mathsf{H}}\Big) \times S_{\mathcal{T}_\mathsf{H}}. \tag{2.39}$$

A pair $(\mathbf{u}_\mathsf{H}, p_\mathsf{H}) \in \mathbf{X}^{\mathrm{mini_D}}_\mathsf{H} \times \left(\mathrm{M}^{\mathrm{mini}}_\mathsf{H} \cap \mathrm{L}^2_0(\Omega_\mathsf{H})\right)$ is regarded as the Galerkin approximation if it fulfills the discrete variational system:

$$\begin{array}{lcll} \mathfrak{a}_\mathsf{H}(\mathbf{u}_\mathsf{H}, \mathbf{v}_\mathsf{H}) & + & \mathfrak{b}_\mathsf{H}(\mathbf{v}_\mathsf{H}, p_\mathsf{H}) & = \langle \mathbf{f}_\mathsf{H}, \mathbf{v}_\mathsf{H} \rangle_{0,\Omega_\mathsf{H}} \quad \forall \mathbf{v}_\mathsf{H} \in \mathbf{X}^{\mathrm{mini_D}}_\mathsf{H}, \\ \mathfrak{b}_\mathsf{H}(\mathbf{u}_\mathsf{H}, q_\mathsf{H}) & & & = 0 \qquad\qquad\quad \forall q_\mathsf{H} \in \mathrm{M}^{\mathrm{mini}}_\mathsf{H} \cap \mathrm{L}^2_0(\Omega_\mathsf{H}). \end{array} \tag{2.40}$$

where the bilinear forms are defined with respect to Ω_H:

$$\begin{aligned} &\mathfrak{a}_\mathsf{H} : \mathbf{H}^1(\Omega_\mathsf{H}) \times \mathbf{H}^1(\Omega_\mathsf{H}) \to \mathbb{R}, \quad \mathfrak{a}_\mathsf{H}(\mathbf{u}, \mathbf{v}) := 2 \int_{\Omega_\mathsf{H}} (\mathbf{D}\mathbf{u}) : (\mathbf{D}\mathbf{v}), \\ &\mathfrak{b}_\mathsf{H} : \mathbf{H}^1(\Omega_\mathsf{H}) \times \mathrm{L}^2(\Omega_\mathsf{H}) \to \mathbb{R}, \quad \mathfrak{b}_\mathsf{H}(\mathbf{v}, q) := -\int_{\Omega_\mathsf{H}} q \operatorname{div} \mathbf{v}. \end{aligned} \tag{2.41}$$

The right-hand side $\mathbf{f}_\mathsf{H}$ is a suitable approximation of the original outer force $\mathbf{f}$. Provided the continuous solution $(\mathbf{u}, p) \in \mathbf{H}^2(\Omega) \times \mathrm{H}^1(\Omega)$, the resulting method was proved to be convergent

of order one (cf. [Girault and Raviart, 1986]). Supposing $\Omega = \Omega_{\mathsf{H}}$ for all H this can be expressed in the following error estimate

$$\left\|\mathbf{u} - \mathbf{u}_{\mathsf{H}}\right\|_{1,\Omega} + \left\|p - p_{\mathsf{H}}\right\|_{0,\Omega} \leq C\mathsf{H}\left(\left|\mathbf{u}\right|_{2,\Omega} + \left|p\right|_{1,\Omega}\right),$$

where $C > 0$ is a constant which neither depends on H, $\mathbf{u}$, nor p. A main key role in the proof is the discrete stability, which we will present for later use: *There exists a constant* $\beta_{\mathrm{mini}} > 0$ *such that*

$$\inf_{0 \neq p_{\mathsf{H}} \in \mathrm{M}_{\mathsf{H}}^{\mathrm{mini}} \cap L_0^2(\Omega)} \sup_{\mathbf{0} \neq \mathbf{u}_{\mathsf{H}} \in \mathbf{X}_{\mathsf{H}}^{\mathrm{mini_D}}} \frac{\mathfrak{b}_{\mathsf{H}}(\mathbf{u}_{\mathsf{H}}, p_{\mathsf{H}})}{\left\|p_{\mathsf{H}}\right\|_{0,\Omega} \left\|\mathbf{u}_{\mathsf{H}}\right\|_{1,\Omega}} \geq \beta_{\mathrm{mini}} > 0 \quad \forall \mathsf{H} > 0. \tag{2.42}$$

The Mini Element (Slip Boundary Condition)

In the slip case, the element can be defined in a similar way. Again, piecewise affine functions are used to approximate the solution. And again the essential part of the boundary condition is enforced pointwise[5] in the boundary vertices, cf. [Verfürth, 1985], where the technique was used in a piecewise quadratic velocity space. For the mini element we get the following velocity space

$$\mathbf{X}_{\mathsf{H}}^{\mathrm{mini_s}} := \left\{\mathbf{v} \in \mathbf{S}_{\mathcal{T}_{\mathsf{H}}} \mid \langle \mathbf{v}(\mathbf{x}), \boldsymbol{\nu}(\mathbf{x})\rangle = 0 \quad \forall \mathbf{x} \in \Theta_{\mathsf{H}}^{\Gamma}\right\} \oplus \mathbf{B}_{\mathcal{T}_{\mathsf{H}}},$$

while the pressure space is still $\mathrm{M}_{\mathsf{H}}^{\mathrm{mini}}$. Here $\boldsymbol{\nu}$ denotes the outer normal with respect to the physical domain Ω[6]. This time we are looking for a pair $(\mathbf{u}_{\mathsf{H}}, p_{\mathsf{h}}) \in \mathbf{X}_{\mathsf{H}}^{\mathrm{mini_s}} \times \left(\mathrm{M}_{\mathsf{H}}^{\mathrm{mini}} \cap \mathrm{L}_0^2(\Omega_{\mathsf{H}})\right)$ fulfilling the discrete variational system:

$$\begin{aligned} \mathfrak{a}_{\mathsf{H}}(\mathbf{u}_{\mathsf{H}}, \mathbf{v}_{\mathsf{H}}) \;+\; \mathfrak{b}_{\mathsf{H}}(\mathbf{v}_{\mathsf{H}}, p_{\mathsf{H}}) &= \int_{\Omega_{\mathsf{H}}} \langle \mathbf{f}_{\mathsf{H}}, \mathbf{v}_{\mathsf{H}}\rangle \quad \forall \mathbf{v}_{\mathsf{H}} \in \mathbf{X}_{\mathsf{H}}^{\mathrm{mini_s}}, \\ \mathfrak{b}_{\mathsf{H}}(\mathbf{u}_{\mathsf{H}}, q_{\mathsf{H}}) &= 0 \qquad\qquad\quad \forall q_{\mathsf{H}} \in \mathrm{M}_{\mathsf{H}}^{\mathrm{mini}} \cap \mathrm{L}_0^2(\Omega_{\mathsf{H}}). \end{aligned} \tag{2.43}$$

The ideas and proofs in [Verfürth, 1987] and their generalized versions in [Knobloch, 2000] and [Bänsch and Deckelnick, 1999] can be combined with the approximation theory of the original mini element to prove optimal order (linear) convergence of the slip version of the mini element, provided the continuous solution $(\mathbf{u}, p) \in \mathbf{H}^2(\Omega) \times \mathrm{H}^1(\Omega)$.

2.2.3 Notes on the Resolution Condition

As already seen in the introduction, replacing the physical domain by polyhedrons might cause significant errors in the approximation. This effect is not restricted to a near boundary zone but pollutes the accuracy in the whole domain. The question is, under which conditions on Ω_{H} such an error can be neglected in comparison to the approximation error of the method itself. Such conditions are addressed to the local grid size near the boundary. In case of Dirichlet boundary condition Strang and Fix [1973] extended piecewise linear trial functions by zero to fit them in a

[5] In the literature, other approaches of handling the slip boundary condition can be found, for instance penalty methods or extended mixed formulations (cf. [Verfürth, 1987] and [Verfürth, 1991]).

[6] The use of the normal with respect to Ω_{H} is not sufficient to ensure optimal convergence (cf. [Verfürth, 1987]) but it is possible to define approximative normals depending only on Ω_{H} that allow optimal convergence (cf. [Bänsch and Deckelnick, 1999]).

conforming framework which works of course only under the additional assumption $\Omega_\mathsf{H} \subseteq \Omega$. This is a very strong condition since families of triangulations $\{\mathcal{T}_\mathsf{H}\}_{\mathsf{H}>0}$ with this property exist only for convex domains. Furthermore, extension by zero produces only poor approximation results near the boundary, which forces $\Omega \setminus \Omega_\mathsf{H}$ to be very thin, i.e.

$$\sup_{\mathbf{x}\in\partial\Omega_\mathsf{H}} \inf_{\mathbf{y}\in\Gamma} \operatorname{dist}(\mathbf{x},\mathbf{y}) \leq \mathsf{H}^2.$$

It is not clear for both, the Dirichlet and the slip case, how necessary this resolution condition is for the mini element on more general domains in practical applications.

We will present resolution conditions for both types of boundary conditions which can also be applied to non-convex domains and which are based on the shape of the mini element functions. They will provide sufficient conditions and help to analyze the numerical experiments.

The problem in the analysis lies in the fact that the solutions and its approximation are defined on different domains. Therefore it is unavoidable to define liftings between these spaces. In [Bänsch and Deckelnick, 1999] a homeomorphism is introduced to do the job but the conditions on its existence are very restrictive. It is assumed that Γ can be projected onto its approximations $\partial\Omega_\mathsf{H}$ in a very smooth way. The C^k-norms of this mapping appear in the convergence proof up to order $k = 3$ and are therefore supposed to be moderately bounded. In contrast to this homeomorphism strategy we employ a simple extension operator to match the discrete spaces with the continuous one and apply the abstract theory from Section 2.2.1. To reduce the technical effort we restrict to two dimensions and assume that $\tilde{T} := T \cap \Omega$ [7] is connected and that $\operatorname{diam}(\tilde{T}) \approx \operatorname{diam}(T)$ [7] for all simplices T in $\mathcal{T}_\mathsf{H}$. If this is the case then Θ_H determines an exact subdivision of Ω as follows: We connect the vertices which are adjacent in $\mathcal{T}_\mathsf{H}$ by a piece of Γ if they lie on the boundary or the corresponding edge of $\mathcal{T}_\mathsf{H}$ otherwise. We will denote the resulting exact subdivision by $\mathcal{T}_\mathsf{H}^\Omega$. Now, functions in the space $S_{\mathcal{T}_\mathsf{H}}$ are extrapolated to $\Omega \cup \Omega_\mathsf{H}$ piecewise by itself, i.e. functions are extended locally affine from $T \cap \tilde{T}$ to $T \cup \tilde{T}$. By restriction, a space of functions which are piecewise affine with respect to $\mathcal{T}_\mathsf{H}^\Omega$ is given by

$$S_{\mathcal{T}_\mathsf{H}^\Omega} := \left\{ v \in C^0(\overline{\Omega}) \mid \forall \tilde{T} \in \mathcal{T}_\mathsf{H}^\Omega : \, v|_{\tilde{T}} \in \mathbb{P}_1 \right\}.$$

Incorporating the boundary condition pointwise in $\Theta_\mathsf{H} \cap \Gamma$ as before we get the following finite element spaces on $\mathcal{T}_\mathsf{H}^\Omega$

$$\begin{aligned}
\mathbf{X}_{\mathrm{D},\mathsf{H}}^\Omega &:= \left\{ \mathbf{v} \in \mathbf{S}_{\mathcal{T}_\mathsf{H}^\Omega} \mid \mathbf{v}(\mathbf{x}) = \mathbf{0} \quad \forall \mathbf{x} \in \Theta_\mathsf{H}^\Gamma \right\} \oplus \mathbf{B}_{\mathcal{T}_\mathsf{H}^\Omega}, \\
\mathbf{X}_{\mathrm{s},\mathsf{H}}^\Omega &:= \left\{ \mathbf{v} \in \mathbf{S}_{\mathcal{T}_\mathsf{H}^\Omega} \mid \langle \mathbf{v}(\mathbf{x}), \boldsymbol{\nu}(\mathbf{x}) \rangle = 0 \quad \forall \mathbf{x} \in \Theta_\mathsf{H}^\Gamma \right\} \oplus \mathbf{B}_{\mathcal{T}_\mathsf{H}^\Omega}, \\
\mathrm{M}_\mathsf{H}^\Omega &:= S_{\mathcal{T}_\mathsf{H}^\Omega}.
\end{aligned}$$

$\mathbf{B}_{\mathcal{T}_\mathsf{H}^\Omega}$ can be chosen such that the discrete inf-sup condition is fulfilled[8]. We do not elaborate on this aspect here but focus on a minimal resolution condition. We suppose that all functions in $\mathbf{B}_{\mathcal{T}_\mathsf{H}^\Omega}$

[7] Note that this condition is already a restriction on the gridsize near the boundary, which is additionally affected by what follows.

[8] For instance, if a triangle $T \in \mathcal{T}_H$ is not a subset of Ω then the corresponding bubble function can be defined only on a sub-triangle $\tilde{T} \subseteq T \cap \Omega$ (cf. Ullmann [2006]).

vanish on Γ. Since we extrapolate piecewise affine the approximability conditions with respect to $\mathcal{T}_{\mathsf{H}}^{\Omega}$ can be retrieved by using techniques which will be presented in the fourth chapter (cf. Lemma 4.1). Therefore the error due the domain approximation can be handled via the measure of non-conformity K_{H} as in Theorem 2.4. We only have to check under which conditions it is of order H. In case of Dirichlet boundary condition we will use the identity

$$\int_{\Omega} \mathbf{D}\mathbf{u} : \mathbf{D}\mathbf{v} + \int_{\Omega} p \operatorname{div} \mathbf{v} - \langle \mathbf{f}, \mathbf{v} \rangle_{\mathrm{L}^2(\Omega)} = \int_{\Gamma} \langle \boldsymbol{\sigma}_{\boldsymbol{\nu}}(\mathbf{u}, p), \mathbf{v} \rangle \,, \tag{2.44}$$

which holds for the solution $(\mathbf{u}, p)$ to the weak Stokes problem (2.15) and an arbitrary $\mathbf{v} \in \mathbf{H}^1(\Omega)$. It allows us to rewrite the nonconformity error

$$K_{\mathsf{H}} = \sup_{\mathbf{0} \neq \mathbf{v}_{\mathsf{H}} \in \mathbf{X}_{\mathsf{H}}^{\mathrm{mini}_{\mathrm{D}}}} \frac{\int_{\Gamma} \langle \boldsymbol{\sigma}_{\boldsymbol{\nu}}(\mathbf{u}, p), \mathbf{v}_{\mathsf{H}} \rangle}{\|\mathbf{v}_{\mathsf{H}}\|_{1,\Omega}} \tag{2.45}$$

and in order to ensure the linear (optimal) convergence of the method it is sufficient (cf. Theorem 2.4) to show

$$\|\mathbf{v}_{\mathsf{H}}\|_{0,\Gamma} \leq C\mathsf{H} \|\mathbf{v}_{\mathsf{H}}\|_{1,\Omega} \quad \forall \mathbf{v}_{\mathsf{H}} \in \mathbf{X}_{\mathrm{D},\mathsf{H}}^{\Omega} \setminus \mathbf{B}_{\mathcal{T}_{\mathsf{H}}^{\Omega}}.$$

Let us take a $\mathbf{v}_{\mathsf{H}} \in \mathbf{X}_{\mathrm{D},\mathsf{H}}^{\Omega} \setminus \mathbf{B}_{\mathcal{T}_{\mathsf{H}}^{\Omega}}$ and a simplex $\tilde{T} \in \mathcal{T}_{\mathsf{H}}^{\Omega}$ such that $|\Gamma \cap \tilde{T}| > 0$. We will use the Taylor expansion to estimate $\mathbf{v}_{\mathsf{H}}$ a point $\mathbf{x} \in \Gamma \cap \tilde{T}$:

$$|\mathbf{v}_{\mathsf{H}}(\mathbf{x})| = |\nabla \mathbf{v}_{\mathsf{H}}|_{\tilde{T}} \cdot (\mathbf{x} - \bar{\mathbf{x}})| \leq C \frac{|\mathbf{x} - \bar{\mathbf{x}}|}{\operatorname{diam}(T)} |\mathbf{v}_{\mathsf{H}}|_{1,\tilde{T}}, \tag{2.46}$$

where $\bar{\mathbf{x}}$ denotes a projection of $\mathbf{x}$ onto $\Gamma_{\mathsf{H}} \cap T$. This leads to the $\mathbf{L}^2$ estimate

$$\|\mathbf{v}_{\mathsf{H}}\|_{0,\Gamma\cap\tilde{T}} \leq C \frac{\sqrt{|\Gamma \cap \tilde{T}|}}{\operatorname{diam}(T)} \left(\sup_{\mathbf{x} \in \Gamma \cap \tilde{T}} \inf_{\mathbf{y} \in \Gamma_{\mathsf{H}} \cap T} \operatorname{dist}(\mathbf{x}, \mathbf{y}) \right) |\mathbf{v}_{\mathsf{H}}|_{1,\tilde{T}}.$$

This gives us the specification of the resolution condition[9]:

$$\frac{\sqrt{|\Gamma \cap \tilde{T}|}}{\operatorname{diam}(T)} \left(\sup_{\mathbf{x} \in \Gamma \cap \tilde{T}} \inf_{\mathbf{y} \in \Gamma_{\mathsf{H}} \cap T} \operatorname{dist}(\mathbf{x}, \mathbf{y}) \right) \leq \mathsf{H} \quad \forall T \in \mathcal{T}_{\mathsf{H}}^{\Gamma}. \tag{2.47}$$

If the relative boundary length $|\Gamma \cap \tilde{T}|/\operatorname{diam}(T)$ can be bounded moderately [10], then a quasi uniform grid [11] can be used if

$$\sup_{\mathbf{x} \in \partial\Omega_{\mathsf{H}}} \inf_{\mathbf{y} \in \Gamma} \operatorname{dist}(\mathbf{x}, \mathbf{y}) \leq \mathsf{H}^{\frac{3}{2}}. \tag{2.48}$$

For slip boundary condition the resolution condition is more restrictive. K_{H} can be rewritten using

$$\int_{\Omega} \mathbf{D}\mathbf{u} : \mathbf{D}\mathbf{v} + \int_{\Omega} p \operatorname{div} \mathbf{v} - \int_{\Omega} \langle \mathbf{f}, \mathbf{v} \rangle = \int_{\Gamma} \langle \boldsymbol{\nu}, \boldsymbol{\sigma}_{\boldsymbol{\nu}}(\mathbf{u}, p) \rangle \langle \mathbf{v}_{\mathsf{H}}, \boldsymbol{\nu} \rangle \,, \tag{2.49}$$

[9] Note that, additional conditions can arise from the integration on Ω_{H} instead of Ω or from the approximation of the right-hand side. We do not elaborate on these perturbations.

[10] $\frac{|\Gamma \cap \tilde{T}|}{\operatorname{diam}(T)}$ converges to a constant $C \in [0, 1]$ as H tends to zero

[11] Quasi uniformity means that, in addition to shape regularity, all triangles have almost the same size, i.e. there exists a moderate constant $C > 0$ such that $\operatorname{diam}(T) \geq \frac{1}{C}\mathsf{H}$ for all $T \in \mathcal{T}_{\mathsf{H}}^{\Omega}$.

which holds for the solution $(\mathbf{u}, p)$ of the weak Stokes problem (2.20) and an arbitrary $\mathbf{v} \in \mathbf{H}^1(\Omega)$. Therefore

$$K_{\mathsf{H}} = \sup_{\mathbf{0} \neq \mathbf{v}_{\mathsf{H}} \in \mathbf{X}_{\mathsf{H}}^{\mathrm{mini_s}}} \frac{\int_\Gamma \langle \boldsymbol{\nu}, \boldsymbol{\sigma}_{\boldsymbol{\nu}}(\mathbf{u}, p) \rangle \langle \mathbf{v}_{\mathsf{H}}, \boldsymbol{\nu} \rangle}{\|\mathbf{v}_{\mathsf{H}}\|_{1,\Omega}} \tag{2.50}$$

and it is sufficient to show

$$\|\langle \mathbf{v}_{\mathsf{H}}, \boldsymbol{\nu} \rangle\|_{0,\Gamma} \leq CH \|\mathbf{v}_{\mathsf{H}}\|_{1,\Omega} \quad \forall \mathbf{v}_{\mathsf{H}} \in \mathbf{X}_{\mathsf{H}}^{\mathrm{mini_s}} \setminus \mathbf{B}_{\mathcal{T}_{\mathsf{H}}^\Omega}.$$

Here, we cannot apply (2.46), since $\mathbf{v}_{\mathsf{H}}$ does not vanish on Γ_{h} in general. We will use an interpolation argument which requires Γ to be of class C^2.

Let again $\mathbf{v}_{\mathsf{H}} \in \mathbf{X}_{\mathrm{D},\mathsf{H}}^\Omega \setminus \mathbf{B}_{\mathcal{T}_{\mathsf{H}}^\Omega}$ and $\tilde{T} \in \mathcal{T}_{\mathsf{H}}^\Omega$ such that $|\Gamma \cap \tilde{T}| > 0$. By

$$\phi : [0, \underbrace{|\Gamma \cap \tilde{T}|}_{=:L}] \to \Gamma \cap \tilde{T}$$

we denote the arc length parametrization of $\Gamma \cap \tilde{T}$, i.e.

$$|\dot{\phi}(s)| = 1 \quad \forall s \in [0, L].$$

Since $\langle \mathbf{v}_{\mathsf{H}}(\phi(0)), \boldsymbol{\nu}(\phi(0)) \rangle = \langle \mathbf{v}_{\mathsf{H}}(\phi(L)), \boldsymbol{\nu}(\phi(L)) \rangle = 0$ and $\left\langle \boldsymbol{\nu}(\phi(s)), \dot{\phi}(s) \right\rangle = 0$ we get

$$\|\langle \mathbf{v}_{\mathsf{H}}, \boldsymbol{\nu} \rangle\|_{0,\Gamma\cap\tilde{T}} = \|\left\langle \mathbf{v}_{\mathsf{H}} \circ \phi, (\dot{\phi})^\perp \right\rangle\|_{0,[0,L]} \leq CL |\left\langle \mathbf{v}_{\mathsf{H}} \circ \phi, (\dot{\phi})^\perp \right\rangle|_{1,[0,L]},$$

where $(\dot{\phi})^\perp := (\dot{\phi}_2, -\dot{\phi}_1)^T$. The seminorm on the right-hand side can be bounded by the $\mathbf{H}^1$ norm of $\mathbf{v}_{\mathsf{H}}$ and the maximal curvature of $\Gamma \cap \tilde{T}$ denoted by κ_T. This gives us the estimate

$$\|\langle \mathbf{v}_{\mathsf{H}}, \boldsymbol{\nu} \rangle\|_{0,\Gamma\cap\tilde{T}} \leq C \frac{L}{\mathrm{diam}(T)} (1 + \kappa_T) \|\mathbf{v}_{\mathsf{H}}\|_{1,\tilde{T}}.$$

The resolution condition in case of slip boundary reads[9,12]:

$$\frac{|\Gamma \cap \tilde{T}|}{\sqrt{\mathrm{diam}(T)}} (1 + \kappa_T) \leq \mathsf{H} \quad \forall T \in \mathcal{T}_{\mathsf{H}}^\Gamma. \tag{2.51}$$

This is more restrictive than in the Dirichlet case. If the relative boundary length is moderately bounded it still remains to satisfy

$$\mathrm{diam}(T) \leq \frac{\mathsf{H}^2}{1 + \kappa^2} \quad \forall T \in \mathcal{T}_{\mathsf{H}}^\Gamma. \tag{2.52}$$

This consideration explains why the uniform approach in the introduction failed and a near boundary refinement process is necessary. It will turn out that there is a certain redundancy of information in the resulting boundary concentrating spaces. The method of the next chapter provides a way to compress these spaces without loss of the principal information.

[12] For sufficiently small relative curvatures $(\kappa_T \cdot \mathrm{diam}(T))$ the resolution condition can be improved in such a way that it also allows quasi uniform approaches for sufficiently small choices of H.

3

Composite Mini Elements

In this chapter we define a new mixed finite element for the Stokes equations, the *composite mini element* (CME). It decouples the minimal space dimension of the approximation space from the domain geometry. Element functions of a certain refinement level are thereby composed by elements from the classical mini element space of a finer level. Therefore we introduce two scale grids and define extension operators that map functions from the coarse part of the grid to the refined one.

3.1 Two Scale Grids

In the previous chapter, approximative subdivisions of the physical domain Ω have been used to introduce a finite element method. We required that all boundary vertices lie on Γ and that Γ is resolved. Even for large mesh widths H this may lead to a huge number of elements. We weaken the resolution condition by adapting the shape of the element functions. To this end, we need to equip the triangulations with more structure: A second parameter h (fine scale mesh width in a vicinity of the boundary) measures the boundary resolution. Let $\{\mathcal{T}_{\mathsf{H},\mathsf{h}}\}_{\mathsf{H}\geq\mathsf{h}>0}$ be a family of subdivisions of Ω into closed simplices. Any two different elements are either disjoint or share exactly either one face or one side or one vertex. Moreover, $\mathcal{T}_{\mathsf{H},\mathsf{h}}$ is supposed to fulfill the following conditions:

1. $\Omega \subseteq \Omega_{\mathsf{H},\mathsf{h}} := \operatorname{int}\Big(\bigcup_{t\in\mathcal{T}_{\mathsf{H},\mathsf{h}}} t\Big)$,
2. $t \cap \bar{\Omega} \neq \emptyset \quad \forall t \in \mathcal{T}_{\mathsf{H},\mathsf{h}}$,
3. $\operatorname{diam}(t) \leq \mathsf{H} \quad \forall t \in \mathcal{T}_{\mathsf{H},\mathsf{h}}$ and $\operatorname{diam}(t) \leq \mathsf{h} \quad \forall t \in \mathcal{T}_{\mathsf{H},\mathsf{h}} : t \cap \Gamma \neq \emptyset$.

The first condition means that $\mathcal{T}_{\mathsf{H},\mathsf{h}}$ overlaps Ω but simplices lying outside are forbidden (cf. 2.). We define shape functions depending only on a subset of nodes of $\mathcal{T}_{\mathsf{H},\mathsf{h}}$; the remaining nodes are

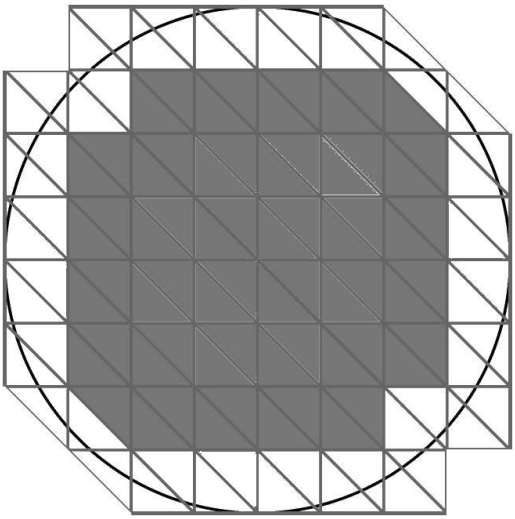

(a) Initial uniform overlapping triangulation $\mathcal{T}_H$.

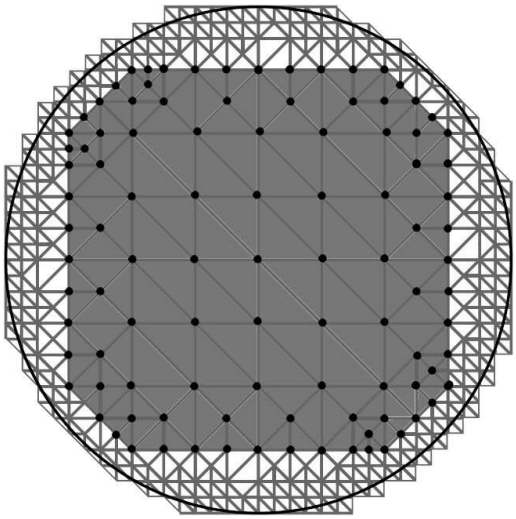

(b) Refined two scale overlapping grid $\mathcal{T}_{H,h}$ with degrees of freedom (•)

Figure 3.1: Generation of an overlapping two scale grid for the unit circle using the algorithm introduced in [Rech, 2006] and [Rech et al., 2006] respectively.

slave nodes and used to define the shape of the composite mini element functions. We split the subdivision into two parts, a possibly coarse (inner) part $\mathcal{T}_H^{\mathrm{dof}}$ and a refined (boundary) part $\mathcal{T}_{H,h}^{\Gamma}$:

$$\mathcal{T}_{H,h} = \mathcal{T}_H^{\mathrm{dof}} \cup \mathcal{T}_{H,h}^{\Gamma}.$$

Accordingly, the set of vertices $\Theta_{H,h}$ is decomposed into

$$\Theta_{H,h} = \Theta_H^{\mathrm{dof}} \cup \Theta_{H,h}^{\Gamma},$$

where Θ_H^{dof} is set of vertices of $\mathcal{T}_H^{\mathrm{dof}}$ and $\Theta_{H,h}^{\Gamma} := \Theta_{H,h} \setminus \Theta_{H,h}^{\mathrm{dof}}$. The common vertices of $\mathcal{T}_H^{\mathrm{dof}}$ and $\mathcal{T}_{H,h}^{\Gamma}$ have been put into Θ_H^{dof}, the elements of which are called *degrees of freedom*. We refer to the vertices in $\Theta_{H,h}^{\Gamma}$ as *slave nodes* since later, the values therein are defined via extension from the inner degrees of freedom toward the essential boundary conditions. So the number of unknowns is only of order $\sharp\Theta_H^{\mathrm{dof}}$, which is not correlated to any geometric resolution conditions. Convergence is measured in terms of H. For the definition of suitable extension operators we also make use of a (coarse) overlapping grid $\mathcal{T}_H$ satisfying

1. $\Omega_H := \mathrm{int}\Big(\bigcup_{T\in\mathcal{T}_H} T\Big) \supseteq \Omega_{H,h} \supseteq \Omega$,
2. $T \cap \bar{\Omega} \neq \emptyset \qquad \forall T \in \mathcal{T}_H$,
3. $\mathrm{diam}(T) \leq H \qquad \forall T \in \mathcal{T}_H$,

4. $\mathcal{T}_\mathsf{H}^{\mathrm{dof}} \subsetneq \mathcal{T}_\mathsf{H}$ and
5. $\forall T \in \mathcal{T}_\mathsf{H}^\Gamma := \mathcal{T}_\mathsf{H} \setminus \mathcal{T}_\mathsf{H}^{\mathrm{dof}}\ \exists \tilde{T} \in \mathcal{T}_\mathsf{H}^{\mathrm{dof}}\ :\ T \cap \tilde{T} \neq \emptyset$.

$\mathcal{T}_\mathsf{H}$ can be regarded as a parent grid of $\mathcal{T}_{\mathsf{H},\mathsf{h}}$ in a near boundary refinement process as illustrated in Figure 3.1. However, we allow that $\mathcal{T}_{\mathsf{H},\mathsf{h}}$ resolves Ω (cf. Figure 3.2). In such cases, a parent grid may not be available and one has to define it separately.

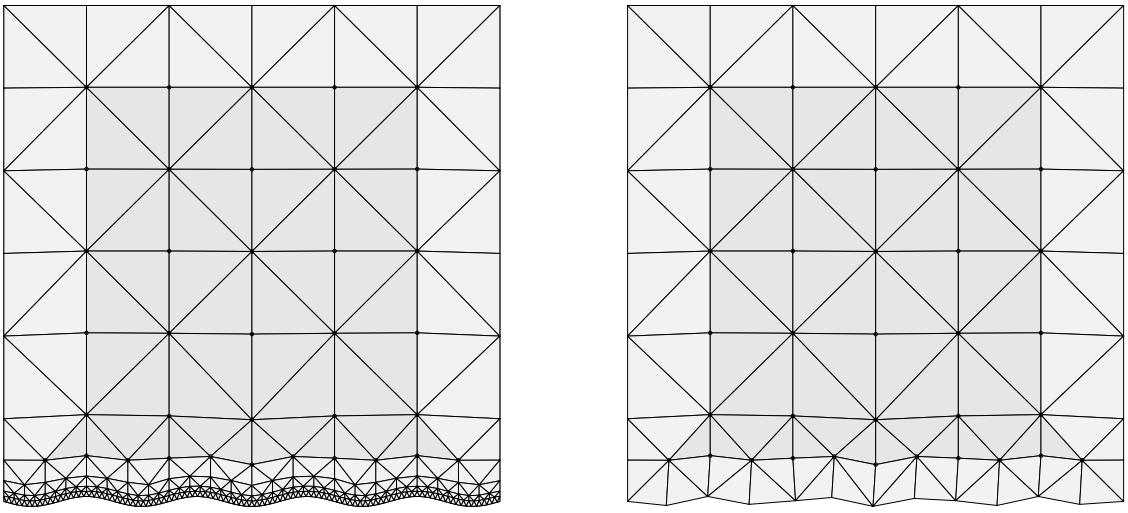

(a) Initial resolving triangulation $\mathcal{T}_{\mathsf{H},\mathsf{h}}$. The inner part with the degrees of freedom (•) is shaded darkly.

(b) Artificial coarse grid $\mathcal{T}_\mathsf{H}$. The darkly shaded inner part coincides with that of the left grid.

Figure 3.2: Two scale grid $\mathcal{T}_{\mathsf{H},\mathsf{h}}$ resolving the domain.

We will assign some more information to the grids. First, we assign a closest boundary point $\mathbf{x}^\Gamma \in \Gamma$ to every slave node $\mathbf{x} \in \Theta_{\mathsf{H},\mathsf{h}}^\Gamma$ by

$$\Theta_{\mathsf{H},\mathsf{h}}^\Gamma \ni \mathbf{x} \mapsto \mathbf{x}^\Gamma \in \arg\inf_{\mathbf{y}\in\Gamma} \operatorname{dist}(\mathbf{x},\mathbf{y})\,.$$

A similar mapping is used to define a closest inner simplex $T_\mathbf{x} \in \mathcal{T}_\mathsf{H}^{\mathrm{dof}}$ [1]:

$$\Theta_{\mathsf{H},\mathsf{h}}^\Gamma \ni \mathbf{x} \mapsto T_\mathbf{x} \in \arg\min_{T\in\mathcal{T}_\mathsf{H}^{\mathrm{dof}}} \operatorname{dist}(\mathbf{x},T)\,. \tag{3.1}$$

Both mappings are illustrated in Figure 3.3. By fixing a vertex $\mathbf{x}_t$ in every simplex $t \in \mathcal{T}_{\mathsf{H},\mathsf{h}}^\Gamma$ we can also assign an inner simplex to t:

$$\mathcal{T}_{\mathsf{H},\mathsf{h}}^\Gamma \ni t \mapsto T_t := T_{\mathbf{x}_t}\,.$$

The values of a finite element function in a slave node will depend on its values in the corresponding inner simplex. Another point of view for this construction is that the values in an inner

[1] The same can be done to define closest inner simplices for the boundary nodes $\mathbf{x} \in \Theta_\mathsf{H}^\Gamma$ of the coarse triangulation $\mathcal{T}_\mathsf{H}$. We will need this to define suitable extension of the discrete pressure functions.

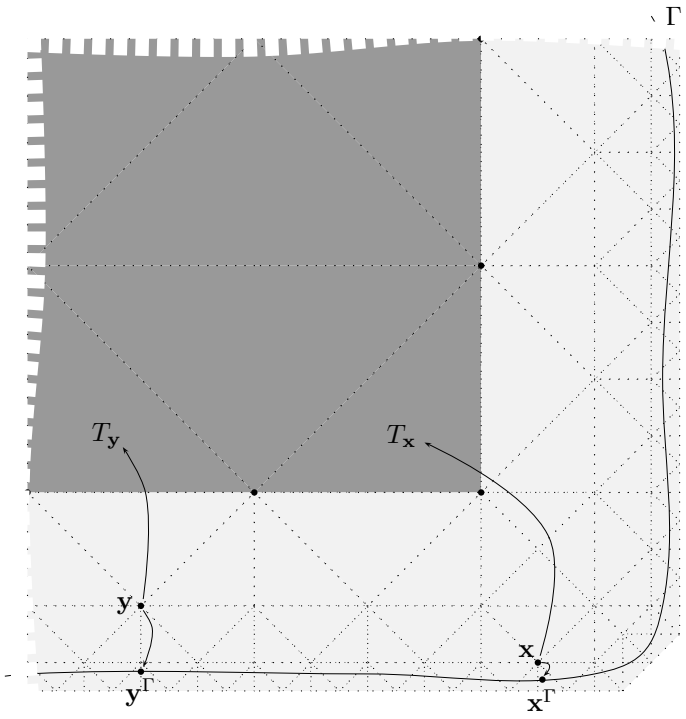

Figure 3.3: The choice of closest boundary point and closest inner triangle.

simplex T determine the values in all vertices t where T is the closest inner simplex in at least one of the vertices. For every $T \in \mathcal{T}_{\mathsf{H}}^{\mathrm{dof}}$ we define the set of slave simplices

$$\mathcal{T}^{\mathrm{T}} := \{t \in \mathcal{T}_{\mathsf{H,h}}^{\Gamma} \mid \exists \mathbf{x} \in V(t) \ : \ T_{\mathbf{x}} = T\} \subseteq \mathcal{T}_{\mathsf{H,h}}^{\Gamma}, \ ^{2}$$

where $V(T)$ denotes the set of vertices of T. We collect all the simplices of $\mathcal{T}_{\mathsf{H,h}}$ where $T_{\mathbf{x}} = T$ for all vertices $\mathbf{x} \in V(t)$ in the subset

$$\hat{\mathcal{T}}^{\mathrm{T}} := \left\{t \in \mathcal{T}^{\mathrm{T}} \mid \forall \mathbf{x} \in V(t) \ : \ T_{\mathbf{x}} = T\right\} \subseteq \mathcal{T}^{\mathrm{T}}. \ ^{2}$$

An example is depicted in Figure 3.4. If $\mathcal{T}^{\mathrm{T}} \neq \emptyset$ we call T an extension simplex.

We assume that both, the coarse mesh $\mathcal{T}_{\mathsf{H}}$ and the refined mesh $\mathcal{T}_{\mathsf{H,h}}$, are shape regular, i.e., there exists $\rho > 0$ such that

$$\rho_t := \frac{\operatorname{diam}(B_t)}{\operatorname{diam}(t)} \geq \rho \qquad \forall t \in \mathcal{T}_{\mathsf{H}} \cup \mathcal{T}_{\mathsf{H,h}}, \tag{3.2}$$

where B_t denotes the largest ball contained in t (cf. [Brenner and Scott, 1994]).

[2] Since $\mathcal{T}^{\mathrm{T}}$ and $\hat{\mathcal{T}}^{\mathrm{T}}$ are always subsets of $\mathcal{T}_{\mathsf{H,h}}^{\Gamma}$ we do not subscript the symbols by the mesh width parameters.

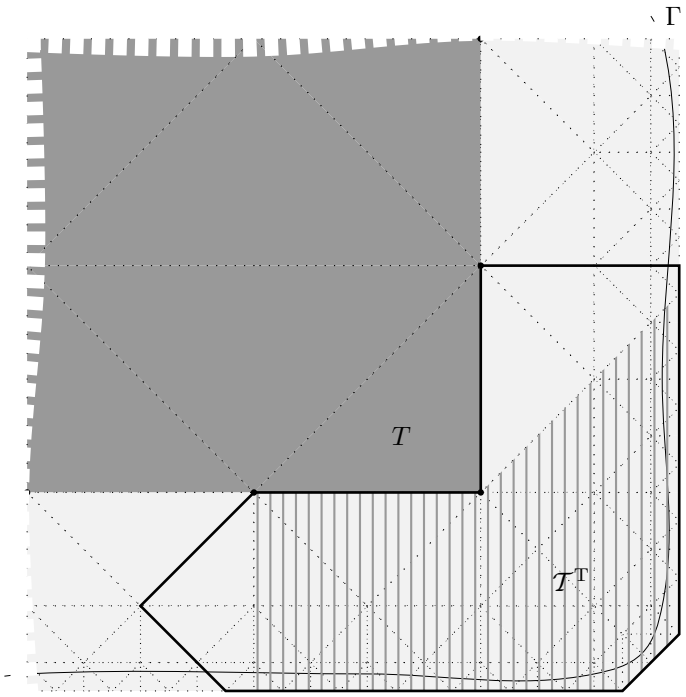

Figure 3.4: Inner triangle T with its domain of influence $\mathcal{T}^{\mathrm{T}}$ (black bordered). The hatched subset depicts $\hat{\mathcal{T}}^{\mathrm{T}}$.

Let us fix two more constants characterizing the grids $\mathcal{T}_{\mathsf{H}}$ and $\mathcal{T}_{\mathsf{H},\mathsf{h}}$. As the shape regularity they will appear in the convergence analysis. We suppose that

$$C_1^{\mathcal{T}} := \max_{t\in\mathcal{T}_{\mathsf{H},\mathsf{h}}^{\Gamma}} \frac{\operatorname{dist}(t,\Gamma)}{\operatorname{diam}(t)} \text{ and } C_2^{\mathcal{T}} := \max_{\mathbf{x}\in\Theta_{\mathsf{H},\mathsf{h}}^{\Gamma}} \frac{\operatorname{dist}(\mathbf{x},T_{\mathbf{x}})}{\operatorname{diam}(T_{\mathbf{x}})} \tag{3.3}$$

are moderately bounded. This condition is a strengthening of shape regularity in the near boundary zone. Note that, due to shape regularity, the left ratio in (3.3) changes only slightly for simplices $T \in \mathcal{T}_{\mathsf{H}}^{\mathrm{dof}}$ intersecting $\mathcal{T}_{\mathsf{H},\mathsf{h}}^{\Gamma}$, especially for the extension simplices, i.e.

$$\frac{\operatorname{dist}(T,\Gamma)}{\operatorname{diam}(T)} \leq C(C_1^{\mathcal{T}}).$$

The grids depicted in Figure 3.1 and Figure 3.2 fulfill these conditions. Moreover, the constants are moderately bounded if the algorithm introduced in [Rech et al., 2006] is employed for the mesh generation.

3.2 Extension Operators

In Section 2.2.2 we have defined spaces of functions that are continuous and piecewise affine with respect to a simplicial subdivision (cf. (2.35)). Now we consider such spline spaces on a part of a

triangulation and show how functions can be extrapolated to the whole grid. We start by giving scalar operators that are the basis for the definition of vector valued versions.

3.2.1 Scalar Operators

We define two different types of operators, simple linear extensions and extensions taking a zero boundary condition on Γ into account. In any case we start with functions u from the space $S_{\mathcal{T}_\mathsf{H}^{\mathrm{dof}}}$. Since the restriction of u to a simplex $T \in \mathcal{T}_\mathsf{H}^{\mathrm{dof}}$ is affine we can analytically extend this restriction to the whole space $\mathbb{R}^d$. So let u_T always denote the affine extension (extension by itself) of $u|_T$ to $\mathbb{R}^d$. We use this extension piecewise to define the first extension operator $\mathcal{E}_{\mathsf{H},\mathsf{h}}$ mapping functions from $S_{\mathcal{T}_\mathsf{H}^{\mathrm{dof}}}$ to $S_{\mathcal{T}_{\mathsf{H},\mathsf{h}}}$:

$$\mathcal{E}_{\mathsf{H},\mathsf{h}} : S_{\mathcal{T}_\mathsf{H}^{\mathrm{dof}}} \to S_{\mathcal{T}_{\mathsf{H},\mathsf{h}}}, \quad \big(\mathcal{E}_{\mathsf{H},\mathsf{h}} u\big)(\mathbf{x}) := \begin{cases} u(\mathbf{x}) & \mathbf{x} \in \Theta_\mathsf{H}^{\mathrm{dof}} \\ u_{T_\mathbf{x}}(\mathbf{x}) & \mathbf{x} \in \Theta_{\mathsf{H},\mathsf{h}}^{\Gamma} \end{cases} . \tag{3.4}$$

Since the image function $\mathcal{E}_{\mathsf{H},\mathsf{h}} u$ is an element of $S_{\mathcal{T}_{\mathsf{H},\mathsf{h}}}$ it is sufficient to define it pointwise in the vertices of $\mathcal{T}_{H,h}$. Thereby function values in the slave nodes are defined by extrapolation from the corresponding closest inner simplex. An example is given in Figure 3.5.

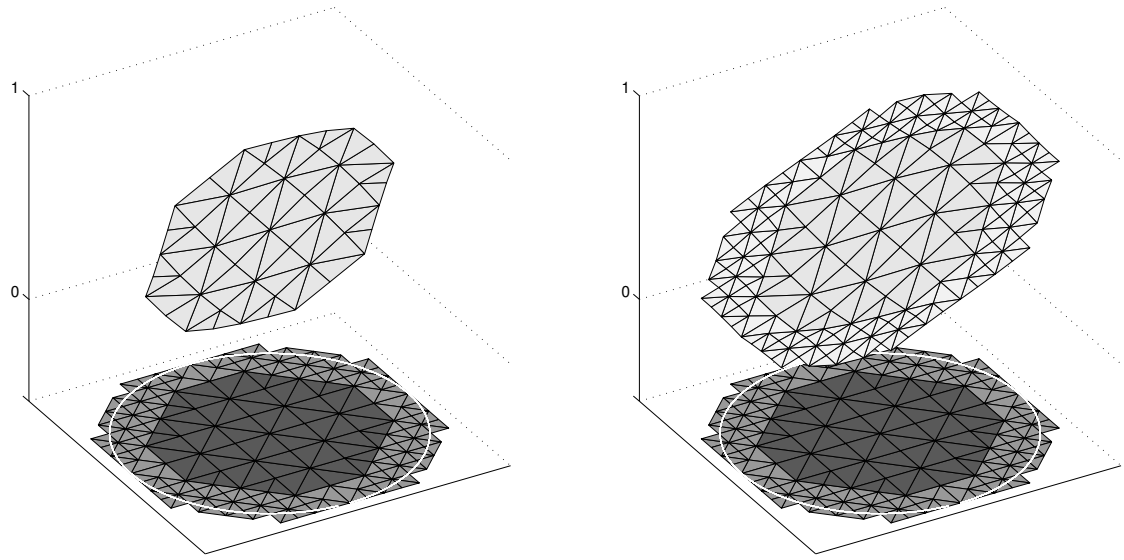

(a) $u \in S_{\mathcal{T}_\mathsf{H}^{\mathrm{dof}}}$. (b) $\mathcal{E}_{\mathsf{H},\mathsf{h}} u \in S_{\mathcal{T}_{\mathsf{H},\mathsf{h}}}$.

Figure 3.5: Extension of a scalar functions defined on $\mathcal{T}_\mathsf{H}^{\mathrm{dof}}$.

If we want the extrapolated functions to be zero on the domain boundary Γ, we have to modify the operator $\mathcal{E}_{\mathsf{H},\mathsf{h}}$. In [Rech, 2006], it is suggested to add a correction term to $\mathcal{E}_{\mathsf{H},\mathsf{h}}$ resulting in the

operator

$$\mathcal{E}^D_{\mathsf{H},\mathsf{h}} : S_{\mathcal{T}^{\mathrm{dof}}_{\mathsf{H}}} \to S_{\mathcal{T}_{\mathsf{H},\mathsf{h}}}, \quad \big(\mathcal{E}^D_{\mathsf{H},\mathsf{h}} u\big)(\mathbf{x}) := \begin{cases} u(\mathbf{x}) & \mathbf{x} \in \Theta^{\mathrm{dof}}_{\mathsf{H}} \\ u_{T_{\mathbf{x}}}(\mathbf{x}) - u_{T_{\mathbf{x}}}(\mathbf{x}^{\Gamma}) & \mathbf{x} \in \Theta^{\Gamma}_{\mathsf{H},\mathsf{h}} \end{cases}.$$

Note that $\big(\mathcal{E}^D_{\mathsf{H},\mathsf{h}} u\big)(\mathbf{x}) = 0$ if $\mathbf{x} \in \Gamma$ which is observable in Figure 3.6 and especially in Figure 3.7.

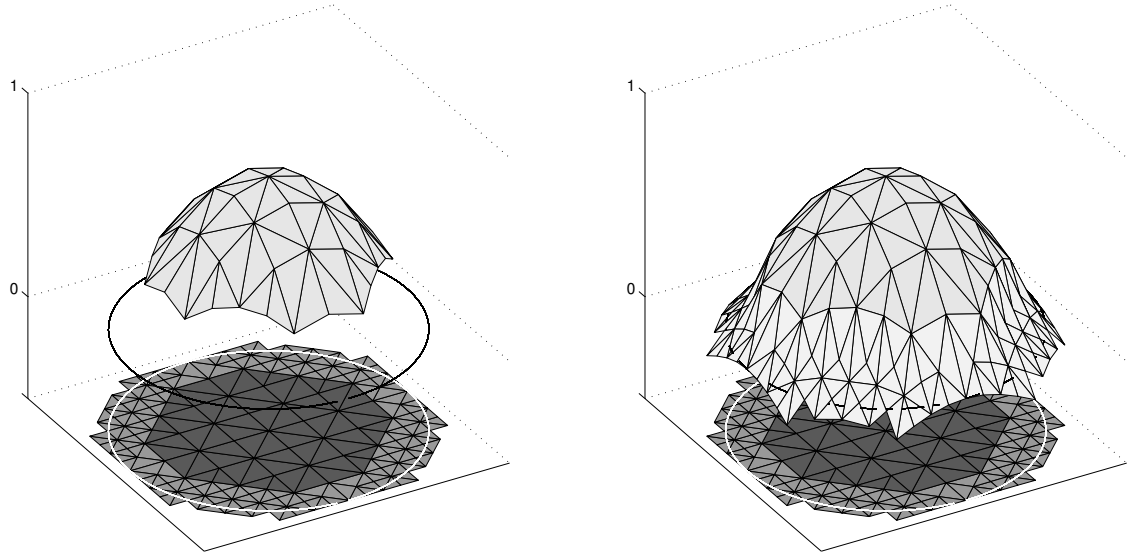

(a) $u \in S_{\mathcal{T}^{\mathrm{dof}}_{\mathsf{H}}}$. (b) $\mathcal{E}^D_{\mathsf{H},\mathsf{h}} u \in S_{\mathcal{T}_{\mathsf{H},\mathsf{h}}}$.

Figure 3.6: Extension of a scalar function defined on $\mathcal{T}^{\mathrm{dof}}_{\mathsf{H}}$ taking into account zero boundary conditions on Γ (black line).

Using the mean value theorem $\big(\mathcal{E}^D_{\mathsf{H},\mathsf{h}} u\big)(\mathbf{x})$ can be rewritten in the following form

$$\big(\mathcal{E}^D_{\mathsf{H},\mathsf{h}} u\big)(\mathbf{x}) = (\nabla u_{T_{\mathbf{x}}})(\mathbf{x} - \mathbf{x}^{\Gamma}) \quad \forall \mathbf{x} \in \Theta^{\Gamma}_{\mathsf{H},\mathsf{h}},$$

where $\nabla u_{T_{\mathbf{x}}}$ is the (constant) gradient of $u_{T_{\mathbf{x}}}$.

The operators $\mathcal{E}_{\mathsf{H},\mathsf{h}}$ and $\mathcal{E}^D_{\mathsf{H},\mathsf{h}}$ are the basis for the definition of vector valued extension operators fulfilling the Dirichlet and slip boundary conditions of the velocity. For the pressure which is free from boundary conditions, the application of $\mathcal{E}_{\mathsf{H},\mathsf{h}}$ appears to be reasonable. However, the stability of this operator in H^1 depends critically on the small scale h. The reason is that there are always simplices with diameter h in which the closest inner triangle is not the same for all vertices. This might result in steep gradients of the extrapolated function. This is the point where the coarse triangulation $\mathcal{T}_{\mathsf{H}}$ comes into play. Applying the same technique as in (3.4) on the coarse grid $\mathcal{T}_{\mathsf{H}}$ results in the operator $\mathcal{E}_{\mathsf{H}}$:

$$\mathcal{E}_{\mathsf{H}} : S_{\mathcal{T}^{\mathrm{dof}}_{\mathsf{H}}} \to S_{\mathcal{T}_{\mathsf{H}}}, \quad \big(\mathcal{E}_{\mathsf{H}} u\big)(\mathbf{x}) := \begin{cases} u(\mathbf{x}) & \mathbf{x} \in \Theta^{\mathrm{dof}}_{\mathsf{H}} \\ u_{T_{\mathbf{x}}}(\mathbf{x}) & \mathbf{x} \in \Theta^{\Gamma}_{\mathsf{H}} \end{cases}.$$

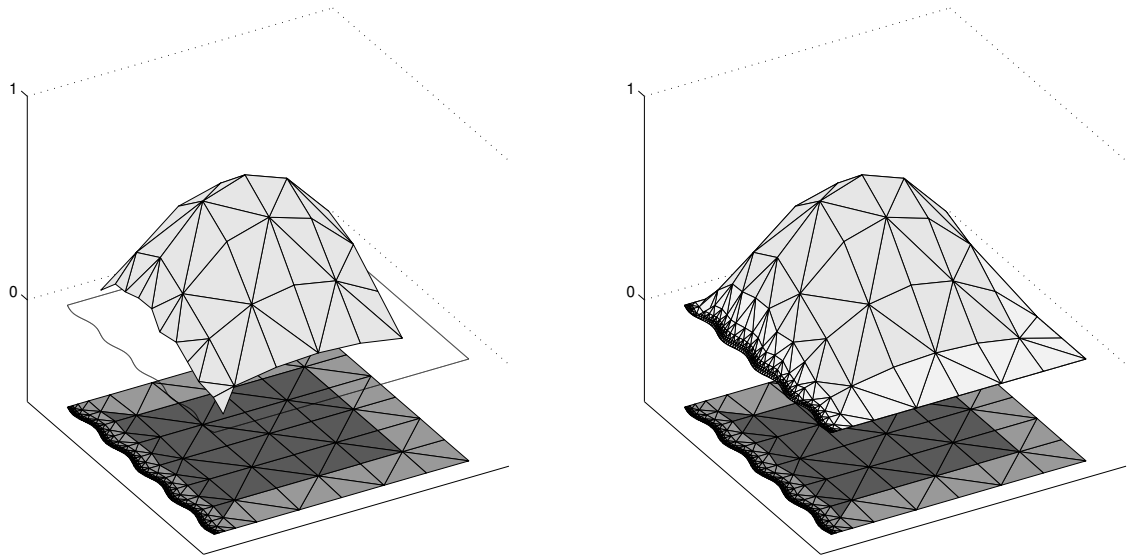

(a) $u \in S_{\mathcal{T}_\mathsf{H}^{\mathrm{dof}}}$. (b) $\mathcal{E}^D_{\mathsf{H},\mathsf{h}} u \in S_{\mathcal{T}_{\mathsf{H},\mathsf{h}}}$.

Figure 3.7: Extension of a scalar function defined on $\mathcal{T}_\mathsf{H}^{\mathrm{dof}}$ taking into account zero boundary conditions on Γ (black line).

With regard to $\Omega_{\mathsf{H},\mathsf{h}} \subseteq \Omega_\mathsf{H}$, the operator $\mathcal{E}_\mathsf{H}$ can also be interpreted as an operator that maps functions from $S_{\mathcal{T}_\mathsf{H}^{\mathrm{dof}}}$ to $S_{\mathcal{T}_{\mathsf{H},\mathsf{h}}}$. For the purpose of application in the pressure part of the space, we rename it:

$$\mathcal{E}^{\mathrm{p}}_\mathsf{H} : S_{\mathcal{T}_\mathsf{H}^{\mathrm{dof}}} \to S_{\mathcal{T}_{\mathsf{H},\mathsf{h}}},\ q \mapsto \mathcal{E}^{\mathrm{p}}_\mathsf{H} q := \mathcal{E}_\mathsf{H} q.$$

Note that, there is no h-dependence in the operator $\mathcal{E}^p_\mathsf{H}$ and, in contrast to $\mathcal{E}_{\mathsf{H},\mathsf{h}}$, there are no problems in bounding $\mathcal{E}^p_\mathsf{H}$ moderately. In Figure 3.8, it is applied in the case of the resolving grid from Figure 3.2.

3.2.2 Vector Valued Operators

In the problems under considerations, boundary conditions affect the vector valued function. Therefore we adapt the operators from the previous paragraph to this case. For Dirichlet boundary condition, this is quite simple. We just use $\mathcal{E}^D_{\mathsf{H},\mathsf{h}}$ in every component and define

$$\boldsymbol{\mathcal{E}}^{\mathrm{D}}_{\mathsf{H},\mathsf{h}} : \mathbf{S}_{\mathcal{T}_\mathsf{H}^{\mathrm{dof}}} \to \mathbf{S}_{\mathcal{T}_{\mathsf{H},\mathsf{h}}}, \quad \boldsymbol{\mathcal{E}}^{\mathrm{D}}_{\mathsf{H},\mathsf{h}}\, \mathbf{u}(\mathbf{x}) := \begin{cases} \mathbf{u}(\mathbf{x}) & \mathbf{x} \in \Theta^{\mathrm{dof}}_\mathsf{H} \\ \mathbf{u}_{T_\mathbf{x}}(\mathbf{x}) - \mathbf{u}_{T_\mathbf{x}}(\mathbf{x}^\Gamma) & \mathbf{x} \in \Theta^\Gamma_{\mathsf{H},\mathsf{h}} \end{cases}. \tag{3.5}$$

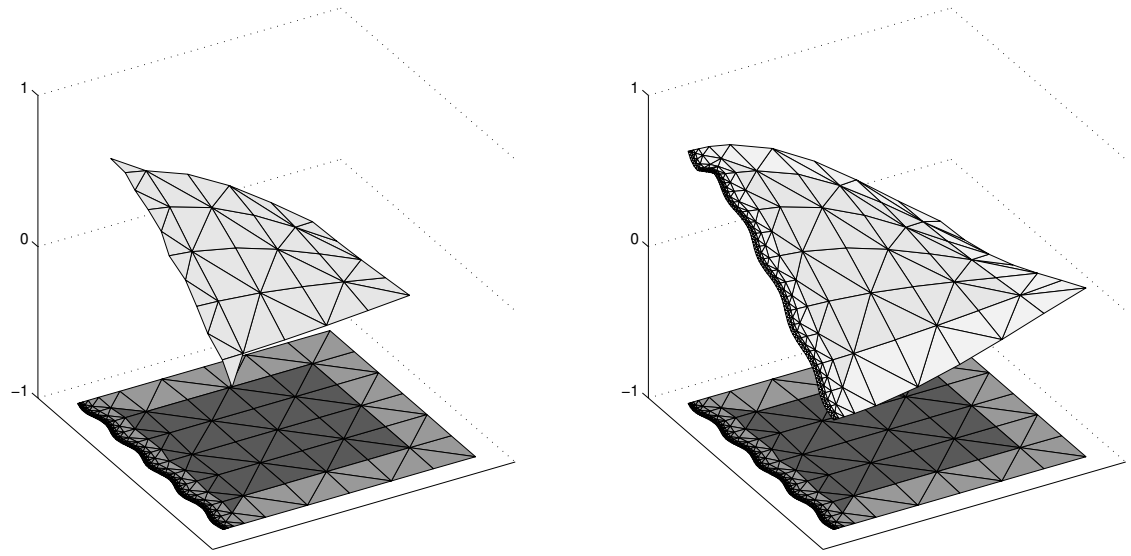

(a) $u \in S_{\mathcal{T}_\mathsf{H}^{\mathrm{dof}}}$. (b) $\mathcal{E}_\mathsf{H} u \in S_{\mathcal{T}_{\mathsf{H},\mathsf{h}}}$.

Figure 3.8: Extension of a scalar functions defined on $\mathcal{T}_\mathsf{H}^{\mathrm{dof}}$.

Equivalent formulations are given by

$$\left(\boldsymbol{\mathcal{E}}^{\mathrm{D}}_{\mathsf{H},\mathsf{h}}\,\mathbf{u}\right)(\mathbf{x}) = (\nabla \mathbf{u}_{T_\mathbf{x}})(\mathbf{x}-\mathbf{x}^\Gamma) = \begin{pmatrix} \left(\mathcal{E}^D_{\mathsf{H},\mathsf{h}} u^1\right)(\mathbf{x}) \\ \vdots \\ \left(\mathcal{E}^D_{\mathsf{H},\mathsf{h}} u^d\right)(\mathbf{x}) \end{pmatrix} \quad \forall \mathbf{x} \in \Theta^\Gamma_{\mathsf{H},\mathsf{h}},$$

where $\mathbf{u} = (u^1, \ldots, u^d)^T$ and $\nabla \mathbf{u}_{T_\mathbf{x}}$ is the (constant) Jacobian matrix of $\mathbf{u}$ on $T_\mathbf{x}$.

For slip boundary conditions, we combine $\boldsymbol{\mathcal{E}}^{\mathrm{D}}_{\mathsf{H},\mathsf{h}}$ with the vector valued version of $\mathcal{E}_{\mathsf{H},\mathsf{h}}$:

$$\boldsymbol{\mathcal{E}}_{\mathsf{H},\mathsf{h}} : \mathbf{S}_{\mathcal{T}_\mathsf{H}^{\mathrm{dof}}} \to \mathbf{S}_{\mathcal{T}_{\mathsf{H},\mathsf{h}}},\ \mathbf{u} \mapsto \boldsymbol{\mathcal{E}}_{\mathsf{H},\mathsf{h}}\,\mathbf{u} := \begin{pmatrix} \mathcal{E}_{\mathsf{H},\mathsf{h}} u^1 \\ \vdots \\ \mathcal{E}_{\mathsf{H},\mathsf{h}} u^d \end{pmatrix}.$$

$\boldsymbol{\mathcal{E}}_{\mathsf{H},\mathsf{h}}$ is used to define the tangential component of a discrete velocity field $\mathbf{u}$ while $\boldsymbol{\mathcal{E}}^{\mathrm{D}}_{\mathsf{H},\mathsf{h}}$ is responsible for the vanishing normal component. More precisely, $\boldsymbol{\mathcal{E}}^{\mathrm{s}}_{\mathsf{H},\mathsf{h}} : \mathbf{S}_{\mathcal{T}_\mathsf{H}^{\mathrm{dof}}} \to \mathbf{S}_{\mathcal{T}_{\mathsf{H},\mathsf{h}}}$ is given by

$$\boldsymbol{\mathcal{E}}^{\mathrm{s}}_{\mathsf{H},\mathsf{h}}\,\mathbf{u}(\mathbf{x}) := \begin{cases} \mathbf{u}(\mathbf{x}) & \mathbf{x} \in \Theta^{\mathrm{dof}}_\mathsf{H} \\ \left(\boldsymbol{\mathcal{E}}_{\mathsf{H},\mathsf{h}}\,\mathbf{u}\right)(\mathbf{x}) - \left(\left(\boldsymbol{\mathcal{E}}_{\mathsf{H},\mathsf{h}}\,\mathbf{u}\right)(\mathbf{x})\right)_{\boldsymbol{\nu}(\mathbf{x}^\Gamma)} + \left(\left(\boldsymbol{\mathcal{E}}^{\mathrm{D}}_{\mathsf{H},\mathsf{h}}\,\mathbf{u}\right)(\mathbf{x})\right)_{\boldsymbol{\nu}(\mathbf{x}^\Gamma)} & \mathbf{x} \in \Theta^\Gamma_{\mathsf{H},\mathsf{h}} \end{cases}, \tag{3.6}$$

where $\boldsymbol{\nu}\left(\mathbf{x}^\Gamma\right)$ denotes the outer normal of Ω at $\mathbf{x}^\Gamma$. It is well defined since we assumed the boundary to be of class C^1. If a vector is subscripted by a normal vector, we mean its normal component (cf. Footnote 2 on page 6). In Figure 3.9, an example of the use of $\boldsymbol{\mathcal{E}}^{\mathrm{s}}_{\mathsf{H},\mathsf{h}}$ is depicted. In order

to fulfill the slip boundary condition it would have been sufficient to define $\boldsymbol{\mathcal{E}}^{\mathrm{s}}_{\mathsf{H},\mathsf{h}}\,\mathbf{u}$ in $\mathbf{x} \in \Theta^{\Gamma}_{\mathsf{H},\mathsf{h}}$ without the use of $\boldsymbol{\mathcal{E}}^{\mathrm{D}}_{\mathsf{H},\mathsf{h}}$ by $\big(\boldsymbol{\mathcal{E}}_{\mathsf{H},\mathsf{h}}\,\mathbf{u}\big)(\mathbf{x}) - \big(\big(\boldsymbol{\mathcal{E}}_{\mathsf{H},\mathsf{h}}\,\mathbf{u}\big)\,(\mathbf{x})\big)_{\boldsymbol{\nu}(\mathbf{x}^{\Gamma})}$. The term related to $\boldsymbol{\mathcal{E}}^{\mathrm{D}}_{\mathsf{H},\mathsf{h}}$ in (3.6) can be regarded as a smoothing term avoiding steep gradients in the extrapolated function, especially if its tangential component is small compared to the normal one.

Finally, we mention that functions from $\mathbf{S}_{\mathcal{T}^{\mathrm{dof}}_{\mathsf{H}}}$ could easily be extended pointwise by zero, which is the simplest way to extend a function. Although the resulting functions fulfill the Dirichlet boundary condition on Γ approximately (in many cases even exactly) and though it coincides with the operator $\boldsymbol{\mathcal{E}}^{\mathrm{D}}_{\mathsf{H},\mathsf{h}}$ for constant functions, it is no alternative to $\boldsymbol{\mathcal{E}}^{\mathrm{D}}_{\mathsf{H},\mathsf{h}}$, because in general, it has worse approximation properties in the near boundary zone. But it is the right choice to extend the bubble functions $\mathbf{u} \in \mathbf{B}_{\mathcal{T}^{\mathrm{dof}}_{\mathsf{H}}}$ which, as usual, enrich our space only for purposes of stabilization:

$$\boldsymbol{\mathcal{E}}^{\mathbf{0}} : \mathbf{B}_{\mathcal{T}^{\mathrm{dof}}_{\mathsf{H}}} \to \mathbf{B}_{\mathcal{T}_{\mathsf{H},\mathsf{h}}}, \quad \mathbf{u} \mapsto \big(\boldsymbol{\mathcal{E}}^{\mathbf{0}}\mathbf{u}\big)(\mathbf{x}) := \begin{cases} \mathbf{u}(\mathbf{x}) & \mathbf{x} \in \Theta^{\mathrm{dof}}_{\mathsf{H}} \\ \mathbf{0} & \mathbf{x} \in \Theta^{\Gamma}_{\mathsf{H},\mathsf{h}} \end{cases} . \tag{3.7}$$

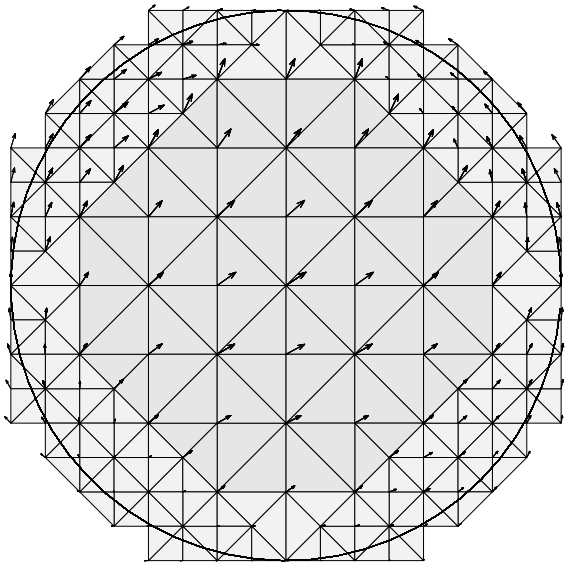

Figure 3.9: Extension of a vector field defined on $\mathcal{T}^{\mathrm{dof}}_{\mathsf{H}}$ by the operator $\boldsymbol{\mathcal{E}}^{\mathrm{s}}_{\mathsf{H},\mathsf{h}}$.

3.3 The Composite Mini Element for Dirichlet Condition

With the help of the extension operators of the previous section, we can now define the composite mini element space. It is the image of the full mini space on $\mathcal{T}^{\mathrm{dof}}_{\mathsf{H}}$ under the linear mapping $\boldsymbol{\mathcal{E}}^{\mathrm{CME_D}}$ that is composed of the extensions as in the previous section. We apply $\boldsymbol{\mathcal{E}}^{\mathrm{D}}_{\mathsf{H},\mathsf{h}}$ to the piecewise affine

part of the velocity space, $\mathcal{E}_{\mathsf{H}}^{\mathrm{p}}$ to the pressure and $\boldsymbol{\mathcal{E}}^{\mathbf{0}}$ for the bubbles:

$$\begin{aligned}\boldsymbol{\mathcal{E}}^{\mathrm{CME_D}} : \overbrace{\left(\mathbf{S}_{\mathcal{T}_{\mathsf{H}}^{\mathrm{dof}}} \oplus \mathbf{B}_{\mathcal{T}_{\mathsf{H}}^{\mathrm{dof}}}\right) \times S_{\mathcal{T}_{\mathsf{H}}^{\mathrm{dof}}}}^{\mathbf{X}^{\mathrm{mini}}_{\mathcal{T}_{\mathsf{H}}^{\mathrm{dof}}} \times \mathrm{M}^{\mathrm{mini}}_{\mathcal{T}_{\mathsf{H}}^{\mathrm{dof}}}}} &\to \overbrace{\left(\mathbf{S}_{\mathcal{T}_{\mathsf{H},\mathsf{h}}} \oplus \mathbf{B}_{\mathcal{T}_{\mathsf{H},\mathsf{h}}}\right) \times S_{\mathcal{T}_{\mathsf{H},\mathsf{h}}}}^{\mathbf{X}^{\mathrm{mini}}_{\mathcal{T}_{\mathsf{H},\mathsf{h}}} \times \mathrm{M}^{\mathrm{mini}}_{\mathcal{T}_{\mathsf{H},\mathsf{h}}}} } \\ \left(\mathbf{u}^S + \mathbf{u}^B, p\right) &\mapsto \left(\boldsymbol{\mathcal{E}}^{\mathrm{D}}_{\mathsf{H},\mathsf{h}}\, \mathbf{u}^S + \boldsymbol{\mathcal{E}}^{\mathbf{0}} \mathbf{u}^B, \mathcal{E}^{\mathrm{p}}_{\mathsf{H}} p\right).\end{aligned} \tag{3.8}$$

Here, $\mathbf{u}^S \in \mathbf{S}_{\mathcal{T}_{\mathsf{H}}^{\mathrm{dof}}}$ and $\mathbf{u}^B \in \mathbf{B}_{\mathcal{T}_{\mathsf{H}}^{\mathrm{dof}}}$. The operator $\boldsymbol{\mathcal{E}}^{\mathrm{CME_D}}$ is injective, provided $\mathcal{T}_{\mathsf{H}}^{\mathrm{dof}} \neq \emptyset$, since functions are not changed on $\mathcal{T}_{\mathsf{H}}^{\mathrm{dof}}$. If any two elements of $\left(\mathbf{S}_{\mathcal{T}_{\mathsf{H}}^{\mathrm{dof}}} \oplus \mathbf{B}_{\mathcal{T}_{\mathsf{H}}^{\mathrm{dof}}}\right) \times S_{\mathcal{T}_{\mathsf{H}}^{\mathrm{dof}}}$ are different, so are their images. The composite mini element space in the case of the Dirichlet boundary condition is defined by

$$\begin{aligned}\mathbf{X}^{\mathrm{CME_D}}_{\mathsf{H},\mathsf{h}} \times \mathrm{M}^{\mathrm{CME}}_{\mathsf{H}} &:= \boldsymbol{\mathcal{E}}^{\mathrm{CME_D}}\left(\left(\mathbf{S}_{\mathcal{T}_{\mathsf{H}}^{\mathrm{dof}}} \oplus \mathbf{B}_{\mathcal{T}_{\mathsf{H}}^{\mathrm{dof}}}\right) \times S_{\mathcal{T}_{\mathsf{H}}^{\mathrm{dof}}}\right) \\ &\subseteq \left(\mathbf{S}_{\mathcal{T}_{\mathsf{H},\mathsf{h}}} \oplus \mathbf{B}_{\mathcal{T}_{\mathsf{H},\mathsf{h}}}\right) \times S_{\mathcal{T}_{\mathsf{H},\mathsf{h}}}.\end{aligned}$$

In general, the space $\mathbf{X}^{\mathrm{CME_D}}_{\mathsf{H},\mathsf{h}}$ is nonconforming since the essential Dirichlet boundary condition is satisfied only in an approximate way. The nonconformity in the space can be controlled in an a priori resp. in an a posteriori way by the small scale parameter h of the underlying triangulation $\mathcal{T}_{\mathsf{H},\mathsf{h}}$. There are two things to note about the pressure part of the space: First, it does not depend on the small scale parameter h and, second, there is no nonconformity arising from the pressure part of the space.

Now we can define composite mini element approximations of the solution of the weak Stokes problem (2.15) as pairs $(\mathbf{u}_{\mathsf{H},\mathsf{h}}, p_{\mathsf{H}}) \in \mathbf{X}^{\mathrm{CME_D}}_{\mathsf{H},\mathsf{h}} \times \mathrm{M}^{\mathrm{CME}}_{\mathsf{H}} \cap \mathrm{L}^2_0(\Omega)$ satisfying the discrete variational system:

$$\begin{aligned} \mathfrak{a}(\mathbf{u}_{\mathsf{H},\mathsf{h}}, \mathbf{v}_{\mathsf{H},\mathsf{h}}) \;+\; \mathfrak{b}(\mathbf{v}_{\mathsf{H},\mathsf{h}}, p_{\mathsf{H}}) &= \langle \mathbf{f}, \mathbf{v}_{\mathsf{H},\mathsf{h}} \rangle_{0,\Omega} \quad \forall \mathbf{v}_{\mathsf{H},\mathsf{h}} \in \mathbf{X}^{\mathrm{CME_D}}_{\mathsf{H},\mathsf{h}}, \\ \mathfrak{b}(\mathbf{u}_{\mathsf{H},\mathsf{h}}, q_{\mathsf{H}}) &= 0 \quad \forall q_{\mathsf{H}} \in \mathrm{M}^{\mathrm{CME}}_{\mathsf{H}} \cap \mathrm{L}^2_0(\Omega). \end{aligned} \tag{3.9}$$

The bilinear forms are defined as in (2.16).

3.4 The Composite Mini Element for Slip Condition

We define an injective linear mapping $\boldsymbol{\mathcal{E}}^{\mathrm{CME_s}}$ in an analogous way as for Dirichlet boundary condition while replacing $\boldsymbol{\mathcal{E}}^{\mathrm{D}}_{\mathsf{H},\mathsf{h}}$ by $\boldsymbol{\mathcal{E}}^{\mathrm{s}}_{\mathsf{H},\mathsf{h}}$:

$$\boldsymbol{\mathcal{E}}^{\mathrm{CME_s}} : \overbrace{\left(\mathbf{S}_{\mathcal{T}_{\mathsf{H}}^{\mathrm{dof}}} \oplus \mathbf{B}_{\mathcal{T}_{\mathsf{H}}^{\mathrm{dof}}}\right) \times S_{\mathcal{T}_{\mathsf{H}}^{\mathrm{dof}}}}^{\mathbf{X}^{\mathrm{mini}}_{\mathcal{T}_{\mathsf{H}}^{\mathrm{dof}}} \times \mathrm{M}^{\mathrm{mini}}_{\mathcal{T}_{\mathsf{H}}^{\mathrm{dof}}}}} \to \overbrace{\left(\mathbf{S}_{\mathcal{T}_{\mathsf{H},\mathsf{h}}} \oplus \mathbf{B}_{\mathcal{T}_{\mathsf{H},\mathsf{h}}}\right) \times S_{\mathcal{T}_{\mathsf{H},\mathsf{h}}}}^{\mathbf{X}^{\mathrm{mini}}_{\mathcal{T}_{\mathsf{H},\mathsf{h}}} \times \mathrm{M}^{\mathrm{mini}}_{\mathcal{T}_{\mathsf{H},\mathsf{h}}}}} \tag{3.10}$$

$$\left(\mathbf{u}^S + \mathbf{u}^B, p\right) \mapsto \left(\boldsymbol{\mathcal{E}}^{\mathrm{s}}_{\mathsf{H},\mathsf{h}}\, \mathbf{u}^S + \boldsymbol{\mathcal{E}}^{\mathbf{0}} \mathbf{u}^B, \mathcal{E}^{\mathrm{p}}_{\mathsf{H}} p\right). \tag{3.11}$$

The composite mini element space in the case of the slip boundary condition is defined by

$$\begin{aligned}\mathbf{X}^{\mathrm{CME_s}}_{\mathsf{H},\mathsf{h}} \times \mathrm{M}^{\mathrm{CME}}_{\mathsf{H}} &:= \boldsymbol{\mathcal{E}}^{\mathrm{CME_s}}\left(\left(\mathbf{S}_{\mathcal{T}_{\mathsf{H}}^{\mathrm{dof}}} \oplus \mathbf{B}_{\mathcal{T}_{\mathsf{H}}^{\mathrm{dof}}}\right) \times S_{\mathcal{T}_{\mathsf{H}}^{\mathrm{dof}}}\right) \\ &\subseteq \left(\mathbf{S}_{\mathcal{T}_{\mathsf{H},\mathsf{h}}} \oplus \mathbf{B}_{\mathcal{T}_{\mathsf{H},\mathsf{h}}}\right) \times S_{\mathcal{T}_{\mathsf{H},\mathsf{h}}}.\end{aligned}$$

Again, the space $\mathbf{X}_{\mathsf{H},\mathsf{h}}^{\mathrm{CME_s}}$ is nonconforming in general since the essential slip boundary condition is satisfied only approximately. The nonconformity can be controlled by the small scale parameter h. The pressure part of the space is the same as for Dirichlet boundary.

Composite mini element approximations of the solution of the weak Stokes problem (2.20) are pairs $(\mathbf{u}_{\mathsf{H},\mathsf{h}}, p_{\mathsf{H}}) \in \mathbf{X}_{\mathsf{H},\mathsf{h}}^{\mathrm{CME_s}} \times \mathrm{M}_{\mathsf{H}}^{\mathrm{CME}} \cap \mathrm{L}_0^2(\Omega)$ which fulfill the discrete variational system:

$$\begin{array}{lll} \mathfrak{a}(\mathbf{u}_{\mathsf{H},\mathsf{h}}, \mathbf{v}_{\mathsf{H},\mathsf{h}}) \;+\; \mathfrak{b}(\mathbf{v}_{\mathsf{H},\mathsf{h}}, p_{\mathsf{H}}) & = \langle \mathbf{f}, \mathbf{v}_{\mathsf{H},\mathsf{h}} \rangle_{0,\Omega} & \forall \mathbf{v}_{\mathsf{H},\mathsf{h}} \in \mathbf{X}_{\mathsf{H},\mathsf{h}}^{\mathrm{CME_s}}, \\ \mathfrak{b}(\mathbf{u}_{\mathsf{H},\mathsf{h}}, q_{\mathsf{H}}) & = 0 & \forall q_{\mathsf{H}} \in \mathrm{M}_{\mathsf{H}}^{\mathrm{CME}} \cap \mathrm{L}_0^2(\Omega) \end{array} . \tag{3.12}$$

3.5 CME and Matrix Compression

From Chapter 2 we know that variational equations can be written as operator equations and, moreover, that they can be represented by linear systems in the coefficients of the basis representation of the solution if they are discrete. If we apply the techniques of Section 2.1.3 and 2.1.5 to the full mini element space $\mathbf{X}_{\mathcal{T}_{\mathsf{H},\mathsf{h}}}^{\mathrm{mini}} \times \mathrm{M}_{\mathcal{T}_{\mathsf{H},\mathsf{h}}}^{\mathrm{mini}}$ on $\mathcal{T}_{\mathsf{H},\mathsf{h}}$ we obtain the linear equation

$$\underbrace{\begin{bmatrix} \mathfrak{A} & \mathfrak{B} & \mathbf{0} \\ \mathfrak{B}^* & \mathbf{0} & \mathfrak{C} \\ \mathbf{0} & \mathfrak{C}^* & 0 \end{bmatrix}}_{\mathfrak{G}^{\mathrm{mini}}} \begin{bmatrix} \mathbf{u} \\ p \\ \lambda \end{bmatrix} = \begin{bmatrix} \mathbf{f} \\ \mathbf{0} \\ 0 \end{bmatrix}, \tag{3.13}$$

where the linear operators $\mathfrak{A} : \mathbf{X}_{\mathcal{T}_{\mathsf{H},\mathsf{h}}}^{\mathrm{mini}} \to \mathbf{X}_{\mathcal{T}_{\mathsf{H},\mathsf{h}}}^{\mathrm{mini}}$, $\mathfrak{B} : \mathrm{M}_{\mathcal{T}_{\mathsf{H},\mathsf{h}}}^{\mathrm{mini}} \to \mathbf{X}_{\mathcal{T}_{\mathsf{H},\mathsf{h}}}^{\mathrm{mini}}$ and $\mathfrak{C} : \mathrm{M}_{\mathcal{T}_{\mathsf{H},\mathsf{h}}}^{\mathrm{mini}} \to \mathbb{R}$ are given by

$$\begin{aligned} \langle \mathbf{u}, \mathfrak{A}\mathbf{v} \rangle_{\mathbf{H}^1(\Omega)} &:= \mathfrak{a}(\mathbf{u}, \mathbf{v}), \quad \mathbf{u}, \mathbf{v} \in \mathbf{X}_{\mathcal{T}_{\mathsf{H},\mathsf{h}}}^{\mathrm{mini}}, \\ \langle \mathbf{u}, \mathfrak{B}p \rangle_{\mathbf{H}^1(\Omega)} &:= \mathfrak{b}(\mathbf{u}, p), \quad \mathbf{u} \in \mathbf{X}_{\mathcal{T}_{\mathsf{H},\mathsf{h}}}^{\mathrm{mini}},\ p \in \mathrm{M}_{\mathcal{T}_{\mathsf{H},\mathsf{h}}}^{\mathrm{mini}}, \\ \langle \lambda, \mathfrak{C}q \rangle_{\mathrm{L}^2(\Omega)} &:= \mathfrak{c}(\lambda, q), \quad \lambda \in \mathbb{R},\ q \in \mathrm{M}_{\mathcal{T}_{\mathsf{H},\mathsf{h}}}^{\mathrm{mini}}. \end{aligned} \tag{3.14}$$

In general, (3.13) does not have a unique solution since no boundary condition was taken into account. But this system is the starting point for deriving formulations of the composite mini element systems. It turns out that the discrete variational equations (3.9) and (3.12) can be written in the form

$$\left[\boldsymbol{\mathcal{E}}^* \mathfrak{G}^{\mathrm{mini}} \boldsymbol{\mathcal{E}}\right] \begin{bmatrix} \mathbf{u}_{\mathsf{H},\mathsf{h}} \\ p_{\mathsf{H}} \\ \lambda \end{bmatrix} = \left[\boldsymbol{\mathcal{E}}^*\right] \begin{bmatrix} \mathbf{f} \\ \mathbf{0} \\ 0 \end{bmatrix}, \tag{3.15}$$

where $\boldsymbol{\mathcal{E}}$ is the slight modification of the extension operators $\boldsymbol{\mathcal{E}}^{\mathrm{CME_D}}$ resp. $\boldsymbol{\mathcal{E}}^{\mathrm{CME_s}}$ by mapping the multiplier identically. We justify (3.15) on an abstract level: Let D be real a Hilbert space, $\mathfrak{d}$ a bilinear form on $\mathrm{D} \times \mathrm{D}$. Related to $\mathfrak{d}$ we can define an operator $\mathfrak{D} : \mathrm{D} \to \mathrm{D}'$ by

$$\langle u, \mathfrak{D}v \rangle_{\mathrm{D}} = \mathfrak{d}(u, v) \quad \forall u, v \in \mathrm{D}. \tag{3.16}$$

Let $\tilde{\mathrm{D}}$ be a Hilbert space and $\mathcal{E} : \tilde{\mathrm{D}} \to \mathrm{D}$ be a linear operator. We are interested in solutions $u \in \mathcal{E}(\mathrm{D})$ of the variational system

$$\mathfrak{d}(u, v) = \langle f, v \rangle_{\mathrm{D}} \quad \forall v \in \mathcal{E}(\mathrm{D}), \tag{3.17}$$

where f is a linear form on D. We reformulate this as an operator equation. With the help of (3.16) we get

$$\mathfrak{d}(\mathcal{E}\tilde{u}, \mathcal{E}\tilde{v}) = \langle \mathcal{E}\tilde{u}, \mathfrak{D}\mathcal{E}\tilde{v}\rangle_{\mathrm{D}} = \langle \tilde{u}, \mathcal{E}^*\mathfrak{D}\mathcal{E}\tilde{v}\rangle_{\tilde{\mathrm{D}}} \quad \forall \tilde{u}, \tilde{v} \in \tilde{\mathrm{D}}, \tag{3.18}$$

where $\mathcal{E}^* : \mathrm{D}' \to \tilde{\mathrm{D}}'$ denotes the adjoint operator to $\mathcal{E}$. The right-hand side of (3.17) can be written as follows

$$\langle f, \mathcal{E}\tilde{v}\rangle_{\mathrm{D}} = \langle \mathcal{E}^* f, \tilde{v}\rangle_{\tilde{\mathrm{D}}} \quad \forall \tilde{v} \in \tilde{\mathrm{D}}. \tag{3.19}$$

So (3.17) can be formulated as a linear operator equation on the space $\tilde{\mathrm{D}}$:

$$\mathcal{E}^*\mathfrak{D}\mathcal{E}\tilde{u} = f. \tag{3.20}$$

This proves (3.15).
For a matrix version of (3.15) we employ the basis of $\mathbf{X}^{\mathrm{mini}}_{\mathcal{T}_{\mathsf{H},\mathsf{h}}} \times \mathrm{M}^{\mathrm{mini}}_{\mathcal{T}_{\mathsf{H},\mathsf{h}}}$ made up of hat and bubble functions (cf. (2.36) and (2.37))

$$\Bigg(\Big(\underbrace{\{\boldsymbol{\lambda}_i\}_{i=1}^{d\cdot\sharp\Theta_{\mathsf{H}}^{\mathrm{dof}}} \cup \{\boldsymbol{\psi}_j\}_{j=1}^{d\cdot\sharp\mathcal{T}_{\mathsf{H}}^{\mathrm{dof}}}}_{=:\{\mathbf{v}_l\}_{l=1}^{n}}\Big) \times \{0\}\Bigg) \cup \Bigg(\{\mathbf{0}\} \times \underbrace{\{\lambda_k\}_{k=1}^{\sharp\Theta_{\mathsf{H}}^{\mathrm{dof}}}}_{\{q_k\}_{k=1}^{m}}\Bigg).$$

We obtain the equivalent linear system

$$\left[\mathbf{S}^{\mathrm{CME_D}}\right] \begin{bmatrix} \mathbf{u}_{\mathsf{H},\mathsf{h}} \\ p_{\mathsf{H}} \\ \lambda \end{bmatrix} = \begin{bmatrix} \tilde{\mathbf{f}} \\ \mathbf{0} \\ 0 \end{bmatrix}. \tag{3.21}$$

Figure 3.10 gives a more detailed visualization of (3.21). All appearing matrices (dotted) are sparse. This is well known for $\mathbf{S}^{\mathrm{mini}}$, but also true for the extension matrices where at most three entries per line are nonzero, and transmitted to the composite mini element system matrix $\mathbf{S}^{\mathrm{CME_D}}$. Moreover, there are additional substructures hidden in the matrices, which we do not want to describe in detail here. For an implementation of the method it is of course not necessary to compute the global matrices. The whole assembly process can be localized to element matrix computations as usual in finite element methods. This is described in detail in [Rech, 2006]. The computational effort for calculating the composite system matrix is comparable to that of the mini element, but the storage requirement and the effort for solving the system can be much smaller. The next chapter shows that the error is hardly affected by this reduction. The extension strategy reduces the dimension of the original full mini matrix, which is comparable to the system matrix $\mathbf{S}^{\mathrm{mini_D}}$ of the mini element taking the Dirichlet boundary condition into account. In the case where $\mathcal{T}_{\mathsf{H},\mathsf{h}}$ resolves the domain, $\mathbf{S}^{\mathrm{CME_D}}$ can even be viewed as a compression of $\mathbf{S}^{\mathrm{mini_D}}$, since $\mathbf{X}^{\mathrm{CME_D}}_{\mathsf{H},\mathsf{h}} \subseteq \mathbf{X}^{\mathrm{mini_D}}_{\mathsf{H}}$.

All results of this section can be applied to the slip condition in an analog way by simply replacing $\boldsymbol{\mathcal{E}}^{\mathrm{D}}_{\mathsf{H},\mathsf{h}}$ by $\boldsymbol{\mathcal{E}}^{\mathrm{s}}_{\mathsf{H},\mathsf{h}}$.

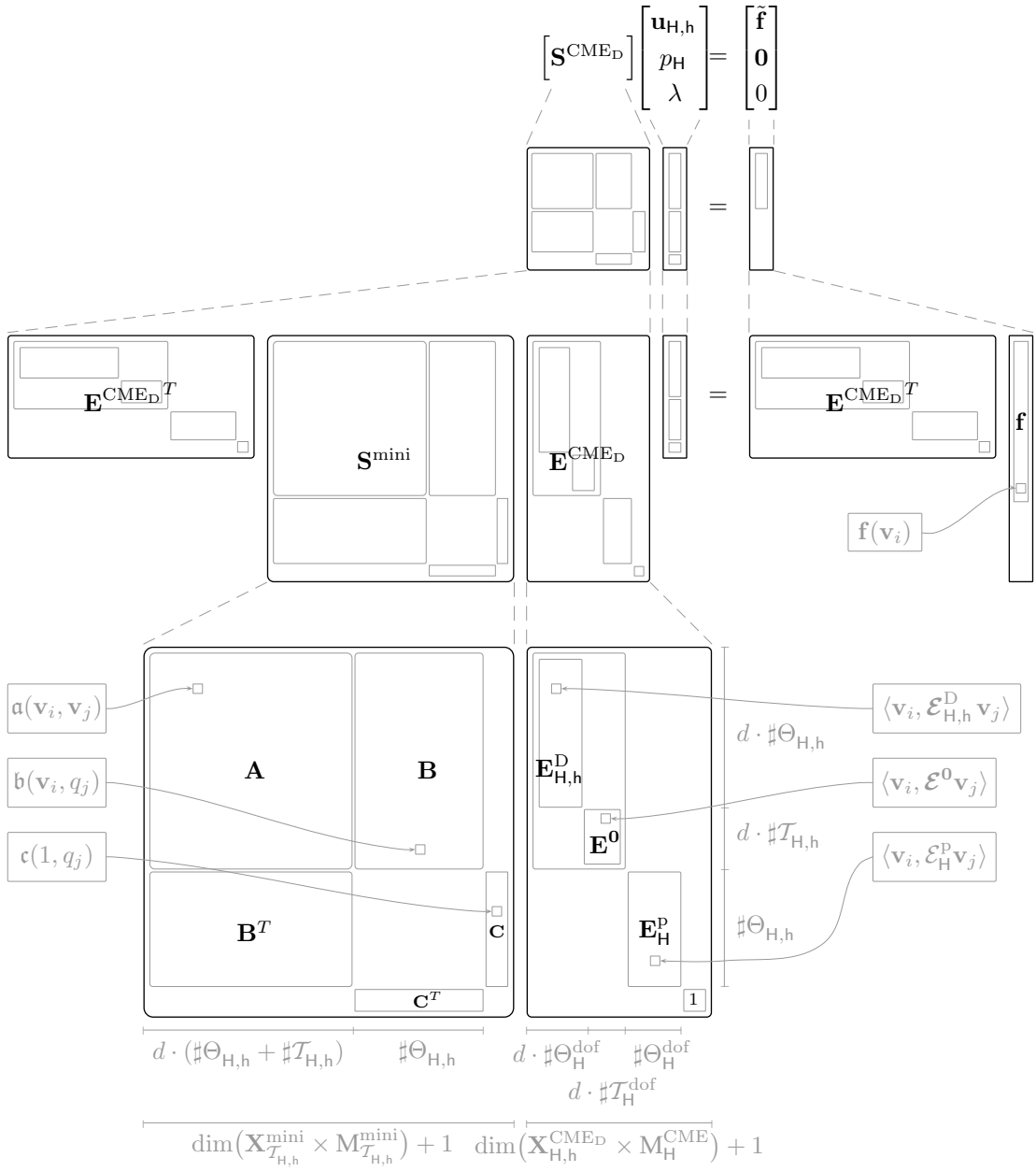

Figure 3.10: Structure of the composite mini element linear system (3.21). All appearing matrix blocks have a sparse structure, empty parts represent zero blocks. The gray shaded terms provide information on matrix entries and dimension.

4

Convergence Analysis

In this chapter we will present the main theorem on the convergence of the composite mini element method. We apply the theory presented in 2.2.1. The main steps are the investigation of the approximation properties and stability. The results are based on the interpolation error estimates which will be derived in Section 4.1.

4.1 Interpolation and Extrapolation Estimates

The convergence analysis makes use of the existence of an appropriate extension operator for the given domain Ω. It is known that, if Ω is bounded and Lipschitz, there exists a continuous, linear extension operator $\mathfrak{E} : \mathrm{H}^k(\Omega) \to \mathrm{H}^k(\mathbb{R}^d)$, $k \in \mathbb{N}_0$, such that

$$\forall u \in \mathrm{H}^k(\Omega): \quad \mathfrak{E}u|_\Omega = u \ \text{ and } \ \|\mathfrak{E}u\|_{\mathrm{H}^k(\mathbb{R}^d)} \leq C_{\mathrm{ext}} \|u\|_{\mathrm{H}^k(\Omega)}, \tag{4.1}$$

with a constant C_{ext} depending only on k and Ω (cf. [Stein, 1970]). It is worth noting that for domains containing a large number of holes and a possibly rough outer boundary, there exists an extension operator with moderately small norm C_{ext} under mild assumptions on the geometry. For all details including the characterization of the class of domain geometries, we refer to [Sauter and Warnke, 1999]. In the following we always identify a function $u \in \mathrm{H}^k(\Omega)$ with its minimal extension $\mathfrak{E}u$ without mentioning this explicitly.

To get an optimal convergence result, we show that $\mathbf{H}^1_{\mathrm{D}}(\Omega)$- and $\mathbf{H}^1_{\mathrm{s}}(\Omega)$- functions can be approximated by the velocity part of the composite mini space in a way that can be controlled by the large scale parameter H. Usually, a piecewise affine interpolant $\mathcal{I}_{\mathcal{T}_{\mathsf{H},\mathsf{h}}}$ with respect to the grid $\mathcal{T}_{\mathsf{H},\mathsf{h}}$ is used to prove this property. However, this is not possible in our situation because the simplices in $\mathcal{T}^{\Gamma}_{\mathsf{H},\mathsf{h}}$ do not contain degrees of freedom. We use the extensions of the affine interpolants $\mathcal{I}_{\mathcal{T}^{\mathrm{dof}}_{\mathsf{H}}}$ on the inner grid $\mathcal{T}^{\mathrm{dof}}_{\mathsf{H}}$ instead. That is why we get error estimates in terms of H, even on the fine part of the grid. The small scale h is necessary to control the non-conformity in the velocity space.

One problem is that standard interpolation error estimates can be applied only inside the underlying triangulation that is $\mathcal{T}^{\mathrm{dof}}_{\mathsf{H}}$ in our case. However, we are interested in the error in Ω.

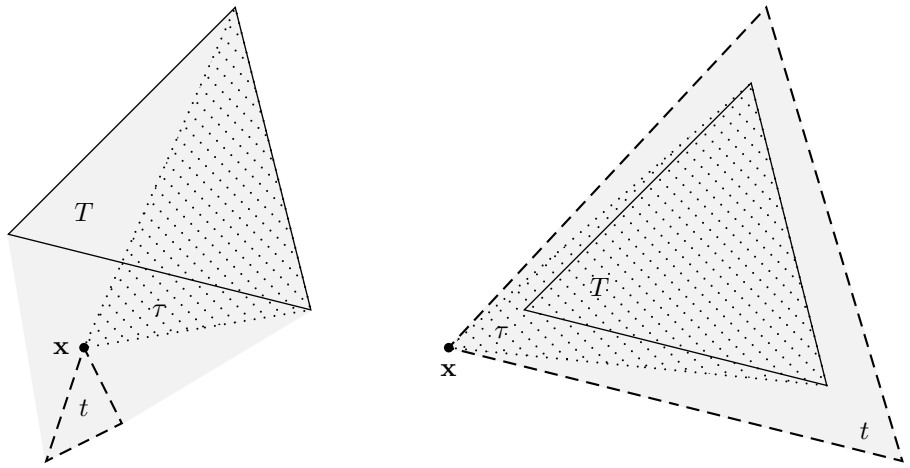

(a) $t \cap T = \emptyset$, $C_{\mathrm{dist}} \approx C_{\mathrm{size}} \approx \frac{1}{3}$, $t, T \subsetneq \mathrm{conv}(T \cup t)$

(b) $T \subseteq t$, $C_{\mathrm{dist}} = 0$, $C_{\mathrm{size}} \approx \frac{3}{2}$, $\mathrm{conv}(T \cup t) = t$

Figure 4.1: Two typical situations for the simplices t and T from Lemma 4.1.

It is well known (cf. [Ciarlet, 1978, Theorem 16.1]) that, for an arbitrary simplex $T \subseteq \mathbb{R}^d$ with regularity constant ρ_T, there exists a constant $C_{\mathrm{int}} = C_{\mathrm{int}}(m, p, d)$ such that

$$\left|u - \mathcal{I}_{\mathrm{T}} u\right|_{m,p,T} \leq \frac{C_{\mathrm{int}}}{\rho_T^m} \operatorname{diam}(T)^{\left(2 - \frac{d}{2} + \frac{d}{p} - m\right)} \left|u\right|_{2,T} \qquad \forall u \in \mathrm{H}^2(T), \tag{4.2}$$

where $m \in \{0, 1\}$ and $1 \leq p \leq \infty$, provided $\mathrm{W}_p^m(\Omega) \subseteq \mathrm{H}^2(\Omega)$ [1]. $\mathcal{I}_{\mathrm{T}} u \in \mathbb{P}_1(\mathbb{R}^d)$ denotes the linear interpolant of u in the vertices of T. The subsequent lemma analyzes the approximation quality of $\mathcal{I}_{\mathrm{T}} u$ in a neighborhood of the convex hull of the interpolation points, i.e. outside of T.

Lemma 4.1 (Neighborhood property)
Let T be an arbitrary simplex with regularity constant ρ_T, t be an arbitrary simplex with regularity constant ρ_t. Let the ratio of the diameters of t and T be denoted by C_{size} and the distance between T and t relative to the size of T by C_{dist}, i.e.

$$C_{\mathrm{size}} := \frac{\operatorname{diam}(t)}{\operatorname{diam}(T)} \quad \textit{and} \quad C_{\mathrm{dist}} := \frac{\operatorname{dist}(t, T)}{\operatorname{diam}(T)}.$$

Furthermore let $u \in H^2(\mathrm{conv}(T \cup t))$ and let $\mathcal{I}_{\mathrm{T}} u \in \mathbb{P}_1(\mathbb{R}^d)$ denote the affine interpolation of u at the vertices of T. Then, for $m \in \{0, 1\}$ and $1 \leq p \leq \infty$, provided $W_p^m(\Omega) \subseteq H^2(\Omega)$, there exists a constant $C = C(C_{\mathrm{int}}, d, C_{\mathrm{size}}, C_{\mathrm{dist}}) > 0$ such that

$$\left|u - \mathcal{I}_{\mathrm{T}} u\right|_{m,p,t} \leq \frac{C}{\rho_t^m \rho_T^{\left(1 + \frac{d}{2}\right)}} \operatorname{diam}(T)^{\left(2 - \frac{d}{2}\right)} \operatorname{diam}(t)^{\left(\frac{d}{p} - m\right)} \left|u\right|_{2,\mathrm{conv}\left(T \cup t\right)},$$

[1] The condition $\mathrm{W}_p^m(\Omega) \subseteq \mathrm{H}^2(\Omega)$ restricts the choices of m and p depending on the dimension d. The combinations of m and p that will be useful later ($(m, p) = (0, 2), (0, \infty), (1, 2)$) are allowed in two as well as three dimensions.

where $\operatorname{conv}(T \cup t)$ *denotes the convex hull of* $T \cup t$.

Proof. Let $\mathcal{I}_{\mathrm{t}} u \in \mathbb{P}_1(\mathbb{R}^d)$ denote the affine interpolation of u at the vertices of t. We define $\mathsf{h}_t := \operatorname{diam}(t)$ and $\mathsf{h}_T := \operatorname{diam}(T)$. The use of triangle inequality, (4.2), and the inverse estimate (which is valid for $m \in \{0,1\}$ and all $p \in \mathbb{N} \cup \{\infty\}$)

$$\big|q\big|_{m,p,t} \leq \left(\frac{2}{\rho_t}\right)^m \mathsf{h}_t^{\left(\frac{d}{p}-m\right)} \big\|q\big\|_{0,\infty,t} \quad \forall q \in \mathbb{P}_1(\mathbb{R}^d) \tag{4.3}$$

lead to

$$\begin{aligned} \big|u - \mathcal{I}_{\mathrm{T}} u\big|_{m,p,t} &\leq \big|u - \mathcal{I}_{\mathrm{t}} u\big|_{m,p,t} + \big|\mathcal{I}_{\mathrm{t}} u - \mathcal{I}_{\mathrm{T}} u\big|_{m,p,t} \\ &\leq \frac{C_{\mathrm{int}}}{\rho_t^m}\, \mathsf{h}_t^{\left(2-\frac{d}{2}+\frac{d}{p}-m\right)} \big|u\big|_{2,t} + \left(\frac{2}{\rho_t}\right)^m \mathsf{h}_t^{\left(\frac{d}{p}-m\right)} \big\|\mathcal{I}_{\mathrm{t}} u - \mathcal{I}_{\mathrm{T}} u\big\|_{0,\infty,t}. \end{aligned} \tag{4.4}$$

Note that $\big\|\mathcal{I}_{\mathrm{t}} u - \mathcal{I}_{\mathrm{T}} u\big\|_{0,\infty,t} = \max_{\mathbf{x} \in V(t)} \big|\mathcal{I}_{\mathrm{t}} u(\mathbf{x}) - \mathcal{I}_{\mathrm{T}} u(\mathbf{x})\big|$. Before we can estimate $\big\|\mathcal{I}_{\mathrm{t}} u - \mathcal{I}_{\mathrm{T}} u\big\|_{0,\infty,t}$ or $\big|\mathcal{I}_{\mathrm{t}} u(\mathbf{x}) - \mathcal{I}_{\mathrm{T}} u(\mathbf{x})\big|$ for a vertex $\mathbf{x} \in V(t)$, we have to investigate the set

$$\Lambda_{\mathbf{x}} := \big\{\tau \mid \tau \text{ is a simplex, } \mathbf{x} \in V(\tau) \subseteq (V(T) \cup \{\mathbf{x}\})\big\}$$

containing $(d+1)$ simplices. There is at least one $\tau \in \Lambda_{\mathbf{x}}$ that fulfills $\big|\tau \cap T\big| \geq \frac{1}{d+1}\big|T\big|$. Obviously, its diameter is bounded by $(1 + C_{\mathrm{dist}} + C_{\mathrm{size}})\mathsf{h}_T$. Since $\tau \cap T$ is a simplex, we can use HERON's formula to derive

$$\operatorname{diam}(B_\tau) \geq \operatorname{diam}(B_{\tau\cap T}) = \frac{d\big|\tau \cap T\big|}{\big|\partial(\tau \cap T)\big|} \geq \frac{1}{d+1}\frac{d\big|T\big|}{\big|\partial T\big|} = \frac{1}{d+1}\operatorname{diam}(B_T)$$

and therefore $\rho_\tau \geq \dfrac{1}{d+1}\dfrac{\mathsf{h}_T}{\operatorname{diam}(\tau)} \geq \dfrac{\rho_T}{(d+1)(1 + C_{\mathrm{dist}} + C_{\mathrm{size}})}$. According to $\mathbf{x} \in V(t)$, we can choose a simplex τ with the following properties (see also Figure 4.1):

1. $\mathbf{x} \in V(\tau) \subseteq (V(T) \cup \{\mathbf{x}\})$, $\tau \subseteq \operatorname{conv}(T \cup \{\mathbf{x}\})$, $\operatorname{diam}(\tau) \leq (1 + C_{\mathrm{dist}} + C_{\mathrm{size}})\mathsf{h}_T$,

2. $\big|\tau \cap T\big| \geq \frac{1}{d+1}\big|T\big|$ and

3. $\rho_\tau \geq \dfrac{\rho_T}{(d+1)(1 + C_{\mathrm{dist}} + C_{\mathrm{size}})}$.

With $\mathbf{y} \in (V(\tau) \cap V(T))$ we get

$$\begin{aligned}
\left|\mathcal{I}_{\mathrm{t}} u(\mathbf{x}) - \mathcal{I}_{\mathrm{T}} u(\mathbf{x})\right| &= \left|\mathcal{I}_\tau u(\mathbf{x}) - \mathcal{I}_{\mathrm{T}} u(\mathbf{x})\right| \\
&= \left|\mathcal{I}_\tau u(\mathbf{y}) - \mathcal{I}_{\mathrm{T}} u(\mathbf{y}) + \nabla\left(\mathcal{I}_\tau u - \mathcal{I}_{\mathrm{T}} u\right) \cdot (\mathbf{x} - \mathbf{y})\right| \\
&\leq \left|\nabla\left(\mathcal{I}_\tau u - \mathcal{I}_{\mathrm{T}} u\right)\right| \operatorname{diam}(\tau) \\
&\leq \left(\frac{1 + C_{\mathrm{dist}} + C_{\mathrm{size}}}{\rho_T^{\frac{d}{2}}}\right) \left|\nabla\left(\mathcal{I}_\tau u - \mathcal{I}_{\mathrm{T}} u\right)\right| |T|^{\frac{1}{2}} \mathsf{h}_T^{\left(1-\frac{d}{2}\right)} \\
&\leq \left(\sqrt{d+1} \frac{1 + C_{\mathrm{dist}} + C_{\mathrm{size}}}{\rho_T^{\frac{d}{2}}}\right) \mathsf{h}_T^{\left(1-\frac{d}{2}\right)} \left|\mathcal{I}_\tau u - \mathcal{I}_{\mathrm{T}} u\right|_{1, T \cap \tau} \\
&\leq \left(\sqrt{d+1} \frac{1 + C_{\mathrm{dist}} + C_{\mathrm{size}}}{\rho_T^{\frac{d}{2}}}\right) \mathsf{h}_T^{\left(1-\frac{d}{2}\right)} \left(\left|\mathcal{I}_\tau u - u\right|_{1,\tau} + \left|u - \mathcal{I}_{\mathrm{T}} u\right|_{1,T}\right) \\
&\leq \left(\sqrt{d+1} C_{\mathrm{int}} \frac{1 + C_{\mathrm{dist}} + C_{\mathrm{size}}}{\rho_T^{\frac{d}{2}}}\right) \mathsf{h}_T^{\left(1-\frac{d}{2}\right)} \left(\frac{\operatorname{diam}(\tau)}{\rho_\tau} + \frac{\mathsf{h}_T}{\rho_T}\right) |u|_{2, \operatorname{conv}\left(T \cup \tau\right)} \\
&\leq \left(2 C_{\mathrm{int}} \frac{(d+1)^{\frac{3}{2}} (1 + C_{\mathrm{dist}} + C_{\mathrm{size}})^3}{\rho_T^{\left(1+\frac{d}{2}\right)}}\right) \mathsf{h}_T^{\left(2-\frac{d}{2}\right)} |u|_{2, \operatorname{conv}\left(T \cup t\right)}. \qquad (4.5)
\end{aligned}$$

We plug this result into (4.4) to bound $\left|u - \mathcal{I}_{\mathrm{T}} u\right|_{m,p,t}$ by

$$\frac{4 C_{\mathrm{int}}\, \mathsf{h}_t^{\left(\frac{d}{p} - m\right)}}{\rho_t^m} \left(\mathsf{h}_T^{\left(2-\frac{d}{2}\right)} + \frac{2(d+1)^{\frac{3}{2}} (1 + C_{\mathrm{dist}} + C_{\mathrm{size}})^3}{\rho_T^{\left(1+\frac{d}{2}\right)}}\, \mathsf{h}_T^{\left(2-\frac{d}{2}\right)}\right) |u|_{2, \operatorname{conv}\left(T \cup t\right)}$$

leading to the final estimate

$$\left|u - \mathcal{I}_{\mathrm{T}} u\right|_{m,p,t} \leq \frac{4(d+1)^{\frac{3}{2}} C_{\mathrm{int}}}{\rho_t^m \rho_T^{\left(1+\frac{d}{2}\right)}} \left(C_{\mathrm{size}}^{\left(2-\frac{d}{2}\right)} + (1 + C_{\mathrm{dist}} + C_{\mathrm{size}})^3\right) \mathsf{h}_t^{\left(\frac{d}{p} - m\right)} \mathsf{h}_T^{\left(2-\frac{d}{2}\right)} |u|_{2, \operatorname{conv}\left(T \cup \tau\right)}.$$

■

This Lemma is useful whenever we are looking for approximations of $\mathbf{H}^2$-functions, which is the regular case in the velocity analysis. It will not be applied to derive approximability results for the pressure space $\mathrm{M}_{\mathsf{H}}^{\mathrm{CME}}$ since, for an optimal convergence result, it is not necessary to make the same regularity assumption as for the velocity. Moreover, it is sufficient to assume that the pressure part of the solution belongs to H^1. This makes the analysis more complicated since the pointwise interpolation operator is no longer well defined. We will use the quasi interpolation operator of Scott and Zhang [1990] instead[2]. We do this in relation to the coarse overlapping grid $\mathcal{T}_{\mathsf{H}}$. For every $\mathbf{x}_i \in \Theta_{\mathsf{H}}$ we fix a face $\boldsymbol{\sigma}_i$ touching $\mathbf{x}_i$. We denote by $\{\phi_{i,j}\}_{j=1}^d$ its affine nodal basis and by $\{\psi_{i,j}\}$ its $\mathrm{L}^2(\boldsymbol{\sigma}_i)$-dual basis. Further let $\{\phi_j\}_{j=1}^N$ be the affine nodal basis of $\mathcal{T}_{\mathsf{H}}$. Then the quasi interpolation operator

$$\Pi_{\mathcal{T}_{\mathsf{H}}} : \mathrm{H}^1(\Omega_{\mathsf{H}}) \to S_{\mathcal{T}_{\mathsf{H}}}$$

[2]Since we only use the approximation property of this operator and not its special structure it is also possible to use the quasi-interpolation operator as introduced by Clément [Clément, 1975] or its modifications as described in [Verfürth, 1996] and [Verfürth, 1999].

is given by

$$\Pi_{\mathcal{T}_\mathsf{H}} p(\mathbf{x}) = \sum_{i=1}^{N} \phi_i(\mathbf{x}) \int_{\boldsymbol{\sigma}_i} \psi_{i,1}(\boldsymbol{\xi}) p(\boldsymbol{\xi}) d\boldsymbol{\xi}.$$

Following [Scott and Zhang, 1990], Theorem 4.1 and Corollary 4.1, the operator is bounded and fulfills the following approximation properties

$$\left\|p - \Pi_{\mathcal{T}_\mathsf{H}} p\right\|_{m,T} \leq C_{\mathrm{qint}} \operatorname{diam}(T)^{1-m} \|p\|_{1,\omega_T} \quad \forall T \in \mathcal{T}_\mathsf{H}\, \forall p \in \mathrm{H}^1(\Omega_\mathsf{H}),\ m \in \{0,1\} \tag{4.6}$$

$$\left\|p - \Pi_{\mathcal{T}_\mathsf{H}} p\right\|_{0,\Omega_H} \leq C_{\mathrm{qint}} \mathsf{H} \|p\|_{1,\Omega_H} \quad \forall p \in \mathrm{H}^1(\Omega_\mathsf{H}). \tag{4.7}$$

The constant $C_{\mathrm{qint}} = C(\rho)$ depends only on the minimal angles in $\mathcal{T}_\mathsf{H}$. This operator is nonlocal in the sense, that the error on a single simplex T depends not only on the derivatives on the simplex itself but a certain neighborhood

$$\omega_T := \{\tau \in \mathcal{T}_\mathsf{H} \mid \bar{\tau} \cap \bar{T} \neq \emptyset\}.$$

That is why Lemma 4.1 does not apply in a straightforward way. We prove an H^1-version instead.

Lemma 4.2 (Neighborhood property for H^1 functions)
Let $p \in H^1(\Omega_\mathsf{H})$ and $T \in \mathcal{T}_\mathsf{H}$. Let $\Pi_\mathrm{T} p \in \mathbb{P}_1(\mathbb{R}^d)$ denote the extension of $p|_T$ to $\mathbb{R}^d$ by itself. Then, for $m \in \{0,1\}$ and all $\tilde{T} \in \omega_T$, there exists a constant $C > 0$ such that

$$\left|p - \Pi_\mathrm{T} p\right|_{m,\tilde{T}} \leq C \operatorname{diam}(T)^{(1-m)} \|p\|_{1,(\omega_T \cup \omega_{\tilde{T}})}.$$

C depends only on C_{qint}, d and the regularity constant ρ (cf. (3.2)).

Proof. We start with an error splitting:

$$\begin{aligned}\left|\Pi_\mathrm{T} p - p\right|_{m,\tilde{T}} &\leq \left|\Pi_{\mathcal{T}_\mathsf{H}} p - \Pi_\mathrm{T} p\right|_{m,\tilde{T}} + \left|\Pi_{\mathcal{T}_\mathsf{H}} p - p\right|_{m,\tilde{T}} \\ &\leq \left(\tfrac{2}{\rho}\right)^m \left|\tilde{T}\right|^{\frac{1}{2}} \max_{\mathbf{x} \in V(\tilde{T})} \left|\Pi_{\mathcal{T}_\mathsf{H}} p(\mathbf{x}) - \Pi_\mathrm{T} p(\mathbf{x})\right| + C_{\mathrm{qint}} \operatorname{diam}(\tilde{T})^{(1-m)} \|p\|_{1,\tilde{T}},\end{aligned} \tag{4.8}$$

where we used (4.3) and (4.6) in the second estimate. Note that T and $\tilde{T}$ share at least one vertex $\mathbf{y} \in V(T) \cap V(\tilde{T})$ which allows the following estimate:

$$\begin{aligned}\left|\Pi_{\mathcal{T}_\mathsf{H}} p(\mathbf{x}) - \Pi_\mathrm{T} p(\mathbf{x})\right| &= \Big|\underbrace{\Pi_{\mathcal{T}_\mathsf{H}} p(\mathbf{y}) - \Pi_\mathrm{T} p(\mathbf{y})}_{=0} + \nabla \left(\Pi_{\mathcal{T}_\mathsf{H}} p - \Pi_\mathrm{T} p\right)\big|_{\tilde{T}} (\mathbf{x} - \mathbf{y})\Big| \\ &\leq \operatorname{diam}(\tilde{T}) \left|\nabla \left(\Pi_{\mathcal{T}_\mathsf{H}} p - \Pi_\mathrm{T} p\right)\big|_{\tilde{T}}\right|.\end{aligned} \tag{4.9}$$

The norm of the gradient on the right-hand side of (4.9) can be bounded, since

$$\begin{aligned}\left|\nabla \left(\Pi_{\mathcal{T}_\mathsf{H}} p - \Pi_\mathrm{T} p\right)\big|_{\tilde{T}}\right| &\leq \left|\nabla\left(\Pi_{\mathcal{T}_\mathsf{H}} p\big|_{\tilde{T}}\right)\right| + \left|\nabla\left(\Pi_\mathrm{T} p\right)\right| \\ &= \left|\Pi_{\mathcal{T}_\mathsf{H}} p\right|_{1,\infty,\tilde{T}} + \left|\Pi_\mathrm{T} p\right|_{1,\infty,T} \\ &\leq \left|\tilde{T}\right|^{-\frac{1}{2}} \left|\Pi_{\mathcal{T}_\mathsf{H}} p\right|_{1,\tilde{T}} + \left|T\right|^{-\frac{1}{2}} \left|\Pi_\mathrm{T} p\right|_{1,T} \\ &\leq \left(1 + \frac{\left|\tilde{T}\right|}{\left|T\right|}\right)^{\frac{1}{2}} \left|T\right|^{-\frac{1}{2}} \left|\Pi_{\mathcal{T}_\mathsf{H}} p\right|_{1,\tilde{T} \cup T} \\ &\leq C(\rho, d) \left|T\right|^{-\frac{1}{2}} \|p\|_{1,\omega_T \cup \omega_{\tilde{T}}},\end{aligned} \tag{4.10}$$

where we used $\operatorname{conv}(T \cup \tilde{T}) \subseteq (\omega_T \cup \omega_{\tilde{T}})$ and $|\tilde{T}| \leq C(\rho)|T|$ as well as the projection property of $\Pi_{\mathcal{T}_\mathsf{H}}$ in the last estimate.

Now combining (4.8), (4.9) and (4.10) yields the assertion. ∎

4.2 Approximability

With suitable interpolation results at hand we analyze the approximation error starting with the Dirichlet velocity space. Throughout this chapter the coarse grid $\mathcal{T}_\mathsf{H}$ is supposed to be a parent of $\mathcal{T}_{\mathsf{H},\mathsf{h}}$, i.e. $\mathcal{T}_{\mathsf{H},\mathsf{h}}$ arises from $\mathcal{T}_\mathsf{H}$ by a refinement process. That allows us to group the simplices in $\mathcal{T}_{\mathsf{H},\mathsf{h}}$ as sons of simplices in $\mathcal{T}_\mathsf{H}$, which simplifies the proofs, especially some counting arguments. We emphasize that this is not a crucial point in the analysis. The condition can be skipped by introducing a suitable weak compatibility condition between the grids.

4.2.1 The CME Velocity Space for Dirichlet Boundary

As a first step for the $\mathbf{H}^1$ approximation result we will prove a local $\mathbf{L}^\infty$ estimate.

Lemma 4.3
For every $\mathbf{u} \in \mathbf{H}^1_\mathrm{D}(\Omega) \cap \mathbf{H}^2(\Omega)$ *there exists* $\mathbf{u}_{\mathsf{H},\mathsf{h}} \in \mathbf{X}^{\mathrm{CME}_\mathrm{D}}_{\mathsf{H},\mathsf{h}}$ *such that*

$$\left\|\mathbf{u} - \mathbf{u}_{\mathsf{H},\mathsf{h}}\right\|_{0,\infty,t} \leq C\left[\left(\operatorname{diam}(t)^{(d-1)}\mathsf{H}\right)^{\frac{1}{d}}\right]^{\left(2-\frac{d}{2}\right)} |\mathbf{u}|_{2,\omega_T} \quad \forall t \in \mathcal{T}_{\mathsf{H},\mathsf{h}},$$

where $C = C(C_\mathrm{int}, \rho, C_1^{\mathcal{T}}, C_2^{\mathcal{T}}, d) > 0$ *is a constant,* $t \subseteq T \in \mathcal{T}_\mathsf{H}$ *and* $\omega_T = \{\tau \in \mathcal{T}_\mathsf{H} \mid \bar{\tau} \cap \bar{T} \neq \emptyset\}$.

Proof. We define $\mathbf{u}_{\mathsf{H},\mathsf{h}} := \boldsymbol{\mathcal{E}}^\mathrm{D}_{\mathsf{H},\mathsf{h}}\left(\mathcal{I}_{\mathcal{T}^\mathrm{dof}_\mathsf{H}}\mathbf{u}\right)$. The result for the inner simplices $T \in \mathcal{T}^\mathrm{dof}_\mathsf{H}$ follows from the standard interpolation estimate (4.2). Hence, it remains to consider $t \in \mathcal{T}^\Gamma_{\mathsf{H},\mathsf{h}}$. Let $\mathsf{h}_t := \operatorname{diam}(t)$ and $\mathcal{I}_\mathrm{t}\mathbf{u}$ denote the affine interpolant of $\mathbf{u}$ at the vertices of t. Then

$$\left\|\mathbf{u} - \mathbf{u}_{\mathsf{H},\mathsf{h}}\right\|_{\infty,t} \leq \left\|\mathbf{u}_{\mathsf{H},\mathsf{h}} - \mathcal{I}_\mathrm{t}\mathbf{u}\right\|_{\infty,t} + \left\|\mathcal{I}_\mathrm{t}\mathbf{u} - \mathbf{u}\right\|_{\infty,t}. \tag{4.11}$$

For the second term in (4.11) we apply (4.2) once more to get the bound $C(C_\mathrm{int}, \rho)\mathsf{h}_t^{\left(2-\frac{d}{2}\right)}|\mathbf{u}|_{2,t}$. It remains to bound the first term in (4.11) or, equivalently, $\left|\mathbf{u}_{\mathsf{H},\mathsf{h}}(\mathbf{x}) - \mathbf{u}(\mathbf{x})\right|$ for every vertex $\mathbf{x} \in V(t)$. We construct a simplex $\tau_\mathbf{x}$ (that does not necessarily belong to $\mathcal{T}_\mathsf{H}$ or $\mathcal{T}_{\mathsf{H},\mathsf{h}}$ (see also Fig. 4.2)):

1. $\mathbf{x} \in \tau_\mathbf{x}$,
2. $\mathbf{x}^\Gamma$ is a vertex of $\tau_\mathbf{x}$,
3. $\mathsf{h}_{\tau_\mathbf{x}} := \operatorname{diam}(\tau_\mathbf{x}) \in \mathcal{O}\left((\mathsf{H}\mathsf{h}_t^{d-1})^{\frac{1}{d}}\right)$, $\rho_{\tau_\mathbf{x}} \geq \rho$ and $\tau_\mathbf{x} \subseteq \omega_T$,

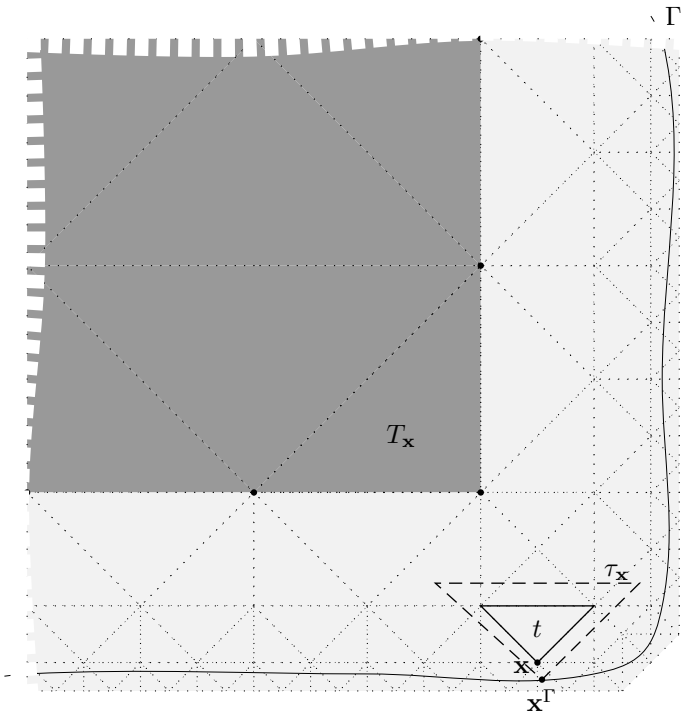

Figure 4.2: Illustration of a slave node $\mathbf{x}$ and the simplex $\tau_{\mathbf{x}}$ from the proof of Lemma 4.3 in $\mathbb{R}^2$.

where $T \in \mathcal{T}_{\mathsf{H}}$ is such that $t \subseteq T$. As before, $\omega_T = \{\tau \in \mathcal{T}_{\mathsf{H}} \mid \tau \cap T \neq \emptyset\}$ denotes the set of neighbors of T in $\mathcal{T}_{\mathsf{H}}$. Due to (3.2) and (3.3) such a simplex always exists. The choice $\mathsf{h}_{\tau_{\mathbf{x}}} \approx \left(\mathsf{H}\mathsf{h}_t^{d-1}\right)^{\frac{1}{d}}$ is made in order to minimize the bound of the pointwise error (see (4.13) in this proof). Let the closest inner simplex according to $\mathbf{x}$ be denoted by $T_{\mathbf{x}}$ and let its diameter be denoted by $\mathsf{h}_{T_{\mathbf{x}}} := \operatorname{diam}(T_{\mathbf{x}})$. Let $\mathcal{I}_{\tau_{\mathbf{x}}}$ and $\mathcal{I}_{\mathrm{T}_{\mathbf{x}}}$ denote the affine interpolation operators corresponding to $\tau_{\mathbf{x}}$ and $T_{\mathbf{x}}$. Then we get

$$
\begin{aligned}
\left|\mathbf{u}_{\mathsf{H},\mathsf{h}}(\mathbf{x}) - \mathbf{u}(\mathbf{x})\right| &= \Big|\nabla \mathcal{I}_{\mathrm{T}_{\mathbf{x}}}\mathbf{u} \cdot \left(\mathbf{x} - \mathbf{x}^{\Gamma}\right) \underbrace{- \overbrace{\left(\mathcal{I}_{\tau_{\mathbf{x}}}\mathbf{u}(\mathbf{x}) - \mathcal{I}_{\tau_{\mathbf{x}}}\mathbf{u}\left(\mathbf{x}^{\Gamma}\right)\right)}^{=\nabla(\mathcal{I}_{\tau_{\mathbf{x}}}\mathbf{u})\cdot\left(\mathbf{x}-\mathbf{x}^{\Gamma}\right)} + \mathcal{I}_{\tau_{\mathbf{x}}}\mathbf{u}(\mathbf{x})}_{=0} - \mathbf{u}(\mathbf{x})\Big| \\
&\leq \left|\nabla\left(\mathcal{I}_{\mathrm{T}_{\mathbf{x}}}\mathbf{u} - \mathcal{I}_{\tau_{\mathbf{x}}}\mathbf{u}\right) \cdot \left(\mathbf{x} - \mathbf{x}^{\Gamma}\right)\right| + \left|\mathbf{u}(\mathbf{x}) - \mathcal{I}_{\tau_{\mathbf{x}}}\mathbf{u}(\mathbf{x})\right| \qquad (4.12) \\
&\leq (1 + C_1^{\mathcal{T}})\mathsf{h}_t \left\|\mathcal{I}_{\mathrm{T}_{\mathbf{x}}}\mathbf{u} - \mathcal{I}_{\tau_{\mathbf{x}}}\mathbf{u}\right\|_{1,\infty,\tau_{\mathbf{x}}} + C_{\mathrm{int}}\mathsf{h}_{\tau_{\mathbf{x}}}^{\left(2-\frac{d}{2}\right)}\left|\mathbf{u}\right|_{2,\tau_{\mathbf{x}}} \\
&\leq \frac{2(1 + C_1^{\mathcal{T}})}{\rho}\frac{\mathsf{h}_t}{\mathsf{h}_{\tau_{\mathbf{x}}}}\left\|\mathcal{I}_{\mathrm{T}_{\mathbf{x}}}\mathbf{u} - \mathcal{I}_{\tau_{\mathbf{x}}}\mathbf{u}\right\|_{0,\infty,\tau_{\mathbf{x}}} + C_{\mathrm{int}}\mathsf{h}_{\tau_{\mathbf{x}}}^{\left(2-\frac{d}{2}\right)}\left|\mathbf{u}\right|_{2,\tau_{\mathbf{x}}} \\
&\leq \frac{2(1 + C_1^{\mathcal{T}})}{\rho}\frac{\mathsf{h}_t}{\mathsf{h}_{\tau_{\mathbf{x}}}}\left(\left\|\mathcal{I}_{\mathrm{T}_{\mathbf{x}}}\mathbf{u} - \mathbf{u}\right\|_{0,\infty,\tau_{\mathbf{x}}} + \left\|\mathbf{u} - \mathcal{I}_{\tau_{\mathbf{x}}}\mathbf{u}\right\|_{0,\infty,\tau_{\mathbf{x}}}\right) + C_{\mathrm{int}}\mathsf{h}_{\tau_{\mathbf{x}}}^{\left(2-\frac{d}{2}\right)}\left|\mathbf{u}\right|_{2,\tau_{\mathbf{x}}} \\
&\leq C\left[\frac{\mathsf{h}_t\mathsf{h}_{T_{\mathbf{x}}}^{\left(2-\frac{d}{2}\right)}}{\mathsf{h}_{\tau_{\mathbf{x}}}} + \mathsf{h}_t\mathsf{h}_{\tau_{\mathbf{x}}}^{\left(1-\frac{d}{2}\right)} + \mathsf{h}_{\tau_{\mathbf{x}}}^{\left(2-\frac{d}{2}\right)}\right]\left|\mathbf{u}\right|_{2,\mathrm{conv}\left(T\cup\tau_{\mathbf{x}}\right)}, \qquad (4.13)
\end{aligned}
$$

where we used (4.2) in the third and the last estimate, (4.3) in the fourth one and Lemma 4.1 for the estimation of $\left\|\mathcal{I}_{\mathrm{T}_\mathbf{x}}\mathbf{u}-\mathbf{u}\right\|_{0,\infty,\tau_\mathbf{x}}$. Now the choice of the diameter of $\tau_\mathbf{x}$ as in 3. becomes clear. The constant C depends only on $C_1^{\mathcal{T}}$, $C_2^{\mathcal{T}}$, ρ, C_{int} and the constant of Lemma 4.1. ∎

The local $\mathbf{L}^2$- respectively $\mathbf{H}^1$-estimates follow at hand.

Lemma 4.4
Let $m \in \{0,1\}$. For every $\mathbf{u} \in \mathbf{H}^1_{\mathrm{D}}(\Omega) \cap \mathbf{H}^2(\Omega)$ there exists $\mathbf{u}_{\mathsf{H},\mathsf{h}} \in \mathbf{X}^{\mathrm{CME_D}}_{\mathsf{H},\mathsf{h}}$ such that

$$\left\|\mathbf{u}-\mathbf{u}_{\mathsf{H},\mathsf{h}}\right\|_{m,t} \leq C\mathsf{H}^{\left(\frac{2}{d}-\frac{1}{2}\right)}\operatorname{diam}(t)^{\left(\frac{5}{2}-m-\frac{2}{d}\right)}\left|\mathbf{u}\right|_{2,\omega_T} \quad \forall t \in \mathcal{T}_{\mathsf{H},\mathsf{h}},$$

where $C = C(C_{\mathrm{int}}, \rho, C_1^{\mathcal{T}}, C_2^{\mathcal{T}}, d) > 0$ is a constant and $t \subseteq T \in \mathcal{T}_{\mathsf{H}}$.

Proof. We define $\mathbf{u}_{\mathsf{H},\mathsf{h}}$ as in the previous proof. We separate the linear part of the error by the triangle inequality, before we can use the inverse inequality (4.3). Estimate (4.2) is employed to estimate the rest:

$$\begin{aligned}\left|\mathbf{u}-\mathbf{u}_{\mathsf{H},\mathsf{h}}\right|_{m,t} &\leq \left|\mathbf{u}_{\mathsf{H},\mathsf{h}}-\mathcal{I}_{\mathrm{t}}(\mathbf{u})\right|_{m,t} + \left|\mathcal{I}_{\mathrm{t}}(\mathbf{u})-\mathbf{u}\right|_{m,t}\\ &\leq \left(\frac{2}{\rho}\right)^m \operatorname{diam}(t)^{\left(\frac{d}{2}-m\right)}\left\|\mathbf{u}_{\mathsf{H},\mathsf{h}}-\mathcal{I}_{\mathrm{t}}(\mathbf{u})\right\|_{\infty,t} + \frac{C_{\mathrm{int}}}{\rho^m}\operatorname{diam}(t)^{(2-m)}\left|\mathbf{u}\right|_{2,t}.\end{aligned}$$

We apply Lemma 4.3 to estimate the first summand and obtain the assertion. The resulting constant C equals $\left(\frac{2}{\rho}\right)^m$ times the constant of Lemma 4.3. ∎

Since the error estimates in Lemma 4.3 and Lemma 4.4 contain positive powers of $\operatorname{diam}(t)$ it is possible to localize the approximation error with respect to the simplices of the refined grid $\mathcal{T}_{\mathsf{H},\mathsf{h}}$. Unfortunately the dependence on the $\mathbf{H}^2$-norm of $\mathbf{u}$ is not local with respect to the fine scale mesh. Thus we cannot simply sum up the local errors to get an optimal global estimate. A deeper analysis is needed to prove the following global approximation property of the velocity space in the Dirichlet case.

Theorem 4.5 (Approximation property of $\mathbf{X}^{\mathrm{CME_D}}_{\mathsf{H},\mathsf{h}}$)
Let $m \in \{0,1\}$. For every $\mathbf{u} \in \mathbf{H}^1_{\mathrm{D}}(\Omega) \cap \mathbf{H}^2(\Omega)$ there exists $\mathbf{u}_{\mathsf{H},\mathsf{h}} \in \mathbf{X}^{\mathrm{CME_D}}_{\mathsf{H},\mathsf{h}}$ such that

$$\left\|\mathbf{u}-\mathbf{u}_{\mathsf{H},\mathsf{h}}\right\|_{m,\Omega} \leq C\mathsf{H}^{(2-m)}\left|\mathbf{u}\right|_{2,\Omega}$$

with some constant $C = C(C_{\mathrm{int}}, \rho, C_1^{\mathcal{T}}, C_2^{\mathcal{T}}, d, C_{\mathrm{ext}}) > 0$ which neither depends on H nor h.

Proof. We define again $\mathbf{u}_{\mathsf{H},\mathsf{h}} := \boldsymbol{\mathcal{E}}^{\mathrm{D}}_{\mathsf{H},\mathsf{h}}\left(\mathcal{I}_{\mathcal{T}_{\mathsf{H}}^{\mathrm{dof}}}\mathbf{u}\right)$ and start with a splitting of the error:

$$\left|\mathbf{u}-\mathbf{u}_{\mathsf{H},\mathsf{h}}\right|^2_{m,\Omega} \leq C\left(\left|\mathbf{u}-\mathcal{I}_{\mathcal{T}_{\mathsf{H},\mathsf{h}}}\mathbf{u}\right|^2_{m,\Omega} + \sum_{T\in\mathcal{T}_{\mathsf{H}}}\sum_{t\in\mathcal{T}^{\mathrm{T}}}\left|\mathcal{I}_{\mathcal{T}_{\mathsf{H},\mathsf{h}}}\mathbf{u}-\mathbf{u}_{\mathsf{H},\mathsf{h}}\right|^2_{m,t}\right). \tag{4.14}$$

As indicated before, the application of Lemma 4.4 would lead to a suboptimal error bound, at least in the $\mathbf{H}^1$-case. In fact, we use Lemma 4.4 only on those triangles whose nodes are assigned to different inner simplices, i.e. $t \notin \hat{\mathcal{T}}^{\mathrm{T}}$ for all $T \in \mathcal{T}_{\mathsf{H}}^{\mathrm{dof}}$. For all other simplices we will need a

more local bound. So let $T \in \mathcal{T}_{\mathsf{H}}^{\mathrm{dof}}$ and $t \in \hat{\mathcal{T}}^{\mathrm{T}}$. By $\mathcal{I}_{\mathrm{t}}\mathbf{u} \subseteq \mathbb{P}_1(\mathbb{R}^d)$ we denote the affine interpolation of $\mathbf{u}$ at the vertices of t, $\mathsf{h}_t := \operatorname{diam}(t)$. Then

$$\begin{aligned}
\left|\mathbf{u}_{\mathsf{H},\mathsf{h}} - \mathcal{I}_{\mathcal{T}_{\mathsf{H},\mathsf{h}}}\mathbf{u}\right|_{m,t} &= \left|\mathbf{u}_{\mathsf{H},\mathsf{h}} - \mathcal{I}_{\mathrm{t}}\mathbf{u}\right|_{m,t} \\
&\leq \left(\frac{2}{\rho}\right)^m \mathsf{h}_t^{\left(\frac{d}{2}-m\right)} \left\|\mathbf{u}_{\mathsf{H},\mathsf{h}} - \mathcal{I}_{\mathrm{t}}\mathbf{u}\right\|_{0,\infty,t} \\
&\leq \left(\frac{2}{\rho}\right)^m \mathsf{h}_t^{\left(\frac{d}{2}-m\right)} \max_{\mathbf{x}\in V(t)} \left|\nabla \mathcal{I}_{\mathrm{T}_{\mathbf{x}}}\mathbf{u} \cdot \left(\mathbf{x}-\mathbf{x}^{\Gamma}\right) - \underbrace{\left(\mathcal{I}_{\mathrm{t}}\mathbf{u}(\mathbf{x}^{\Gamma}) + \nabla \mathcal{I}_{\mathrm{t}}\mathbf{u} \cdot \left(\mathbf{x}-\mathbf{x}^{\Gamma}\right)\right)}_{=\mathcal{I}_{\mathrm{t}}\mathbf{u}(\mathbf{x})}\right| \\
&\leq \left(\frac{2}{\rho}\right)^m \Bigg(C_1^{\mathcal{T}} \mathsf{h}_t^{\left(1+\frac{d}{2}-m\right)} \left\|\nabla\left(\mathcal{I}_{\mathrm{T}_{\mathbf{x}}}\mathbf{u} - \mathcal{I}_{\mathrm{t}}\mathbf{u}\right)\right\|_{0,\infty,t} \\
&\qquad + \mathsf{h}_t^{\left(\frac{d}{2}-m\right)} \max_{\mathbf{x}\in V(t)} \left|\mathcal{I}_{\mathrm{t}}\mathbf{u}(\mathbf{x}^{\Gamma}) - \underbrace{\mathbf{u}(\mathbf{x}^{\Gamma})}_{=0}\right| \Bigg) \qquad (4.15) \\
&\leq C(C_{\mathrm{int}}, C_1^{\mathcal{T}}, \rho, d)\left(\mathsf{h}_t^{(1-m)}\left|\mathcal{I}_{\mathrm{T}}\mathbf{u} - \mathcal{I}_{\mathrm{t}}\mathbf{u}\right|_{1,t} + \mathsf{h}_t^{(2-m)}\left|\mathbf{u}\right|_{2,\tilde{t}}\right), \qquad (4.16)
\end{aligned}$$

where we used (4.3) in the second estimate and Lemma 4.1, (especially (4.5)), in the last one. The set

$$\tilde{t} := \operatorname{conv}\left(t \cup \{\mathbf{x}^{\Gamma} \mid \mathbf{x} \in V(t)\}\right)$$

denotes the convex hull of all the vertices of t and their closest boundary points.

So we get

$$\begin{aligned}
\sum_{T\in\mathcal{T}_{\mathsf{H}}} \sum_{t\in\mathcal{T}^{\mathrm{T}}} \left|\mathcal{I}_{\mathcal{T}_{\mathsf{H},\mathsf{h}}}\mathbf{u} - \mathbf{u}_{\mathsf{H},\mathsf{h}}\right|_{m,t}^2 &\leq \sum_{T\in\mathcal{T}_{\mathsf{H}}} \Bigg(\sum_{t\in\hat{\mathcal{T}}^{\mathrm{T}}} \left|\mathcal{I}_{\mathcal{T}_{\mathsf{H},\mathsf{h}}}\mathbf{u} - \mathbf{u}_{\mathsf{H},\mathsf{h}}\right|_{m,t}^2 + \sum_{t\in\mathcal{T}^{\mathrm{T}}\setminus\hat{\mathcal{T}}^{\mathrm{T}}} \left|\mathcal{I}_{\mathcal{T}_{\mathsf{H},\mathsf{h}}}\mathbf{u} - \mathbf{u}_{\mathsf{H},\mathsf{h}}\right|_{m,t}^2 \Bigg) \\
&\leq \sum_{T\in\mathcal{T}_{\mathsf{H}}} C(C_{\mathrm{int}}, \rho, C_1^{\mathcal{T}}, d)\Bigg(\sum_{t\in\hat{\mathcal{T}}^{\mathrm{T}}} \mathsf{h}_t^{(2-2m)}\left|\mathcal{I}_{\mathrm{T}}\mathbf{u} - \mathcal{I}_{\mathrm{t}}\mathbf{u}\right|_{1,t}^2 + \mathsf{h}_t^{(4-2m)}\left|\mathbf{u}\right|_{2,\tilde{t}}^2 \\
&\qquad + C(C_{\mathrm{int}}, \rho, C_1^{\mathcal{T}}, C_2^{\mathcal{T}}, d) \sum_{t\in\mathcal{T}^{\mathrm{T}}\setminus\hat{\mathcal{T}}^{\mathrm{T}}} \mathsf{H}^{\left(\frac{4}{d}-1\right)}\mathsf{h}_t^{\left(5-2m-\frac{4}{d}\right)}\left|\mathbf{u}\right|_{2,\omega_T}^2 \Bigg) \\
&\leq C(C_{\mathrm{int}}, \rho, C_1^{\mathcal{T}}, C_2^{\mathcal{T}}, d)\mathsf{H}^{(2-2m)}\Bigg(\sum_{T\in\mathcal{T}_{\mathsf{H}}} \underbrace{\left|\mathcal{I}_{\mathrm{T}}\mathbf{u} - \mathcal{I}_{\mathrm{t}}\mathbf{u}\right|_{1,\hat{\mathcal{T}}^{\mathrm{T}}}^2}_{=:M_{1,T}} \\
&\qquad + \sum_{T\in\mathcal{T}_{\mathsf{H}}} \underbrace{\left(\sum_{t\in\hat{\mathcal{T}}^{\mathrm{T}}} \mathsf{h}_t^2\left|\mathbf{u}\right|_{2,\tilde{t}}^2 \right)}_{=:M_{2,T}} + \sum_{T\in\mathcal{T}_{\mathsf{H}}} \underbrace{\left(\sum_{t\in\mathcal{T}^{\mathrm{T}}\setminus\hat{\mathcal{T}}^{\mathrm{T}}} \mathsf{h}_t^2 \right)\left|\mathbf{u}\right|_{2,\omega_T}^2}_{=:M_{3,T}} \Bigg).
\end{aligned}$$

If we could show the existence of constants $C_i > 0$, such that $M_{i,T} \leq C_i \mathsf{H}^2\left|\mathbf{u}\right|_{2,\omega_T}^2$ for all $i \in \{1,2,3\}$, then the proof is finished since

$$\sum_{T\in\mathcal{T}_{\mathsf{H}}} \left|\mathbf{u}\right|_{2,\omega_T}^2 \leq C(\rho, C_{\mathrm{ext}})\left|\mathbf{u}\right|_{2,\Omega}^2.$$

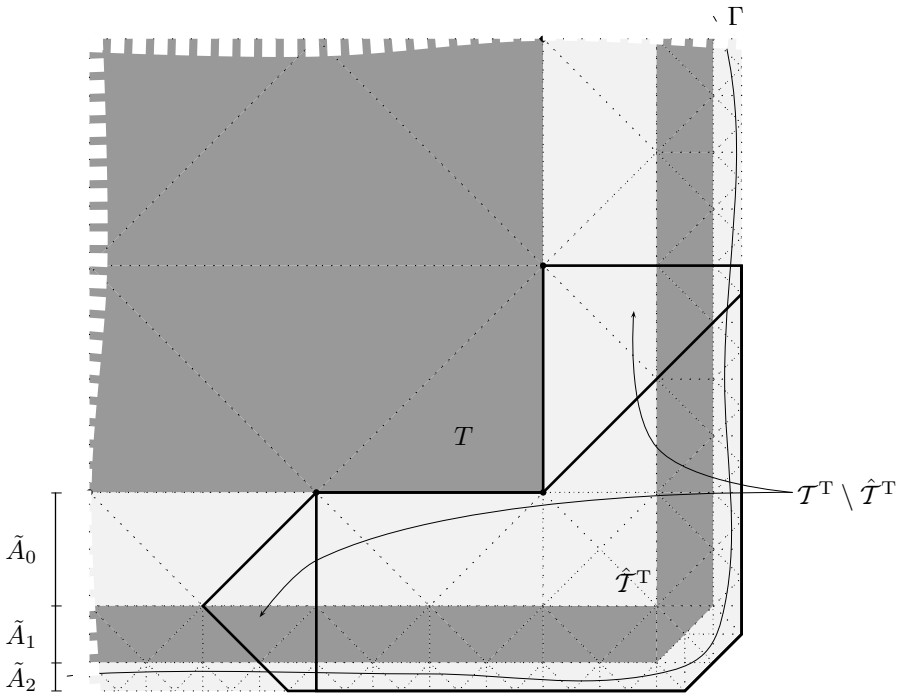

Figure 4.3: The boundary regions $\tilde{A}_i$.

In case of $M_{1,T}$ this can be done by using the triangle inequality, Lemma 4.1 and (4.2):

$$\begin{aligned} M_{1,T} = \left|\mathcal{I}_{\mathrm{T}}\mathbf{u} - \mathcal{I}_{\mathrm{t}}\mathbf{u}\right|^2_{1,\hat{\mathcal{T}}^{\mathrm{T}}} &\leq \left|\mathcal{I}_{\mathrm{T}}\mathbf{u} - \mathbf{u}\right|^2_{1,\hat{\mathcal{T}}^{\mathrm{T}}} + \left|\mathbf{u} - \mathcal{I}_{\mathrm{t}}\mathbf{u}\right|^2_{1,\hat{\mathcal{T}}^{\mathrm{T}}} \\ &\leq \left(C(C_{\mathrm{int}}, \rho, C_2^{\mathcal{T}}, d)^2 + \frac{C_{int}^2}{\rho^2}\right) \mathsf{H}^2 \left|\mathbf{u}\right|^2_{2,\mathrm{conv}\left(\hat{\mathcal{T}}^{\mathrm{T}}\right)} \\ &\leq C(C_{\mathrm{int}}, \rho, C_2^{\mathcal{T}}, d)^2 \mathsf{H}^2 \left|\mathbf{u}\right|^2_{2,\mathrm{conv}\left(\hat{\mathcal{T}}^{\mathrm{T}}\right)}. \end{aligned}$$

For the estimation of $M_{2,T}$ we group simplices from $\mathcal{T}^{\Gamma}_{\mathsf{H},\mathsf{h}}$ not only according to their extrapolation simplices but also according to their boundary distance. We define the sets

$$A_0 := \mathcal{T}^{\Gamma}_{\mathsf{H},\mathsf{h}}, \quad A_k := \left\{t \in \mathcal{T}^{\Gamma}_{\mathsf{H},\mathsf{h}} \mid \max_{\mathbf{x}\in t} \operatorname{dist}(\mathbf{x}, \Gamma) < 2^{-k}\mathsf{H}\right\}, \quad 1 \leq k \leq K := 1 + \left\lceil \log_2\left(\frac{\mathsf{H}}{\mathsf{h}}\right)\right\rceil.$$

Their disjoint versions are given by (cf. Figure 4.3)

$$\tilde{A}_k := A_k \setminus A_{k+1}, \quad 0 \leq k \leq K-1, \quad \tilde{A}_K := A_K. \tag{4.17}$$

The summation in $M_{2,T}$ can be re-sorted using (4.17):

$$M_{2,T} = \sum_{t\in\hat{\mathcal{T}}^{\mathrm{T}}} \mathsf{h}_t^2 \big|\mathbf{u}\big|_{2,\tilde{t}}^2 \le C(C_1^{\mathcal{T}}) \sum_{k=0}^{K} \sum_{t\in\hat{\mathcal{T}}^{\mathrm{T}}\cap\tilde{A}_k} 2^{-2k}\mathsf{H}^2 \Big(\sum_{j=0}^{K} \sum_{\tau\in\tilde{A}_j} \big|\mathbf{u}\big|_{2,\tau\cap\tilde{t}}^2 \Big)$$
$$\le C(C_1^{\mathcal{T}})\mathsf{H}^2 \sum_{k=0}^{K} 2^{-2k} \Big(\sum_{j=0}^{K} \sum_{\tau\in\tilde{A}_j} \sum_{t\in\hat{\mathcal{T}}^{\mathrm{T}}\cap\tilde{A}_k} 2^{-2k} \big|\mathbf{u}\big|_{2,\tau\cap\tilde{t}}^2 \Big)$$
$$\le C(C_1^{\mathcal{T}})\mathsf{H}^2 \sum_{k=0}^{K} 2^{-2k} \Big(\sum_{j=0}^{K} \sum_{\tau\in\tilde{A}_j} \sharp\tilde{A}_{k,\tau} \big|\mathbf{u}\big|_{2,\tau}^2 \Big).$$

Here, $\tilde{A}_{k,\tau} := \{t \in \hat{\mathcal{T}}^{\mathrm{T}} \cap \tilde{A}_k \mid \tau \cap \tilde{t} \neq \emptyset\}$. For $\tau \in \tilde{A}_j$ and $j > k$, $\tilde{A}_{k,\tau}$ is an empty set. In the other cases, $j \le k$, its number of elements is bounded by a moderate constant $C(C_1^{\mathcal{T}}, \rho, d)$ since

$$\operatorname{dist}(t_1, t_2) \le 2 \cdot 2^{-k}\mathsf{H} \ \ \forall t_1, t_2 \in \tilde{A}_{k,\tau} \quad \text{and} \quad \big|t_1\big| \ge C(C_1^{\mathcal{T}}, \rho)(2^{-k}\mathsf{H})^d \ \ \forall t_1 \in \tilde{A}_{k,\tau}.$$

Furthermore, $\tilde{A}_{k,\tau}$ is an empty set if $\tau \notin \omega_T$. This leads to

$$M_{2,T} \le C(C_1^{\mathcal{T}}, \rho, d)\mathsf{H}^2 \sum_{k=0}^{K} 2^{-2k} \sum_{j=0}^{k} \big|\mathbf{u}\big|_{2,\omega_T}^2 \le C(C_1^{\mathcal{T}}, \rho, d)\mathsf{H}^2 \underbrace{\Big(\sum_{k=0}^{K} 2^{-2k} k \Big)}_{\le 2} \big|\mathbf{u}\big|_{2,\omega_T}^2.$$

It remains to estimate $M_{3,T}$. Since $\mathcal{T}^{\mathrm{T}} \setminus \hat{\mathcal{T}}^{\mathrm{T}} \subseteq \bigcup_{\tau\in\omega_T} \mathcal{T}^{\mathrm{T}} \cap \mathcal{T}^{\tau}$ we get

$$M_{3,T} = \Big(\sum_{t\in\mathcal{T}^{\mathrm{T}}\setminus\hat{\mathcal{T}}^{\mathrm{T}}} \mathsf{h}_t^2 \Big) \big|\mathbf{u}\big|_{2,\omega_T}^2 \le \Big(\sum_{k=0}^{K} \sum_{\tau\in\omega_T} \sum_{t\in\mathcal{T}^{\mathrm{T}}\cap\mathcal{T}^{\tau}\cap\tilde{A}_k} 2^{-2k}\mathsf{H}^2 \Big) \big|\mathbf{u}\big|_{2,\omega_T}^2$$
$$\le \mathsf{H}^2 \big|\mathbf{u}\big|_{2,\omega_T}^2 \Big(\sum_{\tau\in\omega_T} \sum_{k=0}^{K} \#\big(\mathcal{T}^{\mathrm{T}} \cap \mathcal{T}^{\tau} \cap \tilde{A}_k\big) 2^{-2k} \Big).$$

by using (4.17). A simplex t belongs to the set $\mathcal{T}^{\mathrm{T}} \cap \mathcal{T}^{\tau}$, $\tau \in \omega_T$, if it intersects the $(d-1)$-dimensional manifold on which the mapping (see also 3.1)

$$\mathbb{R}^d \ni \mathbf{x} \mapsto T_{\mathbf{x}} \in \operatorname{argmin}\{\operatorname{dist}(\mathbf{x}, T), \operatorname{dist}(\mathbf{x}, \tau)\}$$

has a jump. Therefore and due to (3.3) and shape regularity the cardinal number of $\mathcal{T}^{\mathrm{T}} \cap \mathcal{T}^{\tau} \cap \tilde{A}_k$ satisfies

$$\#\big(\mathcal{T}^{\mathrm{T}} \cap \mathcal{T}^{\tau} \cap \tilde{A}_k\big) \le C(C_1^{\mathcal{T}}, C_2^{\mathcal{T}}, \rho, d)(2^k)^{d-2} \quad \forall k = 1, \dots, K.$$

In two dimensions only a moderately bounded number of simplices belongs to $\mathcal{T}^{\mathrm{T}} \cap \mathcal{T}^{\tau} \cap \tilde{A}_k$. This is not true for $d = 3$, but there, the growth in k is sufficiently slow to preserve the final estimate:

$$M_{3,T} \le \Big(\sum_{k=0}^{K} C(C_1^{\mathcal{T}}, C_2^{\mathcal{T}}, \rho, d) 2^{-k} \Big) \mathsf{H}^2 \big|\mathbf{u}\big|_{2,\omega_T}^2 \le 2C(C_1^{\mathcal{T}}, C_2^{\mathcal{T}}, \rho, d)\mathsf{H}^2 \big|\mathbf{u}\big|_{2,\omega_T}^2.$$

■

Thus the Dirichlet case is complete and we turn to the slip boundary condition.

4.2.2 The CME Velocity Space for Slip Boundary

Here, things are getting more complicated due to the free tangential velocity. Due to the loss of information on the boundary a slip analogue of Lemma 4.3 can only give a bound in powers of H.

Lemma 4.6
For every $\mathbf{u} \in \mathbf{H}^1_{\mathrm{s}}(\Omega) \cap \mathbf{H}^2(\Omega)$ *there exists* $\mathbf{u}_{\mathsf{H},\mathsf{h}} \in \mathbf{X}^{\mathrm{CME_s}}_{\mathsf{H},\mathsf{h}}$ *such that*

$$\left\|\mathbf{u} - \mathbf{u}_{\mathsf{H},\mathsf{h}}\right\|_{0,\infty,t} \leq C\mathsf{H}^{\left(2-\frac{d}{2}\right)}\left|\mathbf{u}\right|_{2,\omega_T} \quad \forall t \in \mathcal{T}_{\mathsf{H},\mathsf{h}},$$

where $C = C(C_{\mathrm{int}}, \rho, C_1^{\mathcal{T}}, C_2^{\mathcal{T}}, d) > 0$ *is a constant,* $t \subseteq T \in \mathcal{T}_{\mathsf{H}}$ *and* $\omega_T = \{\tau \in \mathcal{T}_{\mathsf{H}} \mid \tau \cap T \neq \emptyset\}$.

Proof. Let $\mathcal{I}_{\mathcal{T}^{\mathrm{dof}}_{\mathsf{H}}}\mathbf{u}$ denote the piecewise affine interpolant of $\mathbf{u}$ in the nodes of $\mathcal{T}^{\mathrm{dof}}_{\mathsf{H}}$ and define $\mathbf{u}_{\mathsf{H}} := \mathcal{I}_{\mathcal{T}^{\mathrm{dof}}_{\mathsf{H}}}\mathbf{u}$ and $\mathbf{u}_{\mathsf{H},\mathsf{h}} := \boldsymbol{\mathcal{E}}^{\mathrm{s}}_{\mathsf{H},\mathsf{h}}\,\mathbf{u}_{\mathsf{H}}$. We have already proved (cf. proof of Lemma 4.3) that we can restrict ourselves on bounding $\left|\mathbf{u}_{\mathsf{H},\mathsf{h}}(\mathbf{x}) - \mathbf{u}(\mathbf{x})\right|$ for every vertex $\mathbf{x} \in t$. The simplex t is supposed to be contained in $\mathcal{T}^{\mathrm{T}}$ for some $T \in \mathcal{T}^{\mathrm{dof}}_{\mathsf{H}}$. We use the same notation as in the proof of Lemma 4.3 to derive:

$$\begin{aligned}
\left|\mathbf{u}_{\mathsf{H},\mathsf{h}}(\mathbf{x}) - \mathbf{u}(\mathbf{x})\right| &\leq \left|\left(\boldsymbol{\mathcal{E}}^{\mathrm{D}}_{\mathsf{H},\mathsf{h}}\,\mathbf{u}_{\mathsf{H}}(\mathbf{x}) - \mathbf{u}(\mathbf{x})\right)_{\boldsymbol{\nu}(\mathbf{x}^\Gamma)}\right| \\
&\quad + \left|\left(\boldsymbol{\mathcal{E}}_{\mathsf{H},\mathsf{h}}\,\mathbf{u}_{\mathsf{H}}(\mathbf{x}) - \mathbf{u}(\mathbf{x})\right) - \left(\boldsymbol{\mathcal{E}}_{\mathsf{H},\mathsf{h}}\,\mathbf{u}_{\mathsf{H}}(\mathbf{x}) - \mathbf{u}(\mathbf{x})\right)_{\boldsymbol{\nu}(\mathbf{x}^\Gamma)}\right| \\
&\leq \left|\left\langle \nabla\left(\mathcal{I}_{\mathrm{T}_\mathbf{x}}\mathbf{u} - \mathcal{I}_{\tau_\mathbf{x}}\mathbf{u}\right)\cdot\left(\mathbf{x}-\mathbf{x}^\Gamma\right) + \mathcal{I}_{\tau_\mathbf{x}}\mathbf{u}(\mathbf{x}) - \mathbf{u}(\mathbf{x}), \boldsymbol{\nu}(\mathbf{x}^\Gamma)\right\rangle \boldsymbol{\nu}(\mathbf{x}^\Gamma)\right| \\
&\quad + \left|\left(\boldsymbol{\mathcal{E}}_{\mathsf{H},\mathsf{h}}\,\mathbf{u}_{\mathsf{H}}(\mathbf{x}) - \mathbf{u}(\mathbf{x})\right) - \left\langle \boldsymbol{\mathcal{E}}_{\mathsf{H},\mathsf{h}}\,\mathbf{u}_{\mathsf{H}}(\mathbf{x}) - \mathbf{u}(\mathbf{x}), \boldsymbol{\nu}(\mathbf{x}^\Gamma)\right\rangle \boldsymbol{\nu}(\mathbf{x}^\Gamma)\right| \\
&\leq \left|\nabla\left(\mathcal{I}_{\mathrm{T}_\mathbf{x}}\mathbf{u} - \mathcal{I}_{\tau_\mathbf{x}}\mathbf{u}\right)\cdot\left(\mathbf{x}-\mathbf{x}^\Gamma\right) + \mathcal{I}_{\tau_\mathbf{x}}\mathbf{u}(\mathbf{x}) - \mathbf{u}(\mathbf{x})\right| + \left|\boldsymbol{\mathcal{E}}_{\mathsf{H},\mathsf{h}}\,\mathbf{u}_{\mathsf{H}}(\mathbf{x}) - \mathbf{u}(\mathbf{x})\right|.
\end{aligned} \tag{4.18}$$

The first term was estimated in (4.12) by

$$C(C_{\mathrm{int}}, \rho, C_1^{\mathcal{T}}, C_2^{\mathcal{T}}, d)\left[\left(\mathrm{diam}(t)^{d-1}\mathsf{H}\right)^{\frac{1}{d}}\right]^{\left(2-\frac{d}{2}\right)}\left|\mathbf{u}\right|_{2,\omega_T}.$$

The additional second term can only be bounded in terms of H using Lemma 4.1. If $T_1 \in \mathcal{T}^{\Gamma}_{\mathsf{H}}$ such that $\mathbf{x} \in T_1$ ($\Rightarrow T_1 \subseteq \omega_T$), then

$$\begin{aligned}
\left|\boldsymbol{\mathcal{E}}_{\mathsf{H},\mathsf{h}}\,\mathbf{u}_{\mathsf{H}}(\mathbf{x}) - \mathbf{u}(\mathbf{x})\right| &\leq \left\|\boldsymbol{\mathcal{E}}_{\mathsf{H},\mathsf{h}}\,\mathbf{u}_{\mathsf{H}} - \mathbf{u}\right\|_{\infty,T} \leq \left\|\boldsymbol{\mathcal{E}}_{\mathsf{H},\mathsf{h}}\,\mathbf{u}_{\mathsf{H}} - \mathcal{I}_{\mathrm{T}}\mathbf{u}\right\|_{\infty,T} + \left\|\mathcal{I}_{\mathrm{T}}\mathbf{u} - \mathbf{u}\right\|_{\infty,T} \\
&\leq \max_{\mathrm{y}\in V(T)}\left|\mathcal{I}_{\mathrm{T}_\mathrm{y}}\mathbf{u}(\mathbf{y}) - \mathbf{u}(\mathbf{y})\right| + C\mathsf{H}^{\left(2-\frac{d}{2}\right)}\left|\mathbf{u}\right|_{2,T_\mathbf{x}} \leq 2C\mathsf{H}^{\left(2-\frac{d}{2}\right)}\left|\mathbf{u}\right|_{2,\omega_T},
\end{aligned}$$

where C is the constant of Lemma 4.1. ∎

This Lemma is only useful to get a local $\mathbf{L}^2$-estimate but it is not appropriate to derive sharp bounds of the $\mathcal{T}_{\mathsf{H},\mathsf{h}}$-local $\mathbf{H}^1$-norm since the estimate does not contain positive powers of the small scale h, which were the basis of the summing arguments used in the proof of Theorem 4.5. However, the subsequent theorem will show that we get comparable $\mathcal{T}_{\mathsf{H},\mathsf{h}}$-local and global results due to the fact that the problematic term

$$\left|\left(\boldsymbol{\mathcal{E}}_{\mathsf{H},\mathsf{h}}\,\mathbf{u}_{\mathsf{H}}(\mathbf{x}) - \mathbf{u}(\mathbf{x})\right) - \left(\boldsymbol{\mathcal{E}}_{\mathsf{H},\mathsf{h}}\,\mathbf{u}_{\mathsf{H}}(\mathbf{x}) - \mathbf{u}(\mathbf{x})\right)_{\boldsymbol{\nu}(\mathbf{x}^\Gamma)}\right|,$$

which appears in the proof of Lemma 4.6 does not vary to much over a slave simplex.

We need some property of the outer domain normal which we deduce from the assumed boundary regularity:

$$\left|\boldsymbol{\nu}(\mathbf{x}^\Gamma) - \boldsymbol{\nu}(\mathbf{y}^\Gamma)\right| \leq C_{\boldsymbol{\nu}} \left|\mathbf{x} - \mathbf{y}\right| \qquad \forall \mathbf{x}, \mathbf{y} \in \overline{\Omega}. \tag{4.19}$$

If Γ is simply connected, then $C_{\boldsymbol{\nu}}$ is bounded by the square of the maximal curvature of Γ.

Theorem 4.7 (Approximation property of $\mathbf{X}_{\mathsf{H},\mathsf{h}}^{\mathrm{CME_s}}$)
Let $m \in \{0,1\}$. For every $\mathbf{u} \in \mathbf{H}_{\mathrm{s}}^1(\Omega) \cap \mathbf{H}^2(\Omega)$ there exists $\mathbf{u}_{\mathsf{H},\mathsf{h}} \in \mathbf{X}_{\mathsf{H},\mathsf{h}}^{\mathrm{CME_s}}$ such that

$$\left\|\mathbf{u} - \mathbf{u}_{\mathsf{H},\mathsf{h}}\right\|_{m,\Omega} \leq (C + C_{\boldsymbol{\nu}}\mathsf{H})\, \mathsf{H}^{(2-m)} \left|\mathbf{u}\right|_{2,\Omega}$$

with some constant $C = C(C_{\mathrm{int}}, \rho, C_1^{\mathcal{T}}, C_2^{\mathcal{T}}, d, C_{\mathrm{ext}}) > 0$ which neither depends on H nor h.

Proof. We define $\mathbf{u}_{\mathsf{H}} := \mathcal{I}_{\mathcal{T}_{\mathsf{H}}^{\mathrm{dof}}} \mathbf{u}$ and $\mathbf{u}_{\mathsf{H},\mathsf{h}} := \boldsymbol{\mathcal{E}}_{\mathsf{H},\mathsf{h}}^{\mathrm{s}} \mathbf{u}_{\mathsf{H}}$ as in the proof of Lemma 4.6. The proof of the L^2-estimate is a simple consequence of Lemma 4.6 applied to the right-hand side of the Cauchy-Schwarz estimate

$$\left\|\mathbf{u}_{\mathsf{H},\mathsf{h}} - \mathbf{u}\right\|_{0,\Omega}^2 \leq \sum_{t \in \mathcal{T}_{H,h}} |t| \left\|\mathbf{u}_{\mathsf{H},\mathsf{h}} - \mathbf{u}\right\|_{0,\infty,t}^2.$$

To get the $\mathbf{H}^1$-result, we investigate the error $\left|\mathbf{u}_{\mathsf{H},\mathsf{h}} - \mathcal{I}_{\mathcal{T}_{\mathsf{H},\mathsf{h}}} \mathbf{u}\right|_{1,t}$ on a simplex $t \in \mathcal{T}^{\mathrm{T}}$ for some $T \in \mathcal{T}_{\mathsf{H}}^{\mathrm{dof}}$. In contrast to (4.18) we use the fact that the $\mathbf{H}^1$-seminorm of an affine function can not only be bounded by (4.3) but by the scaled maximal difference of function values at two vertices:

$$\left|\mathbf{u}_{\mathsf{H},\mathsf{h}} - \mathcal{I}_{\mathcal{T}_{\mathsf{H},\mathsf{h}}} \mathbf{u}\right|_{1,t} \leq \frac{2}{\rho} \mathsf{h}_t^{\left(\frac{d}{2}-1\right)} \max_{\mathbf{x},\mathbf{y} \in V(t)} \left|\left(\mathbf{u}_{\mathsf{H},\mathsf{h}}(\mathbf{x}) - \mathbf{u}(\mathbf{x})\right) - \left(\mathbf{u}_{\mathsf{H},\mathsf{h}}(\mathbf{y}) - \mathbf{u}(\mathbf{y})\right)\right|.$$

Employing the definition of $\boldsymbol{\mathcal{E}}_{\mathsf{H},\mathsf{h}}^{\mathrm{s}}$ and splitting $\mathbf{u}(\mathbf{x})$ into its components with respect to some normal vectors we further get

$$\begin{aligned}
\left|\mathbf{u}_{\mathsf{H},\mathsf{h}} - \mathcal{I}_{\mathcal{T}_{\mathsf{H},\mathsf{h}}} \mathbf{u}\right|_{1,t} \leq \frac{2}{\rho} \mathsf{h}_t^{\left(\frac{d}{2}-1\right)} \Bigg(& \max_{\mathbf{x},\mathbf{y} \in V(t)} \left| \left(\boldsymbol{\mathcal{E}}_{\mathsf{H},\mathsf{h}}^{\mathrm{D}} \mathbf{u}_{\mathsf{H}}(\mathbf{x}) - \mathbf{u}(\mathbf{x})\right)_{\boldsymbol{\nu}(\mathbf{x}^\Gamma)} - \left(\boldsymbol{\mathcal{E}}_{\mathsf{H},\mathsf{h}}^{\mathrm{D}} \mathbf{u}_{\mathsf{H}}(\mathbf{y}) - \mathbf{u}(\mathbf{y})\right)_{\boldsymbol{\nu}(\mathbf{y}^\Gamma)} \right| \\
& + \max_{\mathbf{x},\mathbf{y} \in V(t)} \left| \boldsymbol{\mathcal{E}}_{\mathsf{H},\mathsf{h}} \mathbf{u}_{\mathsf{H}}(\mathbf{x}) - \mathbf{u}(\mathbf{x}) - \left(\boldsymbol{\mathcal{E}}_{\mathsf{H},\mathsf{h}} \mathbf{u}_{\mathsf{H}}(\mathbf{y}) - \mathbf{u}(\mathbf{y})\right) \right| \\
& + \max_{\mathbf{x},\mathbf{y} \in V(t)} \left| \left(\boldsymbol{\mathcal{E}}_{\mathsf{H},\mathsf{h}} \mathbf{u}_{\mathsf{H}}(\mathbf{x}) - \mathbf{u}(\mathbf{x})\right)_{\boldsymbol{\nu}(\mathbf{x}^\Gamma)} - \left(\boldsymbol{\mathcal{E}}_{\mathsf{H},\mathsf{h}} \mathbf{u}_{\mathsf{H}}(\mathbf{y}) - \mathbf{u}(\mathbf{y})\right)_{\boldsymbol{\nu}(\mathbf{y}^\Gamma)} \right| \Bigg).
\end{aligned}$$

The first maximum is estimated by the absolute maximum of the full error:

$$\max_{\mathbf{x},\mathbf{y} \in V(t)} \left| \left(\boldsymbol{\mathcal{E}}_{\mathsf{H},\mathsf{h}}^{\mathrm{D}} \mathbf{u}_{\mathsf{H}}(\mathbf{x}) - \mathbf{u}(\mathbf{x})\right)_{\boldsymbol{\nu}(\mathbf{x}^\Gamma)} - \left(\boldsymbol{\mathcal{E}}_{\mathsf{H},\mathsf{h}}^{\mathrm{D}} \mathbf{u}_{\mathsf{H}}(\mathbf{y}) - \mathbf{u}(\mathbf{y})\right)_{\boldsymbol{\nu}(\mathbf{y}^\Gamma)} \right| \leq 2 \left|\boldsymbol{\mathcal{E}}_{\mathsf{H},\mathsf{h}}^{\mathrm{D}} \mathbf{u}_{\mathsf{H}} - \mathcal{I}_{\mathrm{t}} \mathbf{u}\right|_{0,\infty,t}.$$

The latter was already estimated twice, in Lemma 4.3 and in the proof of Theorem 4.5 (cf. (4.16)):

$$\begin{aligned}
& \left|\boldsymbol{\mathcal{E}}_{\mathsf{H},\mathsf{h}}^{\mathrm{D}} \mathbf{u}_{\mathsf{H}} - \mathcal{I}_{\mathrm{t}} \mathbf{u}\right|_{0,\infty,t} \\
& \qquad \leq \begin{cases} C(C_{\mathrm{int}}, C_1^{\mathcal{T}}, \rho, d) \left(\mathsf{h}_t^{\left(1-\frac{d}{2}\right)} \left|\mathcal{I}_{\mathrm{T}} \mathbf{u} - \mathcal{I}_{\mathrm{t}} \mathbf{u}\right|_{1,t} + \mathsf{h}_t^{\left(2-\frac{d}{2}\right)} \left|\mathbf{u}\right|_{2,\tilde{t}} \right), & t \in \hat{\mathcal{T}}^{\mathrm{T}} \\ C(C_{\mathrm{int}}, \rho, C_1^{\mathcal{T}}, C_2^{\mathcal{T}}, d) \left[\left(\mathsf{h}_t^{d-1} \mathsf{H}\right)^{\frac{1}{d}} \right]^{\left(2-\frac{d}{2}\right)} \left|\mathbf{u}\right|_{2,\omega_T}, & t \in \mathcal{T}^{\mathrm{T}} \setminus \hat{\mathcal{T}}^{\mathrm{T}}. \end{cases}
\end{aligned}$$

Due to the mean value theorem the second maximum is bounded by

$$\frac{1}{\rho}\,\mathsf{h}_t^{\left(1-\frac{d}{2}\right)}\left|\boldsymbol{\mathcal{E}}_{\mathsf{H},\mathsf{h}}\,\mathbf{u}_{\mathsf{H}}-\mathcal{I}_{\mathcal{T}_{\mathsf{H},\mathsf{h}}}\mathbf{u}\right|_{1,t}.$$

We choose some $\mathbf{x},\mathbf{y}$ in the set of vertices of t to bound the third one with the help of Lemma 4.1 and (4.19) by

$$\begin{aligned}
&\left|\left(\boldsymbol{\mathcal{E}}_{\mathsf{H},\mathsf{h}}\,\mathbf{u}_{\mathsf{H}}\left(\mathbf{x}\right)-\mathbf{u}\left(\mathbf{x}\right)\right)_{\boldsymbol{\nu}(\mathbf{x}^{\Gamma})}-\left(\boldsymbol{\mathcal{E}}_{\mathsf{H},\mathsf{h}}\,\mathbf{u}_{\mathsf{H}}\left(\mathbf{y}\right)-\mathbf{u}(\mathbf{y})\right)_{\boldsymbol{\nu}(\mathbf{y}^{\Gamma})}\right|\\
&\quad\leq\left(\left|\left(\boldsymbol{\mathcal{E}}_{\mathsf{H},\mathsf{h}}\,\mathbf{u}_{\mathsf{H}}\left(\mathbf{x}\right)-\mathbf{u}\left(\mathbf{x}\right)\right)-\left(\boldsymbol{\mathcal{E}}_{\mathsf{H},\mathsf{h}}\,\mathbf{u}_{\mathsf{H}}\left(\mathbf{y}\right)-\mathbf{u}(\mathbf{y})\right)\right|+\left|\boldsymbol{\mathcal{E}}_{\mathsf{H},\mathsf{h}}\,\mathbf{u}_{\mathsf{H}}\left(\mathbf{x}\right)-\mathbf{u}\left(\mathbf{x}\right)\right|\left|\boldsymbol{\nu}(\mathbf{x}^{\Gamma})-\boldsymbol{\nu}(\mathbf{y}^{\Gamma})\right|\right)\\
&\quad\leq\left(\left|\nabla\left(\boldsymbol{\mathcal{E}}_{\mathsf{H},\mathsf{h}}\,\mathbf{u}_{\mathsf{H}}-\mathcal{I}_{\mathrm{t}}\mathbf{u}\right)\cdot\left(\mathbf{x}-\mathbf{y}\right)\right|+C(\rho,d)\mathsf{h}_t^{\left(1-\frac{d}{2}\right)}C_{\boldsymbol{\nu}}\left\|\boldsymbol{\mathcal{E}}_{\mathsf{H},\mathsf{h}}\,\mathbf{u}_{\mathsf{H}}-\mathcal{I}_{\mathcal{T}_{\mathsf{H},\mathsf{h}}}\mathbf{u}\right\|_{0,t}\right)\\
&\quad\leq C(\rho,d)\mathsf{h}_t^{\left(1-\frac{d}{2}\right)}\left(\left|\boldsymbol{\mathcal{E}}_{\mathsf{H},\mathsf{h}}\,\mathbf{u}_{\mathsf{H}}-\mathcal{I}_{\mathrm{t}}\mathbf{u}\right|_{1,t}+C_{\boldsymbol{\nu}}\left\|\boldsymbol{\mathcal{E}}_{\mathsf{H},\mathsf{h}}\,\mathbf{u}_{\mathsf{H}}-\mathcal{I}_{\mathcal{T}_{\mathsf{H},\mathsf{h}}}\mathbf{u}\right\|_{0,t}\right).
\end{aligned}$$

Finally we get

$$\begin{aligned}
\left|\mathbf{u}_{\mathsf{H},\mathsf{h}}-\mathcal{I}_{\mathcal{T}_{\mathsf{H},\mathsf{h}}}\mathbf{u}\right|_{1,t}\leq C(C_{\mathrm{int}},C_1^{\mathcal{T}},\rho,d)\Big(&\left|\mathcal{I}_{\mathrm{T}}\mathbf{u}-\mathcal{I}_{\mathrm{t}}\mathbf{u}\right|_{1,t}+\mathsf{h}_t\left|\mathbf{u}\right|_{2,\tilde{t}}\\
&+\left|\boldsymbol{\mathcal{E}}_{\mathsf{H},\mathsf{h}}\,\mathbf{u}_{\mathsf{H}}-\mathcal{I}_{\mathrm{t}}\mathbf{u}\right|_{1,t}+C_{\boldsymbol{\nu}}\left\|\boldsymbol{\mathcal{E}}_{\mathsf{H},\mathsf{h}}\,\mathbf{u}_{\mathsf{H}}-\mathcal{I}_{\mathcal{T}_{\mathsf{H},\mathsf{h}}}\mathbf{u}\right\|_{0,t}\Big),
\end{aligned}$$

if $t\in\hat{\mathcal{T}}^{\mathrm{T}}$ and

$$\begin{aligned}
\left|\mathbf{u}_{\mathsf{H},\mathsf{h}}-\mathcal{I}_{\mathcal{T}_{\mathsf{H},\mathsf{h}}}\mathbf{u}\right|_{1,t}\leq C(C_{\mathrm{int}},\rho,C_1^{\mathcal{T}},C_2^{\mathcal{T}},d)\Bigg(&\mathsf{h}_t^{\left(\frac{d}{2}-1\right)}\left[\left(\mathsf{h}_t^{d-1}\mathsf{H}\right)^{\frac{1}{d}}\right]^{\left(2-\frac{d}{2}\right)}\left|\mathbf{u}\right|_{2,\omega_T}\\
&+\left|\boldsymbol{\mathcal{E}}_{\mathsf{H},\mathsf{h}}\,\mathbf{u}_{\mathsf{H}}-\mathcal{I}_{\mathrm{t}}\mathbf{u}\right|_{1,t}+C_{\boldsymbol{\nu}}\left\|\boldsymbol{\mathcal{E}}_{\mathsf{H},\mathsf{h}}\,\mathbf{u}_{\mathsf{H}}-\mathcal{I}_{\mathcal{T}_{\mathsf{H},\mathsf{h}}}\mathbf{u}\right\|_{0,t}\Bigg)
\end{aligned}$$

if $t\in\mathcal{T}^{\mathrm{T}}\setminus\hat{\mathcal{T}}^{\mathrm{T}}$. The rest is just summing up as in the proof of Theorem 4.5 and using Lemma 4.1 to estimate

$$\left|\boldsymbol{\mathcal{E}}_{\mathsf{H},\mathsf{h}}\,\mathbf{u}_{\mathsf{H}}-\mathcal{I}_{\mathcal{T}_{\mathsf{H},\mathsf{h}}}\mathbf{u}\right|_{m,(\bigcup_{t\in\mathcal{T}^{\mathrm{T}}}t)}\leq C\mathsf{H}^{(2-m)}\left|\mathbf{u}\right|_{2,\omega_T},\quad m=0,1.$$

■

4.2.3 The CME Pressure Space

As mentioned before we cannot use the pointwise interpolation operator to approximate the pressure $p\in\mathrm{H}^1(\Omega)$. Instead, we employ Lemma 4.2 for the proof of the approximation theorem.

Theorem 4.8 (Approximation property of $\mathbf{M}_{\mathsf{H}}^{\mathrm{CME}}$)
For every $p\in L_0^2(\Omega)\cap H^1(\Omega)$ there exists $p_{\mathsf{H}}\in M_{\mathsf{H}}^{\mathrm{CME}}$ such that

$$\left\|p-p_{\mathsf{H}}\right\|_{0,T}\leq C\,\mathrm{diam}(T)\left\|p\right\|_{1,\tilde{\omega}_T}\quad\forall T\in\mathcal{T}_{\mathsf{H}},\tag{4.20}$$

where $C=C(C_{\mathrm{qint}},\rho,d)>0$ is a constant and $\tilde{\omega}_T:=\bigcup_{\tau\in\omega_T}\omega_\tau$.

Furthermore we have the global estimate

$$\left\|p-p_{\mathsf{H}}\right\|_{0,\Omega}\leq C\mathsf{H}\left\|p\right\|_{1,\Omega},$$

where the constant C depends only on C_{ext}, ρ, and the constant of the local estimate.

Proof. For $p \in \mathrm{H}^1(\Omega)$ we define $p_{\mathsf{H}} := \mathcal{E}^{\mathrm{p}}_{\mathsf{H}}(\Pi_{\mathcal{T}^{\mathrm{dof}}_{\mathsf{H}}} p)$. We start by estimating the local error. For a simplex $T \in \mathcal{T}^{\mathrm{dof}}_{\mathsf{H}}$, p_{H} is equal to $\Pi_{\mathcal{T}_{\mathsf{H}}} p$ and the result follows directly from (4.6).

Let $T \in \mathcal{T}^{\Gamma}_{\mathsf{H}}$. Then

$$\begin{aligned}\left\|p - p_{\mathsf{H}}\right\|_{0,T} &\leq \left\|p - \Pi_{\mathcal{T}_{\mathsf{H}}} p\right\|_{0,T} + \left\|\Pi_{\mathcal{T}_{\mathsf{H}}} p - p_{\mathsf{H}}\right\|_{0,T} \\ &\leq C_{\mathrm{qint}} \operatorname{diam}(T) \left\|p\right\|_{1,\omega_T} + \left|T\right|^{\frac{1}{2}} \left\|\Pi_{\mathcal{T}_{\mathsf{H}}} p - p_{\mathsf{H}}\right\|_{\infty,T}.\end{aligned}$$

The infinity norm of the affine function equals the absolute value of $\left(\Pi_{\mathcal{T}_{\mathsf{H}}} p - p_{\mathsf{H}}\right)$ in some vertex $\mathbf{x} \in V(T)$, which can be estimated by using Lemma 4.2:

$$\begin{aligned}\left|\Pi_{\mathcal{T}_{\mathsf{H}}} p(\mathbf{x}) - p_{\mathsf{H}}(\mathbf{x})\right| &\leq \left|\Pi_{\mathcal{T}_{\mathsf{H}}} p(\mathbf{x}) - p_{T_{\mathbf{x}}}(\mathbf{x})\right| \\ &\leq \left\|\Pi_{\mathcal{T}_{\mathsf{H}}} p - p_{T_{\mathbf{x}}}\right\|_{\infty,T} \\ &\leq 3\left|T\right|^{-\frac{1}{2}} \left\|\Pi_{\mathcal{T}_{\mathsf{H}}} p - \Pi_{T_{\mathbf{x}}} p\right\|_{0,T} \\ &\leq C(C_{\mathrm{qint}}, \rho, d) \operatorname{diam}(T) \left|T\right|^{-\frac{1}{2}} \left\|p\right\|_{1,\tilde{\omega}_T}.\end{aligned}$$

Hence, (4.20) is proved. The global estimate follows immediately, since the overlap of $\tilde{\omega}_T$ can be controlled in terms of ρ. ∎

The preceding approximation result is one basic ingredient of the convergence analysis in the next section. Note that there was no restriction concerning the small scale parameter h. All results are also true for a one-scale method, i.e. $\mathcal{T}_{\mathsf{H},\mathsf{h}} = \mathcal{T}_{\mathsf{H}}$.

Further it is straightforward to generalize the theorems to the case of less regular solutions, say $\mathbf{u} \in \mathbf{H}^{1+s}(\Omega)$ and $p \in \mathrm{H}^{1+t}(\Omega)$ for $s, t \in (0,1)$ by using the interpolation theory of Sobolev spaces.

4.3 Stability and Convergence

In this section, we will investigate the unique solvability of the discrete composite mini element systems and the linear convergence of the method. To fit into the abstract framework of Section 2.2.1, we incorporate the pressure constraint into the space and consider the discrete problems that consist for Dirichlet boundary condition in *finding* $(\mathbf{u}_{\mathsf{H},\mathsf{h}}, p_{\mathsf{H}}) \in \mathbf{X}^{\mathrm{CME_D}}_{\mathsf{H},\mathsf{h}} \times M^{\mathrm{CME}}_{\mathsf{H}} \cap L^2_0(\Omega)$ *such that*

$$\begin{aligned} \mathfrak{a}(\mathbf{u}_{\mathsf{H},\mathsf{h}}, \mathbf{v}) \quad &+\mathfrak{b}(\mathbf{v}, p_{\mathsf{H}}) \quad &&= \langle \mathbf{f}, \mathbf{v} \rangle_{0,\Omega} \quad &&\forall \mathbf{v} \in \mathbf{X}^{\mathrm{CME_D}}_{\mathsf{H},\mathsf{h}}, \\ \mathfrak{b}(\mathbf{u}_{\mathsf{H},\mathsf{h}}, q) \quad & &&= 0 \quad &&\forall q \in \mathrm{M}^{\mathrm{CME}}_{\mathsf{H}} \cap \mathrm{L}^2_0(\Omega), \end{aligned} \tag{4.21}$$

and, for slip boundary condition, in *finding* $(\mathbf{u}_{\mathsf{H},\mathsf{h}}, p_{\mathsf{H}}) \in \mathbf{X}^{\mathrm{CME_s}}_{\mathsf{H},\mathsf{h}} \times M^{\mathrm{CME}}_{\mathsf{H}} \cap L^2_0(\Omega)$ *such that*

$$\begin{aligned} \mathfrak{a}(\mathbf{u}_{\mathsf{H},\mathsf{h}}, \mathbf{v}) \quad &+\mathfrak{b}(\mathbf{v}, p_{\mathsf{H}}) \quad &&= \langle \mathbf{f}, \mathbf{v} \rangle_{0,\Omega} \quad &&\forall \mathbf{v} \in \mathbf{X}^{\mathrm{CME_s}}_{\mathsf{H},\mathsf{h}}, \\ \mathbf{b}(\mathbf{u}_{\mathsf{H},\mathsf{h}}, q) \quad & &&= 0 \quad &&\forall q \in \mathrm{M}^{\mathrm{CME}}_{\mathsf{H}} \cap \mathrm{L}^2_0(\Omega). \end{aligned} \tag{4.22}$$

The problems (4.21) and (4.22) always have a unique solution if the bilinear form $\mathfrak{a}$ is coercive and $\mathfrak{b}$ fulfills the inf-sup condition. As a result of nonconformity it is not obvious that these properties are inherited by the continuous problems (2.15) and (2.20).

The stability proof makes use of the boundedness of the pressure extension $\mathcal{E}^{\mathrm{p}}_{\mathsf{H}}$.

Lemma 4.9
There is a constant $C_{\mathcal{E}^{\mathrm{p}}_{\mathsf{H}}} = C_{\mathcal{E}^{\mathrm{p}}_{\mathsf{H}}}(\rho, d)$ such that $\left\|\mathcal{E}^{\mathrm{p}}_{\mathsf{H}} p\right\|_{0,\Omega} \leq C_{\mathcal{E}^{\mathrm{p}}_{\mathsf{H}}} \|p\|_{0,\Omega^{\mathrm{dof}}}$ for all $p \in M^{\mathrm{mini}}_{\mathcal{T}^{\mathrm{dof}}_{\mathsf{H}}}$.

Proof. Let $p \in \mathrm{M}^{\mathrm{mini}}_{\mathcal{T}^{\mathrm{dof}}_{\mathsf{H}}}$. Then

$$\left\|\mathcal{E}^{\mathrm{p}}_{\mathsf{H}} p\right\|^2_{0,\Omega} \leq \sum_{T \in \mathcal{T}^{\mathrm{dof}}_{\mathsf{H}}} \left\|\mathcal{E}^{\mathrm{p}}_{\mathsf{H}} p\right\|^2_{0,T} + \sum_{T \in \mathcal{T}^{\Gamma}_{\mathsf{H}}} \left\|\mathcal{E}^{\mathrm{p}}_{\mathsf{H}} p\right\|^2_{0,T} \leq \sum_{T \in \mathcal{T}^{\mathrm{dof}}_{\mathsf{H}}} \|p\|^2_{0,T} + \sum_{T \in \mathcal{T}^{\Gamma}_{\mathsf{H}}} |T| \left\|\mathcal{E}^{\mathrm{p}}_{\mathsf{H}} p\right\|^2_{\infty,T}. \tag{4.23}$$

Since $\mathcal{E}^{\mathrm{p}}_{\mathsf{H}} p\,|_T$ takes its maximum on some simplex $T \in \mathcal{T}^{\Gamma}_{\mathsf{H}}$ in a vertex $\mathbf{x}_T \in V(T)$, there holds

$$\left\|\mathcal{E}^{\mathrm{p}}_{\mathsf{H}} p\right\|_{\infty,T} \leq \left\|p_{T_{\mathbf{x}_T}}\right\|_{\infty,T} \leq \left(1 + \frac{\operatorname{diam}(T_{\mathbf{x}_T})}{\operatorname{diam}(T)}\right) \left\|p_{T_{\mathbf{x}_T}}\right\|_{\infty,T_{\mathbf{x}_T}} \leq \frac{C(\rho, d)}{\sqrt{|T_{\mathbf{x}_T}|}} \|p\|_{0,T_{\mathbf{x}_T}},$$

where $p_{T_{\mathbf{x}_T}}$ denotes the extension of $p|_{T_{\mathbf{x}_T}}$ (by itself) to $\mathbb{R}^d$. We plug this into (4.23) and take into account that the overlap on an inner simplex T is bounded by the number of its neighbors, we get

$$\left\|\mathcal{E}^{\mathrm{p}}_{\mathsf{H}} p\right\|^2_{0,\Omega} \leq (1 + C(\rho, d)(\#\omega_T)) \sum_{T \in \mathcal{T}^{\mathrm{dof}}_{\mathsf{H}}} \|p\|^2_{0,T}$$

which finishes the proof, since the number of elements in ω_T can be bounded in terms of ρ. ∎

Now we can show that the composite mini element is stable for the boundary conditions under consideration. The notation "D/slip" means that a formulation holds for both, "*either Dirichlet or slip boundary condition*".

Theorem 4.10 (Stability)
$\mathbf{X}^{\mathrm{CME}_{\mathrm{D/s}}}_{\mathsf{H},\mathsf{h}} \times M^{\mathrm{CME}}_{\mathsf{H}}$ *is a stable pairing for all* $\mathsf{H} > 0$ *and all* $\mathsf{h} > 0$*, i.e. there is a constant* β^{CME} *which depends on* d*,* ρ*, and the discrete inf-sup constant of the mini element* β_{mini} *but neither on* H *or* h *such that*

$$\inf_{p_{\mathsf{H}} \in M^{\mathrm{CME}}_{\mathsf{H}} \cap L^2_0(\Omega)} \sup_{\mathbf{0} \neq \mathbf{u}_{\mathsf{H},\mathsf{h}} \in \mathbf{X}^{\mathrm{CME}_{\mathrm{D/s}}}_{\mathsf{H},\mathsf{h}}} \frac{\mathfrak{b}(\mathbf{u}_{\mathsf{H},\mathsf{h}}, p_{\mathsf{H}})}{\left\|\mathbf{u}_{\mathsf{H},\mathsf{h}}\right\|_{1,\Omega} \left\|p_{\mathsf{H}}\right\|_{0,\Omega}} \geq \beta^{\mathrm{CME}}.$$

Proof. We start with the stability of the classical mini element

$$\mathbf{X}^{\mathrm{mini_D}}_{\mathrm{dof}} \times \mathrm{M}^{\mathrm{mini}}_{\mathrm{dof}} := \mathbf{X}^{\mathrm{mini_D}}_{\mathcal{T}^{\mathrm{dof}}_H} \times \mathrm{M}^{\mathrm{mini}}_{\mathcal{T}^{\mathrm{dof}}_H}$$

with respect to the inner grid $\mathcal{T}^{\mathrm{dof}}_H$ on Ω^{dof}, which is known from (2.42):

$$\inf_{0 \neq p_{\mathsf{H}} \in \mathrm{M}^{\mathrm{mini}}_{\mathrm{dof}} \cap \mathrm{L}^2_0(\Omega^{\mathrm{dof}})} \sup_{\mathbf{0} \neq \mathbf{u}_{\mathsf{H}} \in \mathbf{X}^{\mathrm{mini_D}}_{\mathrm{dof}}} \frac{\mathfrak{b}_{\mathsf{H}}(\mathbf{u}_{\mathsf{H}}, p_{\mathsf{H}})}{\|p_{\mathsf{H}}\|_{0,\Omega^{\mathrm{dof}}} \|\mathbf{u}_{\mathsf{H}}\|_{1,\Omega}} \geq \beta_{\mathrm{mini}} > 0 \quad \forall \mathsf{H} > 0. \tag{4.24}$$

We define two mappings to transport the result to the composite mini element space.

The first one is just a slight modification of $\mathcal{E}^{\mathrm{p}}_{\mathsf{H}}$ in order to handle the L^2_0 intersections:

$$\begin{aligned} \tilde{\mathcal{E}}^{\mathrm{p}}_{\mathsf{H}} : \ \mathrm{M}^{\mathrm{mini}}_{\mathrm{dof}} \cap \mathrm{L}^2_0(\Omega^{\mathrm{dof}}) &\ \to \ \mathrm{M}^{\mathrm{CME}}_{\mathsf{H}} \cap \mathrm{L}^2_0(\Omega)\,, \\ q &\ \mapsto \ \mathcal{E}^{\mathrm{p}}_{\mathsf{H}} q - \frac{1}{|\Omega|} \int_\Omega \mathcal{E}^{\mathrm{p}}_{\mathsf{H}} q. \end{aligned}$$

Due to Lemma 4.9, $\tilde{\mathcal{E}}^{\mathrm{p}}_{\mathsf{H}}$ is bounded and $\|\tilde{\mathcal{E}}^{\mathrm{p}}_{\mathsf{H}} q\|_{0,\Omega} \leq 2C_{\mathcal{E}^{\mathrm{p}}_{\mathsf{H}}} \|p\|_{0,\Omega^{\mathrm{dof}}}$. Furthermore $\tilde{\mathcal{E}}^{\mathrm{p}}_{\mathsf{H}}$ is a bijection since $\mathcal{E}^{\mathrm{p}}_{\mathsf{H}}$ maps constants on constants and the preimage of a constant function is constant.

In a second step we construct a bounded mapping

$$\pi : \mathbf{X}^{\mathrm{mini_D}}_{\mathrm{dof}} \rightarrow \mathbf{X}^{\mathrm{CME_D}}_{\mathsf{H},\mathsf{h}}$$

satisfying

$$\int_{\Omega} \tilde{\mathcal{E}}^{\mathrm{p}}_{\mathsf{H}} q \operatorname{div} \pi\mathbf{u} = \int_{\Omega^{\mathrm{dof}}} q \operatorname{div} \mathbf{u} \qquad \forall q \in \mathrm{M}^{\mathrm{mini}}_{\mathrm{dof}}. \tag{4.25}$$

This step is similar to Fortin's lemma (cf. [Brezzi and Fortin, 1991], Proposition II.2.9), where such a mapping is employed to deduce the discrete stability from the continuous one.
Let us suppose for the moment that π exists. From (4.24) we know that

$$\forall q \in \mathrm{M}^{\mathrm{mini}}_{\mathrm{dof}} \ \exists \mathbf{u}_q \in \mathbf{X}^{\mathrm{mini_D}}_{\mathrm{dof}} \ : \ \int_{\Omega^{\mathrm{dof}}} q \operatorname{div} \mathbf{u}_q \geq \frac{\beta_{\mathrm{mini}}}{2} \|q\|_{0,\Omega^{\mathrm{dof}}} \|\mathbf{u}_q\|_{1,\Omega^{\mathrm{dof}}}.$$

The left-hand side can be replaced using (4.25) and the bijectivity of $\tilde{\mathcal{E}}^{\mathrm{p}}_{\mathsf{H}}$ which leads to:

$$\forall p_{\mathsf{H}} \in \mathrm{M}^{\mathrm{CME}}_{\mathsf{H}} \cap \mathrm{L}^2_0 \ \exists q \in \mathrm{M}^{\mathrm{mini}}_{\mathrm{dof}}, \mathbf{u}_q \in \mathbf{X}^{\mathrm{mini_D}}_{\mathrm{dof}} \ : \ p_{\mathsf{H}} = \tilde{\mathcal{E}}^{\mathrm{p}}_{\mathsf{H}} q \quad \text{and}$$
$$\int_{\Omega} p_{\mathsf{H}} \operatorname{div} \pi\mathbf{u}_q = \int_{\Omega^{\mathrm{dof}}} q \operatorname{div} \mathbf{u}_q \geq \frac{\beta_{\mathrm{mini}}}{2} \|q\|_{0,\Omega^{\mathrm{dof}}} \|\mathbf{u}_q\|_{1,\Omega^{\mathrm{dof}}}.$$

With the help of the operator norm C_π of π and $C_{\mathcal{E}^{\mathrm{p}}_{\mathsf{H}}}$ we get

$$\inf_{p_{\mathsf{H}} \in \mathrm{M}^{\mathrm{CME}}_{\mathsf{H}} \cap \mathrm{L}^2_0(\Omega)} \sup_{\mathbf{0} \neq \mathbf{u}_{\mathsf{H},\mathsf{h}} \in \mathbf{X}^{\mathrm{CME_D}}_{\mathsf{H},\mathsf{h}}} \frac{\mathfrak{b}(\mathbf{u}_{\mathsf{H},\mathsf{h}}, p_{\mathsf{H}})}{\|\mathbf{u}_{\mathsf{H},\mathsf{h}}\|_{1,\Omega} \|p_{\mathsf{H}}\|_{0,\Omega}} \geq \frac{\beta_{\mathrm{mini}}}{4 C_{\mathcal{E}^{\mathrm{p}}_{\mathsf{H}}} C_\pi}.$$

So it remains to define π: Let $\mathbf{u} \in \mathbf{X}^{\mathrm{mini_D}}_{\mathrm{dof}}$. If we extend $\mathbf{u} \in \mathbf{X}^{\mathrm{mini_D}}_{\mathrm{dof}}$ by zero using $\boldsymbol{\mathcal{E}}^{\mathbf{0}}$ (see (3.7)) we can map the result $\boldsymbol{\mathcal{E}}^{\mathbf{0}}\mathbf{u}$ onto $\mathbf{X}^{\mathrm{CME_D}}_{\mathsf{H},\mathsf{h}}$ using the orthogonal projection $\mathcal{P}_{\mathbf{X}^{\mathrm{CME_D}}_{\mathsf{H},\mathsf{h}}}$. In view of Theorem 2.1 and the subsequent remark there is a unique $\mathbf{u}^* \in \mathbf{X}^{\mathrm{mini_D}}_{\mathrm{dof}}$ satisfying the following Stokes problem of Dirichlet type in Ω^{dof}:

$$\begin{aligned} \int_{\Omega^{\mathrm{dof}}} \mathrm{D}(\mathbf{u}^*) : \mathrm{D}(\mathbf{v}) - \int_{\Omega^{\mathrm{dof}}} p \operatorname{div} \mathbf{v} &= \mathbf{0} \qquad \forall \mathbf{v} \in \mathbf{X}^{\mathrm{mini_D}}_{\mathrm{dof}} \\ \int_{\Omega^{\mathrm{dof}}} q \operatorname{div} \mathbf{u}^* &= g(q) \quad \forall q \in \mathrm{M}^{\mathrm{mini}}_{\mathrm{dof}} \cap \mathrm{L}^2_0(\Omega^{\mathrm{dof}}), \end{aligned}$$

where the linear form $g : \mathrm{M}^{\mathrm{mini}}_{\mathrm{dof}} \cap \mathrm{L}^2_0(\Omega^{\mathrm{dof}}) \rightarrow \mathbb{R}$ is given by

$$g(q) := \int_{\Omega} \tilde{\mathcal{E}}^{\mathrm{p}}_{\mathsf{H}} q \operatorname{div}(\boldsymbol{\mathcal{E}}^{\mathbf{0}}\mathbf{u} - \mathcal{P}_{\mathbf{X}^{\mathrm{CME_D}}_{\mathsf{H},\mathsf{h}}} \boldsymbol{\mathcal{E}}^{\mathbf{0}}\mathbf{u}).$$

We define

$$\pi\mathbf{u} := \mathcal{P}_{\mathbf{X}^{\mathrm{CME_D}}_{\mathsf{H},\mathsf{h}}} \boldsymbol{\mathcal{E}}^{\mathbf{0}}\mathbf{u} + \boldsymbol{\mathcal{E}}^{\mathbf{0}}\mathbf{u}^*.$$

Therefore condition (4.25) is obviously fulfilled. The operator π is bounded because of the boundedness of the orthogonal projection (2.11) and Lemma 4.9:

$$\begin{aligned} \|\pi\mathbf{u}\|_{1,\Omega} &\leq \|\mathbf{u}\|_{1,\Omega^{\mathrm{dof}}} + C^* \left(\sup_{0 \neq q \in \mathrm{M}^{\mathrm{mini}}_{\mathrm{dof}} \cap \mathrm{L}^2_0(\Omega^{\mathrm{dof}})} \frac{|g(q)|}{\|q\|_{0,\Omega^{\mathrm{dof}}}} \right) \\ &\leq \underbrace{\left(1 + C^*(1 + 3C_{\mathcal{E}^{\mathrm{p}}_{\mathsf{H}}})\right)}_{=C_\pi} \|\mathbf{u}\|_{1,\Omega^{\mathrm{dof}}}. \end{aligned}$$

For the stability proof of $\mathbf{X}_{\mathsf{H},\mathsf{h}}^{\mathrm{CME_s}} \times \mathrm{M}_{\mathsf{H}}^{\mathrm{CME}}$ we project onto $\mathbf{X}_{\mathsf{H},\mathsf{h}}^{\mathrm{CME_s}}$ by an orthogonal projection $\mathcal{P}_{\mathbf{X}_{\mathsf{H},\mathsf{h}}^{\mathrm{CME_s}}}$ and obtain the analogue result. ∎

It is remarkable that we deduced stability from the mini element with respect to the triangulation $\mathcal{T}_{\mathsf{H}}^{\mathrm{dof}}$ and not from the continuous result on the complicated domain Ω.

The next lemma addresses the boundary resolution of the two scale grid $\mathcal{T}_{\mathsf{H},\mathsf{h}}$.

Lemma 4.11 (Nonconformity)
There is a constant $C = C(\rho, C_3^{\mathcal{T}})$ such that the following estimates hold for all $T \in \mathcal{T}_{\mathsf{H}}^{\Gamma}$:

(a) $\big\|\mathbf{u}_{\mathsf{H},\mathsf{h}}\big\|_{0,\Gamma\cap T} \leq C\Big(\max_{t\in\mathrm{sons}(T):t\cap\Gamma\neq\emptyset} \mathrm{diam}(t)\Big)\,\mathrm{diam}(T)^{-\frac{1}{2}}\big|\mathbf{u}_{\mathsf{H},\mathsf{h}}\big|_{1,\omega_T} \quad \forall \mathbf{u}_{\mathsf{H},\mathsf{h}} \in \mathbf{X}_{\mathsf{H},\mathsf{h}}^{\mathrm{CME_D}}$,

(b) $\big\|\langle \mathbf{u}_{\mathsf{H},\mathsf{h}}, \boldsymbol{\nu}\rangle\big\|_{0,\Gamma\cap T} \leq C\,(1+C_{\boldsymbol{\nu}})\Big(\max_{t\in\mathrm{sons}(T):t\cap\Gamma\neq\emptyset} \mathrm{diam}(t)\Big)\,\mathrm{diam}(T)^{-\frac{1}{2}}\big|\mathbf{u}_{\mathsf{H},\mathsf{h}}\big|_{1,\omega_T}\ \forall \mathbf{u}_{\mathsf{H},\mathsf{h}} \in \mathbf{X}_{\mathsf{H},\mathsf{h}}^{\mathrm{CME_s}}$.

Proof. First we prove the Dirichlet case (a). Let $T \in \mathcal{T}_{\mathsf{H}}^{\Gamma}$ and $t \in \mathcal{T}_{\mathsf{H},\mathsf{h}}^{\Gamma}$ such that $t \subseteq T$ and $t \cap \Gamma \neq \emptyset$. We start estimating the value of $\mathbf{u}_{\mathsf{H},\mathsf{h}}$ in a vertex $\mathbf{x}$ of t:

$$\big|\mathbf{u}_{\mathsf{H},\mathsf{h}}(\mathbf{x})\big| \leq \mathrm{diam}(t)\big|\nabla(\mathbf{u}_{\mathsf{H},\mathsf{h}}|_{T_{\mathbf{x}}})\big| \leq \frac{\mathrm{diam}(t)}{\sqrt{|T_{\mathbf{x}}|}}\big|\mathbf{u}_{\mathsf{H},\mathsf{h}}\big|_{1,T_{\mathbf{x}}}. \tag{4.26}$$

Now we can estimate the $\mathbf{L}^2$-norm of $\mathbf{u}_{\mathsf{H},\mathsf{h}}$ on $\Gamma \cap T$. We use Cauchy-Schwarz inequality and bound the maximum of $\mathbf{u}_{\mathsf{H},\mathsf{h}}$ on $\Gamma \cap t$ by (4.26):

$$\begin{aligned}
\big\|\mathbf{u}_{\mathsf{H},\mathsf{h}}\big\|_{0,\Gamma\cap T}^2 &\leq \sum_{t\in\mathrm{sons}(T):t\cap\Gamma\neq\emptyset} \big|\Gamma\cap t\big|\big|\mathbf{u}_{\mathsf{H},\mathsf{h}}\big|_{\infty,t}^2 \\
&\overset{(4.26)}{\leq} C(\rho) \sum_{t\in\mathrm{sons}(T):t\cap\Gamma\neq\emptyset} \frac{\big|\Gamma\cap t\big|\,\mathrm{diam}(t)^2}{|T_t|}\big|\mathbf{u}_{\mathsf{H},\mathsf{h}}\big|_{1,T_t}^2 \\
&\leq C(\rho)\big|\Gamma\cap T\big|\frac{\mathrm{diam}(t)^2}{\mathrm{diam}(T)^d}\big|\mathbf{u}_{\mathsf{H},\mathsf{h}}\big|_{1,\omega_T}^2 \\
&\leq C(\rho)\underbrace{\left(\max_{T\in\mathcal{T}_{\mathsf{H}}^{\Gamma}} \frac{\big|\Gamma\cap T\big|}{\mathrm{diam}(T)^{(d-1)}}\right)}_{=:C_3^{\mathcal{T}}}\frac{\mathrm{diam}(t)^2}{\mathrm{diam}(T)}\big|\mathbf{u}_{\mathsf{H},\mathsf{h}}\big|_{1,\omega_T}^2.
\end{aligned}$$

It remains to sum up the seminorms using some usual bounded overlap argument.

To prove the slip inequality (b), let $\mathbf{u} \in \mathbf{S}_{\mathcal{T}_{\mathsf{H}}^{\mathrm{dof}}}$ such that $\mathbf{u}_{\mathsf{H},\mathsf{h}} = \boldsymbol{\mathcal{E}}_{\mathsf{H},\mathsf{h}}^{\mathrm{s}}\,\mathbf{u}$ and let $t \in \mathcal{T}_{\mathsf{H},\mathsf{h}}^{\Gamma}$ such that $t \cap \Gamma \neq \emptyset$. By $\{\phi_{t,i}\}_{i=1}^{d+1}$ we denote the affine nodal basis with respect to t. We start with an

L^∞-estimate:

$$\begin{aligned}
\left|\left\langle \mathbf{u}_{\mathsf{H},\mathsf{h}}, \boldsymbol{\nu}\right\rangle\right|_{\infty,\Gamma\cap t} &\leq \sup_{\mathbf{x}\in\Gamma\cap t}\left|\left\langle \sum_{\mathbf{x}_i\in V(t)} \phi_{t,i}(\mathbf{x})\mathbf{u}_{\mathsf{H},\mathsf{h}}(\mathbf{x}_i), \boldsymbol{\nu}(\mathbf{x})\right\rangle\right| \\
&\leq \sup_{\mathbf{x}\in\Gamma\cap t}\Big|\sum_{\mathbf{x}_i\in V(t)} \phi_{t,i}(\mathbf{x})\left\langle \mathbf{u}_{\mathsf{H},\mathsf{h}}(\mathbf{x}_i), \boldsymbol{\nu}(\mathbf{x})\right\rangle\Big| \\
&\leq \sup_{\mathbf{x}\in\Gamma\cap t}\max_{\mathbf{x}_i\in V(t)}\Big(\Big|\Big\langle \boldsymbol{\mathcal{E}}^{\mathrm{D}}_{\mathsf{H},\mathsf{h}}\mathbf{u}(\mathbf{x}_i), \boldsymbol{\nu}(\mathbf{x}_i^\Gamma)\Big\rangle\left\langle \boldsymbol{\nu}(\mathbf{x}_i^\Gamma), \boldsymbol{\nu}(\mathbf{x})\right\rangle\Big| \\
&\qquad\qquad + \Big|\left\langle \boldsymbol{\mathcal{E}}_{\mathsf{H},\mathsf{h}}\mathbf{u}(\mathbf{x}_i), \boldsymbol{\nu}(\mathbf{x})\right\rangle - \left\langle \boldsymbol{\mathcal{E}}_{\mathsf{H},\mathsf{h}}\mathbf{u}(\mathbf{x}_i), \boldsymbol{\nu}(\mathbf{x}_i^\Gamma)\right\rangle\left\langle \boldsymbol{\nu}(\mathbf{x}_i^\Gamma), \boldsymbol{\nu}(\mathbf{x})\right\rangle\Big|\Big) \\
&\leq \left|\boldsymbol{\mathcal{E}}^{\mathrm{D}}_{\mathsf{H},\mathsf{h}}\mathbf{u}\right|_{\infty,t} + C_{\boldsymbol{\nu}}\operatorname{diam}(t)\left|\boldsymbol{\mathcal{E}}_{\mathsf{H},\mathsf{h}}\mathbf{u}\right|_{\infty,t}.
\end{aligned}$$

Since

$$\left\|\boldsymbol{\mathcal{E}}_{\mathsf{H},\mathsf{h}}\mathbf{u}\right\|_{\infty,t} \leq \left\|\boldsymbol{\mathcal{E}}_{\mathsf{H},\mathsf{h}}\mathbf{u}\right\|_{\infty,T} \leq C(\rho)\frac{1}{\operatorname{diam}(T)^{\frac{d}{2}}}\left\|\boldsymbol{\mathcal{E}}_{\mathsf{H},\mathsf{h}}\mathbf{u}\right\|_{0,T}$$

for $T \in \mathcal{T}_\mathsf{H}$ such that $t \subseteq T$, we get

$$\begin{aligned}
\left\|\mathbf{u}_{\mathsf{H},\mathsf{h}}\right\|^2_{0,\Gamma\cap T} &\leq C(\rho)\left|\Gamma\cap T\right|\frac{\operatorname{diam}(t)^2}{\operatorname{diam}(T)^d}\left(\left|\boldsymbol{\mathcal{E}}^{\mathrm{D}}_{\mathsf{H},\mathsf{h}}\mathbf{u}\right|^2_{1,T_t} + C_{\boldsymbol{\nu}}^2\left\|\boldsymbol{\mathcal{E}}_{\mathsf{H},\mathsf{h}}\mathbf{u}\right\|^2_{0,T}\right) \\
&\leq C(\rho)\frac{\left|\Gamma\cap T\right|}{\operatorname{diam}(T)^{(d-1)}}\frac{\operatorname{diam}(t)^2}{\operatorname{diam}(T)}\left(1 + C_{\boldsymbol{\nu}}^2\right)\left\|\mathbf{u}_{\mathsf{H},\mathsf{h}}\right\|^2_{1,\omega_T}.
\end{aligned}$$

■

Lemma 4.11 gives resolution conditions on the overlapping two scale grids of our method. In contrast to the conditions of Section 2.2.3 they can be satisfied by adapting only the fine scale parameter h. This has no influence on the space dimension. In particular, h has to be chosen such that the constant

$$C_K := \max_{T\in\mathcal{T}_\mathsf{H}^\Gamma}\frac{\max_{t\in\operatorname{sons}(T):t\cap\Gamma\neq\emptyset}\operatorname{diam}(t)}{\operatorname{diam}(T)^{\frac{1}{2}}} \tag{4.27}$$

is moderate. For quasi uniform inner grids $\mathcal{T}_\mathsf{H}^{\mathrm{dof}}$ we deduce that the small scale h should be of order $\mathsf{H}^{\frac{3}{2}}$ to preserve the linear convergence. This is optimal as long as the grid is overlapping. If it resolves the domain it is of course sufficient that the fine scale parameter satisfies the standard resolution conditions as proposed in Section 2.2.3. The overlapping approach should not be used if the large scale H is small enough to resolve the domain. In such situations it should be possible to adapt the grid slightly to make it resolving.

The previous lemma also helps to investigate the coercivity of the bilinear form $\mathfrak{a}$ on $\mathbf{X}^{\mathrm{CME_D}}_{\mathsf{H},\mathsf{h}}$ and $\mathbf{X}^{\mathrm{CME_s}}_{\mathsf{H},\mathsf{h}}$ which is the last prerequisite to prove the unique solvability of the discrete problems. Since $\mathfrak{a}$ is coercive on $\mathbf{H}^1_{\mathrm{D/s}}(\Omega)$, it is also coercive on a certain neighborhood of $\mathbf{H}^1_{\mathrm{D/s}}(\Omega)$. By introducing equivalent norms in $\mathbf{H}^1(\Omega)$ the following lemma will show that this neighborhood can be measured by the L^2-norm of the (normal) trace. This will give us discrete coercivity provided the nonconformity in the spaces is small enough, i.e. grid size H is small enough (cf. Lemma 4.11). In Lemma 4.13, the results will be extended to arbitrary values of H.

Lemma 4.12 (Equivalent norms in $\mathbf{H}^1(\Omega)$)

(a) *There is a constant $C > 0$ that does not depend on $\mathbf{u}$ such that*

$$\|\mathbf{u}\|_{1,\Omega}^2 \leq 2\alpha_{\mathrm{D}}^{-1}\mathfrak{a}(\mathbf{u},\mathbf{u}) + (1+2\alpha_{\mathrm{D}}^{-1})C\,\|\mathbf{u}\|_{0,\Gamma}^2 \qquad \forall \mathbf{u} \in \mathbf{H}^1(\Omega)$$

where α_{D} denotes the coercivity constant of $\mathfrak{a}$ with respect to $\mathbf{H}^1_{\mathrm{D}}(\Omega)$ (cf. (2.18)*).*

(b) *Furthermore, if $\mathfrak{a}$ is coercive with respect to $\mathbf{H}^1_{\mathrm{s}}(\Omega)$, i.e.* (2.22) *is true, then there is a constant $C > 0$ such that*

$$\|\mathbf{u}\|_{1,\Omega}^2 \leq 2\alpha_{\mathrm{s}}^{-1}\mathfrak{a}(\mathbf{u},\mathbf{u}) + (1+2\alpha_{\mathrm{s}}^{-1})C\,\|\langle \mathbf{u}, \boldsymbol{\nu}\rangle\|_{0,\Gamma}^2 \qquad \forall \mathbf{u} \in \mathbf{H}^1(\Omega)\,,$$

where C does not depend on $\mathbf{u}$.

Proof. An inequality similar to (b) and therefore implying (a) was proved by Verfürth [1985]. For completeness we present a proof based on the extension of the known inequalities (2.18) and (2.22).

We start proving (a). Given $\mathbf{u} \in \mathbf{H}^1(\Omega)$, let $\mathbf{u}^* \in \mathbf{H}^1_{\mathrm{D}}(\Omega)$ denote its $\mathbf{H}^1$-projection onto the subspace $\mathbf{H}^1_{\mathrm{D}}(\Omega)$, i.e.

$$\langle \mathbf{u}^*, \mathbf{v}\rangle_{\mathbf{H}^1(\Omega)} = \langle \mathbf{u}, \mathbf{v}\rangle_{\mathbf{H}^1(\Omega)} \quad \forall \mathbf{v} \in \mathbf{H}^1_{\mathrm{D}}(\Omega)$$

We can bound $\|\mathbf{u}\|_{1,\Omega}$ using the coercivity of $\mathfrak{a}$ with respect to $\mathbf{H}^1_{\mathrm{D}}(\Omega)$ (cf. (2.18)) and $\|\mathfrak{a}\| = 1$ as follows

$$\begin{aligned}
\|\mathbf{u}\|_{1,\Omega}^2 &= \|\mathbf{u}^*\|_{1,\Omega}^2 + \|\mathbf{u}-\mathbf{u}^*\|_{1,\Omega}^2 \leq \alpha_{\mathrm{D}}^{-1}\mathfrak{a}(\mathbf{u}^*,\mathbf{u}^*) + \|\mathbf{u}-\mathbf{u}^*\|_{1,\Omega}^2 \\
&\leq 2\alpha_{\mathrm{D}}^{-1}\big(\mathfrak{a}(\mathbf{u},\mathbf{u}) + \mathfrak{a}(\mathbf{u}^*-\mathbf{u},\mathbf{u}^*-\mathbf{u})\big) + \|\mathbf{u}-\mathbf{u}^*\|_{1,\Omega}^2 \\
&\leq 2\alpha_{\mathrm{D}}^{-1}\mathfrak{a}(\mathbf{u},\mathbf{u}) + (1+2\alpha_{\mathrm{D}}^{-1})\|\mathbf{u}-\mathbf{u}^*\|_{1,\Omega}^2
\end{aligned} \tag{4.28}$$

If we now could proof the existence of a constant C such that

$$\|\mathbf{u}-\mathbf{u}^*\|_{1,\Omega} \leq C\|\mathbf{u}-\mathbf{u}^*\|_{0,\Gamma}\ \big(= C\|\mathbf{u}\|_{0,\Gamma}\big), \tag{4.29}$$

then we were finished. Inequality (4.29) cannot be true for an arbitrary $\mathbf{H}^1(\Omega)$-function, since a suitable bounded lifting operator can only be defined on $\mathbf{H}^{\frac{1}{2}}(\Gamma)$. We have to use the fact that $\mathbf{u}-\mathbf{u}^*$ is perpendicular to $\mathbf{H}^1_{\mathrm{D}}(\Omega)$. Let us introduce the set of functions with the same property:

$$\mathbf{H}^1_{\mathrm{D}}(\Omega)^{\perp} := \{\mathbf{u} \in \mathbf{H}^1(\Omega)\ \mid\ \langle \mathbf{u}, \mathbf{v}\rangle_{\mathbf{H}^1(\Omega)} = \mathbf{0} \quad \forall \mathbf{v} \in \mathbf{H}^1_{\mathrm{D}}(\Omega)\}.$$

We collect the traces of $\mathbf{H}^1_{\mathrm{D}}(\Omega)^{\perp}$- functions in the space $\mathrm{tr}\big(\mathbf{H}^1_{\mathrm{D}}(\Omega)^{\perp}\big) \subseteq \mathbf{H}^{\frac{1}{2}}(\Gamma)$. If $\|\mathbf{u}_1-\mathbf{u}_2\|_{0,\Gamma} = 0$ for any two different $\mathbf{u}_1, \mathbf{u}_2 \in \mathbf{H}^1_{\mathrm{D}}(\Omega)^{\perp}$ then $\|\mathbf{u}_1-\mathbf{u}_2\|_{\frac{1}{2},\Gamma} = 0$, which means that $\mathbf{u}_1-\mathbf{u}_2 \in \mathbf{H}^1_{\mathrm{D}}(\Omega)$. Since on the other hand $\mathbf{u}_1-\mathbf{u}_2 \in \mathbf{H}^1_{\mathrm{D}}(\Omega)^{\perp}$, we get $\mathbf{u}_1-\mathbf{u}_2 = \mathbf{0}$. So the trace operator is a bijection that maps the Banach space $\big(\mathbf{H}^1_{\mathrm{D}}(\Omega)^{\perp}, \|\cdot\|_{1,\Omega}\big)$ onto the Banach space $\big(\mathrm{tr}(\mathbf{H}^1_{\mathrm{D}}(\Omega)^{\perp}), \|\cdot\|_{0,\Gamma}\big)$. It is well known that the trace operator is bounded (see for instance [Brenner and Scott, 1994]), i.e.

$$\|\mathbf{u}\|_{0,\Gamma} \leq C_{\mathrm{trace}}\|\mathbf{u}\|_{1,\Omega} \qquad \forall \mathbf{w} \in \mathbf{H}^1(\Omega)\,.$$

Therefore, by the inverse-mapping theorem, the inverse trace operator[3] is bounded, i.e. there is a constant C such that

$$\|\mathbf{u}\|_{1,\Omega} \leq C\|\mathbf{u}\|_{0,\Gamma} \qquad \forall \mathbf{u} \in \mathbf{H}^1_{\mathrm{D}}(\Omega)^{\perp}\,.^{4}$$

This proves (4.29).

Assertion (b) can be proved in an analogue way using the normal trace operator mapping $\mathbf{H}^1(\Omega)$-function to the normal components of its traces. $\mathbf{H}^1_{\mathrm{D}}(\Omega)$ needs to replaced by $\mathbf{H}^1_{\mathrm{s}}(\Omega)$ on which $\mathfrak{a}$ is supposed to be coercive. ∎

Lemma 4.13 (Unique discrete solvability)

(a) *The discrete problem with Dirichlet boundary condition (4.21) has a unique solution for all large scale discretization parameters* $\mathsf{H} > 0$ *and for all small scale parameters* $\mathsf{h} > 0$.

(b) *For all large scale discretization parameters* $\mathsf{H} > 0$ *there is a small scale parameter* $\mathsf{h}_0 > 0$ *that only depends on the domain* Ω *such that the discrete problem with slip boundary conditions (4.22) has a unique solution for all* $\mathsf{h} \leq \mathsf{h}_0$.

Proof. In Lemma 4.11 we have seen that the nonconformity tends to zero as H tends to zero. This does not depend on the small scale h since $\mathsf{h} \leq \mathsf{H}$ and the right-hand sides in Lemma 4.11 contain at least a factor $\sqrt{\mathsf{H}}$. So, in view of Lemma 4.12, there is an H_0 such that the bilinear form is coercive for all $\mathsf{H} \leq \mathsf{H}_0$. The case $\mathsf{H} > \mathsf{H}_0$ is discussed in what follows.

(a) Due to (2.23) it remains to show that $\mathbf{X}^{\mathrm{CME_D}}_{\mathsf{H},\mathsf{h}} \cap \mathcal{R} = \{\mathbf{0}\}$, where $\mathcal{R}$ is the set of rigid body motions:

$$\mathcal{R} = \{\mathbf{A}\mathbf{x} + \mathbf{b} \mid \mathbf{A} \in \mathbb{R}^{d\times d} \text{ skew symmetric}, \mathbf{b} \in \mathbb{R}^d\}.$$

Let $\mathbf{u}_{\mathsf{H},\mathsf{h}} \in \mathbf{X}^{\mathrm{CME_D}}_{\mathsf{H},\mathsf{h}}$, $\mathbf{A} \in \mathbb{R}^{d\times d}$ be skew symmetric and $\mathbf{b} \in \mathbb{R}^d$ such that $\mathbf{u}_{\mathsf{H},\mathsf{h}}(\mathbf{x}) = \mathbf{A}\mathbf{x} + \mathbf{b}$. Then, by definition, $\mathbf{u}_{\mathsf{H},\mathsf{h}}(\mathbf{x}) = \mathbf{A}\mathbf{x} + \mathbf{b} = \mathbf{A}\left(\mathbf{x} - \mathbf{x}^{\Gamma}\right)$ in a slave node $\mathbf{x}$ and we get

$$\mathbf{A}\mathbf{x}^{\Gamma} = -\mathbf{b} \qquad \forall \mathbf{x}^{\Gamma} \in \{\mathbf{x}^{\Gamma}_i \mid \mathbf{x}_i \in \Theta^{\Gamma}_{\mathsf{H},\mathsf{h}}\}.$$

Since

$$\operatorname{span}\{\mathbf{x}^{\Gamma}_i \mid \mathbf{x}_i \in \Theta^{\Gamma}_{\mathsf{H},\mathsf{h}}\} = \mathbb{R}^d \quad \forall \mathsf{H} > 0\ \forall \mathsf{h} > 0$$

this can only be true if $\mathbf{A} = \mathbf{0}$ and $\mathbf{b} = \mathbf{0}$.

(b) Let $\mathbf{u}_{\mathsf{H},\mathsf{h}} \in \mathbf{X}^{\mathrm{CME_s}}_{\mathsf{H},\mathsf{h}}$, $\mathbf{A} \in \mathbb{R}^{d\times d}$ be skew symmetric and $\mathbf{b} \in \mathbb{R}^d$ such that $\mathbf{u}_{\mathsf{H},\mathsf{h}}(\mathbf{x}) = \mathbf{A}\mathbf{x} + \mathbf{b}$. Then, by definition, we get

$$\left\langle \mathbf{A}\mathbf{x}^{\Gamma} - \mathbf{b}, \boldsymbol{\nu}(\mathbf{x}^{\Gamma})\right\rangle = 0 \qquad \forall \mathbf{x}^{\Gamma} \in \{\mathbf{x}^{\Gamma}_i \mid \mathbf{x}_i \in \Theta^{\Gamma}_{\mathsf{H},\mathsf{h}}\}.$$

However, this does not imply $\mathbf{X}^{\mathrm{CME_s}}_{\mathsf{H},\mathsf{h}} \cap \mathcal{R} = \{\mathbf{0}\}$. We have to exclude the following case: $\{\mathbf{x}^{\Gamma}_i \mid \mathbf{x}_i \in \Theta^{\Gamma}_{\mathsf{H},\mathsf{h}}\}$ is a subset of ∂G where G is rotationally symmetric with respect to an axis and $\boldsymbol{\nu}_G(\mathbf{x}^{\Gamma}) = \boldsymbol{\nu}(\mathbf{x}^{\Gamma})$ for all $\mathbf{x}^{\Gamma} \in \{\mathbf{x}^{\Gamma}_i \mid \mathbf{x}_i \in \Theta^{\Gamma}_{\mathsf{H},\mathsf{h}}\}$. This can be done for arbitrary H by choosing the small scale h small enough.

[3] The inverse trace operator, often called lifting operator, assigns the solution of the (uniquely solvable) variational problem $\left[\ \langle \mathbf{u}, \mathbf{v}\rangle_{\mathbf{H}^1(\Omega)} = \mathbf{0}\ \ \forall \mathbf{v} \in \mathbf{H}^1_{\mathrm{D}}(\Omega)\,,\quad \mathbf{u}|_{\Gamma} = \mathbf{g}\ \right]$ to every trace function $\mathbf{g} \in \mathfrak{tr}(\mathbf{H}^1_{\mathrm{D}}(\Omega)^{\perp})$.

[4] This means that $\|\cdot\|_{0,\Gamma}$ and $\|\cdot\|_{\frac{1}{2},\Gamma}$ are equivalent norms in $\mathfrak{tr}(\mathbf{H}^1_{\mathrm{D}}(\Omega)^{\perp})$.

■

Finally, we come to the main result on the convergence of the composite finite element solution in the case of the Dirichlet as well as the slip boundary condition.

Theorem 4.14 (Convergence)

(a) *Let* $(\mathbf{u},p)\in\left(\mathbf{H}^1_{\mathrm{D}}\cap\mathbf{H}^2(\Omega)\right)\times\left(L^2_0(\Omega)\cap H^1(\Omega)\right)$ *be the solution of (2.15) and let* $(\mathbf{u}_{\mathsf{H},\mathsf{h}},p_{\mathsf{H}})\in\mathbf{X}^{\mathrm{CME_D}}_{\mathsf{H},\mathsf{h}}\times M^{\mathrm{CME}}_{\mathsf{H}}\cap L^2_0(\Omega)$ *be the unique solution of (4.21). Then there is a* $C>0$*, such that*

$$\left\|\mathbf{u}-\mathbf{u}_{\mathsf{H},\mathsf{h}}\right\|_{1,\Omega}+\left\|p-p_{\mathsf{H}}\right\|_{0,\Omega}\leq C_{\mathrm{D}}\mathsf{H}\left\|\mathbf{f}\right\|_{0,\Omega}.$$

(b) *Let* $(\mathbf{u},p)\in\left(\mathbf{H}^1_{\mathrm{s}}\cap\mathbf{H}^2(\Omega)\right)\times\left(L^2_0(\Omega)\cap H^1(\Omega)\right)$ *be the solution of (2.20) and let* $(\mathbf{u}_{\mathsf{H},\mathsf{h}},p_{\mathsf{H}})\in\mathbf{X}^{\mathrm{CME_s}}_{\mathsf{H},\mathsf{h}}\times M^{\mathrm{CME}}_{\mathsf{H}}\cap L^2_0(\Omega)$ *be the unique solution of (4.22). Then there is a* $C>0$*, such that*

$$\left\|\mathbf{u}-\mathbf{u}_{\mathsf{H},\mathsf{h}}\right\|_{1,\Omega}+\left\|p-p_{\mathsf{H}}\right\|_{0,\Omega}\leq C_{\mathrm{s}}\mathsf{H}\left\|\mathbf{f}\right\|_{0,\Omega}.$$

The constants C_{D} *and* C_{s} *depend only on* α, β^{CME}*, the resolution constant* C_K *(cf.* (4.27)*), the trace constant* C_{trace} *(cf. (4.32)), the regularity constant* C_{reg} *(cf. (2.19) and (2.24)), and the constants from Theorem 4.5, 4.7 and 4.8 and Lemma 4.11.*

Proof. Following Theorem 2.4 and the equations (2.45) and (2.50), we get in the Dirichlet case

$$\begin{aligned}&\left\|\mathbf{u}-\mathbf{u}_{\mathsf{H},\mathsf{h}}\right\|_{1,\Omega}+\left\|p-p_{\mathsf{H}}\right\|_{0,\Omega}\\&\qquad\leq C(\alpha,\beta^{\mathrm{CME}})\Bigg(\inf_{\mathbf{v}_{\mathsf{H},\mathsf{h}}\in\mathbf{X}^{\mathrm{CME_D}}_{\mathsf{H},\mathsf{h}}}\left\|\mathbf{u}-\mathbf{v}_{\mathsf{H},\mathsf{h}}\right\|_{1,\Omega}+\inf_{q_{\mathsf{H}}\in M^{\mathrm{CME}}_{\mathsf{H}}}\left\|p-q_{\mathsf{H}}\right\|_{0,\Omega}\\&\qquad\qquad+\sup_{\mathbf{0}\neq\mathbf{v}_{\mathsf{H},\mathsf{h}}\in\mathbf{X}^{\mathrm{CME_D}}_{\mathsf{H},\mathsf{h}}}\frac{\left|\int_\Gamma\left\langle\boldsymbol{\sigma}_{\boldsymbol{\nu}}(\mathbf{u},p),\mathbf{v}_{\mathsf{H},\mathsf{h}}\right\rangle\right|}{\left\|\mathbf{v}_{\mathsf{H},\mathsf{h}}\right\|_{1,\Omega}}\Bigg)\end{aligned}\tag{4.30}$$

and in the slip case

$$\begin{aligned}&\left\|\mathbf{u}-\mathbf{u}_{\mathsf{H},\mathsf{h}}\right\|_{1,\Omega}+\left\|p-p_{\mathsf{H}}\right\|_{0,\Omega}\\&\qquad\leq C(\alpha,\beta^{\mathrm{CME}})\Bigg(\inf_{\mathbf{v}_{\mathsf{H},\mathsf{h}}\in\mathbf{X}^{\mathrm{CME_s}}_{\mathsf{H},\mathsf{h}}}\left\|\mathbf{u}-\mathbf{v}_{\mathsf{H},\mathsf{h}}\right\|_{1,\Omega}+\inf_{q_{\mathsf{H}}\in M^{\mathrm{CME}}_{\mathsf{H}}}\left\|p-q_{\mathsf{H}}\right\|_{0,\Omega}\\&\qquad\qquad\sup_{\mathbf{0}\neq\mathbf{v}_{\mathsf{H},\mathsf{h}}\in\mathbf{X}^{\mathrm{CME_s}}_{\mathsf{H},\mathsf{h}}}\frac{\left|\int_\Gamma\left\langle\boldsymbol{\nu},\boldsymbol{\sigma}_{\boldsymbol{\nu}}(\mathbf{u},p)\right\rangle\left\langle\mathbf{v}_{\mathsf{H},\mathsf{h}},\boldsymbol{\nu}\right\rangle\right|}{\left\|\mathbf{v}_{\mathsf{H},\mathsf{h}}\right\|_{1,\Omega}}\Bigg).\end{aligned}\tag{4.31}$$

The infima in (4.30) and (4.31) can be estimated using Theorems 4.5, 4.7, and 4.8. The third term of the right-hand side of (4.31) can be estimated as follows

$$\begin{aligned}\left|\int_\Gamma\left\langle\boldsymbol{\nu},\boldsymbol{\sigma}_{\boldsymbol{\nu}}(\mathbf{u},p)\right\rangle\left\langle\mathbf{v}_{\mathsf{H},\mathsf{h}},\boldsymbol{\nu}\right\rangle\right|&\leq\left(\left\|\left\langle\mathrm{D}_{\boldsymbol{\nu}}\,\mathbf{u},\boldsymbol{\nu}\right\rangle\right\|^2_{0,\Gamma}+\left\|p\right\|^2_{0,\Gamma}\right)^{\frac{1}{2}}\left\|\left\langle\mathbf{v}_{\mathsf{H},\mathsf{h}},\boldsymbol{\nu}\right\rangle\right\|_{0,\Gamma}\\&\leq C\left(\left\|\mathbf{u}\right\|^2_{2,\Omega}+\left\|p\right\|^2_{1,\Omega}\right)^{\frac{1}{2}}\left\|\left\langle\mathbf{v}_{\mathsf{H},\mathsf{h}},\boldsymbol{\nu}\right\rangle\right\|_{0,\Gamma},\end{aligned}$$

where we used the trace theorem (cf. [Brenner and Scott, 1994]):

$$\left\|v\right\|_{0,\Gamma}\leq C_{\mathrm{trace}}\left\|v\right\|_{1,\Omega}\qquad\forall v\in\mathrm{H}^1(\Omega)\,.\tag{4.32}$$

The use of Lemma 4.11 and the regularity of the continuous solution $(\mathbf{u}, p)$ proves assertion (b).

By arguing in a similar fashion for the supremum in (4.30) we get

$$\begin{aligned}\left|\int_\Gamma \boldsymbol{\sigma}_{\boldsymbol{\nu}}(\mathbf{u},p)\mathbf{v}_{\mathsf{H},\mathsf{h}}\right| &\leq \left(\|\mathrm{D}_{\boldsymbol{\nu}}\,\mathbf{u}\|_{0,\Gamma}^2 + \|p\|_{0,\Gamma}^2\right)^{\frac{1}{2}} \|\mathbf{v}_{\mathsf{H},\mathsf{h}}\|_{0,\Gamma} \\ &\leq C\left(\|\mathbf{u}\|_{2,\Omega}^2 + \|p\|_{1,\Omega}^2\right)^{\frac{1}{2}} \|\mathbf{v}_{\mathsf{H},\mathsf{h}}\|_{0,\Gamma}\end{aligned}$$

and the proof of (a) is finished by using Lemma 4.11. ∎

5

Numerical Experiments

In this chapter, we will report on the results of some numerical tests. Composite finite elements have been investigated computationally in detail in [Rech, 2006] for the Poisson and the Lamé equation with Dirichlet boundary condition. The element there is comparable to the velocity part of the composite mini element without the bubbles. In [Rech, 2006], overlapping two scale grids were used successfully. Since we could preserve the theoretical results for the Stokes equation we expect a comparable numerical behavior also for the composite mini element. In this thesis we want to concentrate on experiments using resolving boundary concentrated grids as in Figure 3.2.

5.1 Model Problems

We consider the following class of model domains that consist of perturbations of the unit square in $\mathbb{R}^2$:

$$\Omega_{a,b} := \{\mathbf{x} = (x_1, x_2)^T \in \mathbb{R}^2 \mid 0 < x_1 < 1,\ -a\sin(b\pi x_1) < x_2 < 1\}, \quad a \in [0, \tfrac{1}{10}],\ b \in \mathbb{N}_0.$$

We emphasize that the composite mini element method does not require periodicity of the boundary but the choice of Ω allows us to handle the complexity of the domain by two parameters: the amplitude a and the double frequency b. The three choices of interest are depicted in Figure 5.1.

We use the following outer force density

$$\mathbf{f} : \mathbb{R}^2 \to \mathbb{R}^2, \quad \mathbf{x} = (x_1, x_2)^T \mapsto \begin{pmatrix} \cos(\pi x_2)\sin(2\pi x_1) \\ (\frac{3}{2} - \frac{3}{2}x_2)^5 \sin(2\pi x_1)\cos(2\pi x_2) \end{pmatrix} \tag{5.1}$$

as right-hand side. As you can see in Figure 5.2 the force is larger in the lower part of the domain, close to the perturbed boundary. We define a class of model problems for the Dirichlet boundary conditions $\mathcal{M}^{\mathrm{D}}(a, b, \mathbf{f})$ depending on the two domain parameters and the right-hand side $\mathbf{f} \in \mathbf{L}^2(\Omega_{a,b})$ by *seeking pairs* $(\mathbf{u}, p) \in \mathbf{H}^1_{\mathrm{D}}(\Omega_{a,b}) \times L^2_0(\Omega_{a,b})$ *such that*

$$\begin{aligned} \mathfrak{a}(\mathbf{u}, \mathbf{v}) + \mathfrak{b}(\mathbf{v}, p) &= \langle \mathbf{f}, \mathbf{v} \rangle_{0,\Omega_{a,b}} \quad && \forall \mathbf{v} \in \mathbf{H}^1_{\mathrm{D}}(\Omega_{a,b}), \\ \mathfrak{b}(\mathbf{u}, q) &= 0 && \forall q \in \mathrm{L}^2_0(\Omega_{a,b}), \end{aligned} \tag{5.2}$$

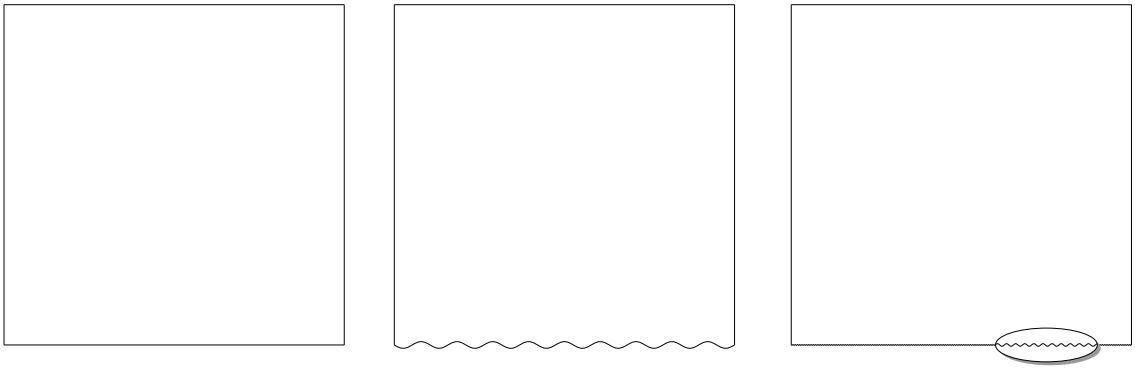

(a) $a = 0$ (unit square). (b) $a = \frac{1}{100}, b = 19$. (c) $a = \frac{1}{1000}, b = 199$.

Figure 5.1: The model domain $\Omega_{a,b}$ from (5.1) for different values of a and b.

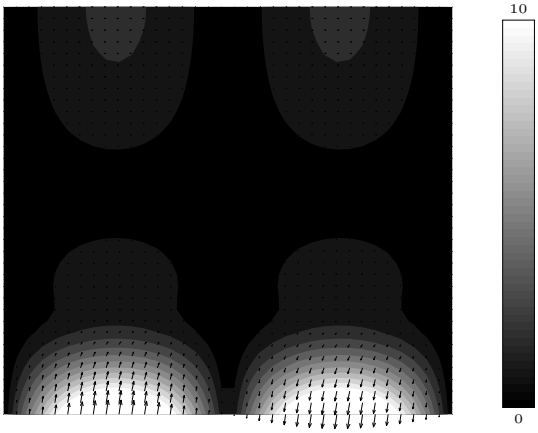

Figure 5.2: Contour plot of the absolute outer force density $\mathbf{f}$ from (5.1). The arrow show the force direction.

In the model problems for slip boundary conditions impose the slip condition only on the oscillating part of the boundary

$$\Gamma^{\mathrm{s}}_{a,b} := \{\mathbf{x} = (x_1, x_2)^T \in \mathbb{R}^2 \mid 0 < x_1 < 1,\ x_2 = -a\sin(b\pi x_1)\}$$

and the Dirichlet condition on the rest $\partial\Omega_{a,b} \setminus \Gamma^{\mathrm{s}}_{a,b}$ including the corners. The appropriate solution space is then

$$\mathbf{H}^1_{\mathrm{s}}(\Omega_{a,b}) := \left\{\mathbf{u} \in \mathbf{H}^1(\Omega) :\ \langle \mathbf{u}, \boldsymbol{\nu}\rangle|_{\Gamma^{\mathrm{s}}_{a,b}} = 0,\ \mathbf{u}|_{\Gamma\setminus\Gamma^{\mathrm{s}}_{a,b}} = 0 \quad \text{in the sense of traces}\right\}.$$

and the class of slip models $\mathcal{M}^{\mathrm{s}}(a, b, \mathbf{f})$ is given by *finding pairs* $(\mathbf{u}, p) \in \mathbf{H}^1_{\mathrm{s}}(\Omega_{a,b}) \times L^2_0(\Omega)$ *such that*

$$\begin{aligned} \mathfrak{a}(\mathbf{u}, \mathbf{v}) + \mathfrak{b}(\mathbf{v}, p) &= \langle \mathbf{f}, \mathbf{v}\rangle_{0,\Omega_{a,b}} \quad && \forall \mathbf{v} \in \mathbf{H}^1_{\mathrm{s}}(\Omega_{a,b}), \\ \mathfrak{b}(\mathbf{u}, q) &= 0 && \forall q \in \mathrm{L}^2_0(\Omega_{a,b}). \end{aligned} \tag{5.3}$$

Due to the complexity of the geometry, analytic solutions are not known. We compute approximations on very fine grids, which we use as references to evaluate the different methods. The

velocity fields of the solutions according to the domains from Figure 5.1 are depicted in Figure 5.3. While differences for Dirichlet boundary are barely observable, the behavior depends critically on the boundary perturbation in the case of the slip condition. For the pressures (see Figure 5.4) the behavior is critical in both cases. The more oscillations the boundary has, the more the pressure has. We emphasize that these oscillations are not a numerical effect. The indentions can be regarded as obstacles. They are attacked by the flow directly on one side while on the other side a flow shadow is observable. This phenomenon leads to the steep pressure gradients.

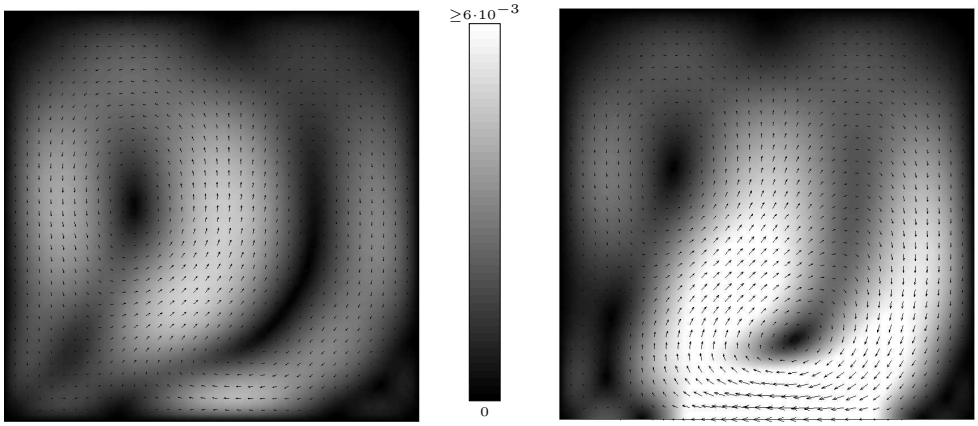

(a) $\mathcal{M}^{\mathrm{D}}(0, 0, \mathbf{f})$. (b) $\mathcal{M}^{\mathrm{s}}(0, 0, \mathbf{f})$.

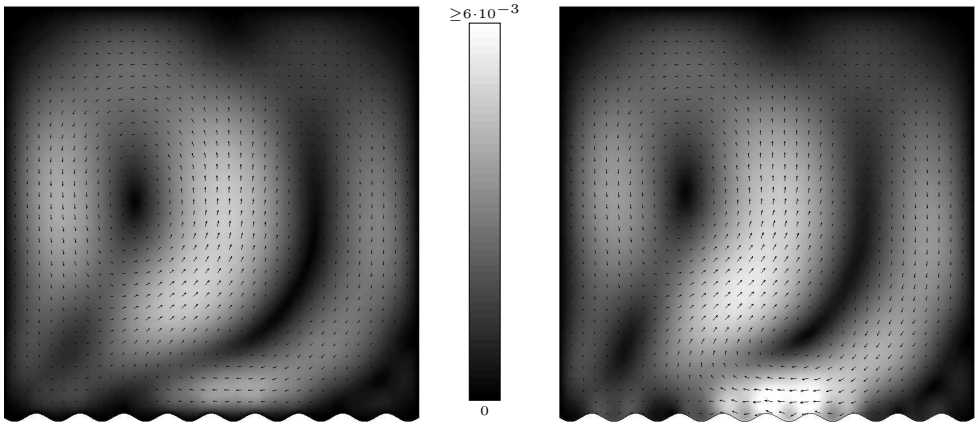

(c) $\mathcal{M}^{\mathrm{D}}(0.1, 19, \mathbf{f})$. (d) $\mathcal{M}^{\mathrm{s}}(0.1, 19, \mathbf{f})$.

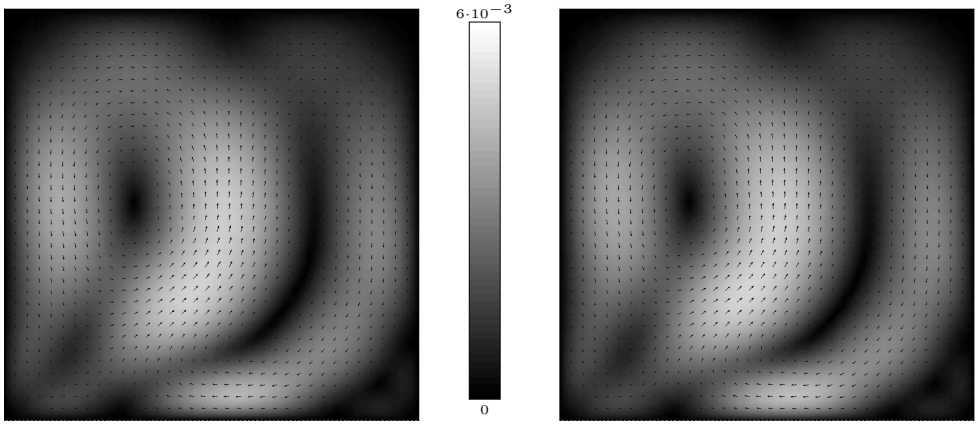

(e) $\mathcal{M}^{\mathrm{D}}(0.001, 199, \mathbf{f})$. (f) $\mathcal{M}^{\mathrm{s}}(0.001, 199, \mathbf{f})$.

Figure 5.3: Solutions to the model problems: The velocity field with direction (arrows) and absolute values (gray intensity).

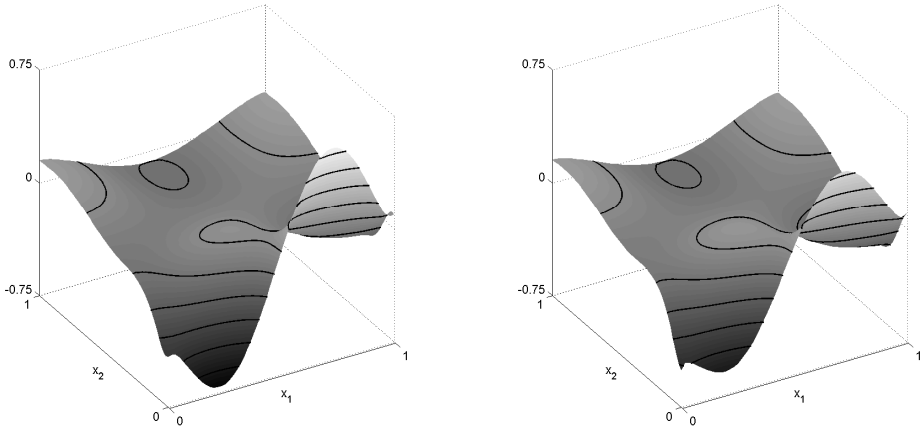

(a) $\mathcal{M}^{\mathrm{D}}(0, 0, \mathbf{f})$.

(b) $\mathcal{M}^{\mathrm{s}}(0, 0, \mathbf{f})$.

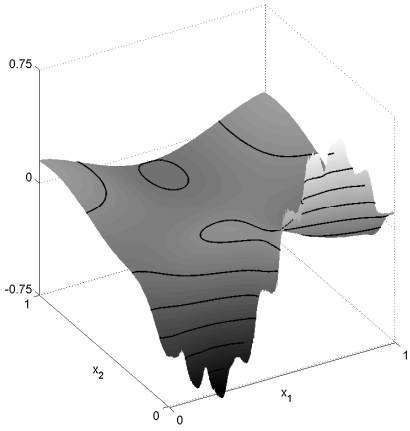

(c) $\mathcal{M}^{\mathrm{D}}(0.1, 19, \mathbf{f})$.

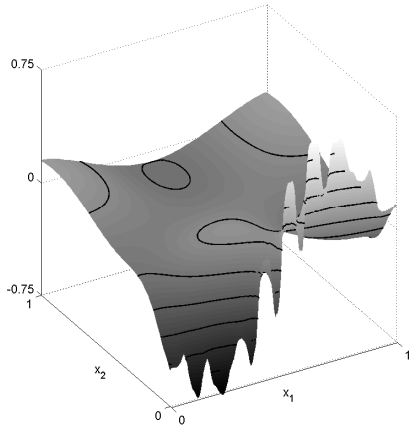

(d) $\mathcal{M}^{\mathrm{s}}(0.1, 19, \mathbf{f})$.

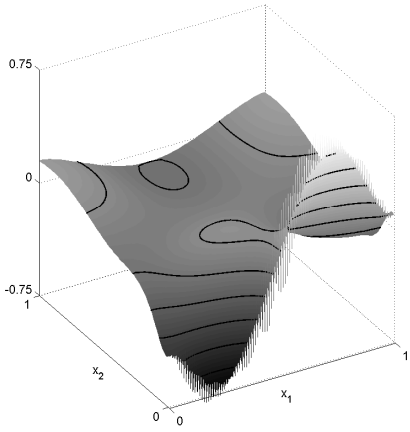

(e) $\mathcal{M}^{\mathrm{D}}(0.001, 199, \mathbf{f})$.

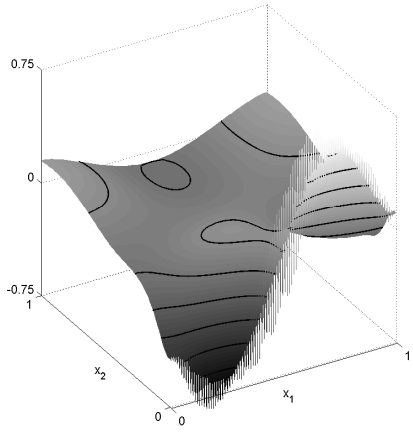

(f) $\mathcal{M}^{\mathrm{s}}(0.001, 199, \mathbf{f})$.

Figure 5.4: Solutions to the model problems: The pressure with contour lines.

5.2 Parameter Tests

In our method there is a certain freedom in choosing the inner grid with the degrees of freedom. If a boundary concentrated grid as in Figure 5.5a is given, the question arises which nodes need to be or should be marked as degrees of freedom. The minimal choice, arising from the assumptions of Chapter 3 and the convergence analysis, is depicted in 5.5a. In this case, the distance between the slave triangles and the extrapolation simplexes is bounded by the coarse grid parameter H, which would produce a factor $2^3 \approx (1 + C_{\mathrm{dist}} + C_{\mathrm{size}})^3$ in the estimate of lemma 4.1. This term also enters the a priori error estimates. A thinner boundary zone might reduce the approximation error. In Figures 5.5b to 5.5d, the inner zone is enlarged layer by layer (we will refer to the number of layers, which are incorporated in the inner zone by l). On the other hand, this increases the computational effort. We compute the corresponding composite mini element approximations. In Figure 5.6a the errors are plotted. For values $l \geq 2$, improvements are hardly observable. But anyway, the error range (all errors lie in the interval $[0.006, 0.022]$) is so small that the choices of $l = 0$ and $l = 1$ are possible as well, especially in view of the increasing system dimension (see Figure 5.6b), which varies between 1000 and 25000. This fact supports the choice of a small l. A good balance is given by $l = 2$ and from now on, we fix $l = 2$ in our composite mini element approximations.

In a second test we investigate the stability of the approximation with respect to the quotient H/h. In the convergence analysis of [Rech, 2006] a factor $\log(\frac{\mathsf{H}}{\mathsf{h}})$ appeared in the error estimates. Since the choice of h is restricted by the boundary resolution condition, this would also restrict the choice of H. Our analysis shows that this factor is of artificial nature. There is no restriction on the ratio of the large scale and the small one. We have performed a numerical experiment for verifying this stability condition. We take the model problem $\mathcal{M}^{\mathrm{D}}(0.01, 19, \mathbf{f})$ and a coarse grid ($\mathsf{H} = 0.1$) and refine it locally near the boundary until $\mathsf{h} = 10^{-4}$ holds which corresponds to the ratio $\frac{\mathsf{H}}{\mathsf{h}} = 1000$. We computed composite mini element approximations with constant inner grid ($l = 0$). The results in Figure 5.7 show that the errors stay constant for increasing ratio. This supports the independence of the approximation error from the ratio $\frac{\mathsf{H}}{\mathsf{h}}$.

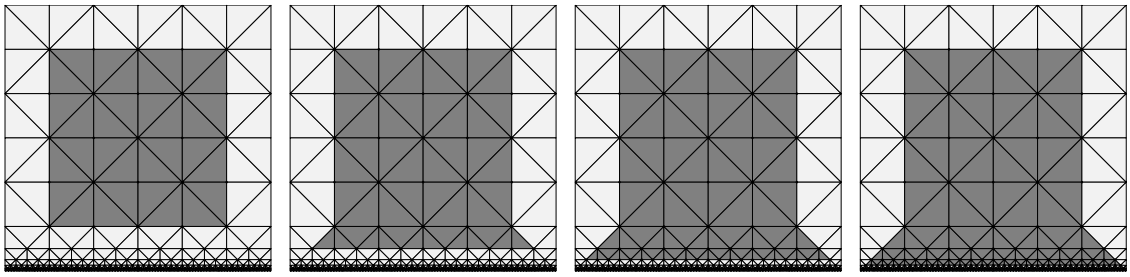

(a) $\mathcal{M}^{\mathrm{D}}(0,0,\mathbf{f})$. (b) $\mathcal{M}^{\mathrm{D}}(0,0,\mathbf{f})$. (c) $\mathcal{M}^{\mathrm{D}}(0,0,\mathbf{f})$. (d) $\mathcal{M}^{\mathrm{D}}(0,0,\mathbf{f})$.

Figure 5.5: Different choices of the inner triangulation with the degrees of freedom in a boundary resolving grid of the model domain $\Omega_{0.001,199}$. The procedure could be continued up to the 8th refinement level which corresponds to the full grid.

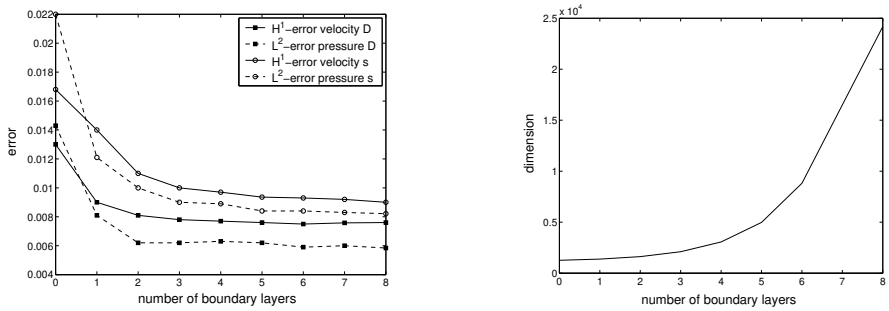

(a) Errors for models $\mathcal{M}^{\mathrm{D}}(0.001,199,\mathbf{f})$ and $\mathcal{M}^{\mathrm{s}}(0.001,199,\mathbf{f})$.

(b) Resulting system dimension.

Figure 5.6: Error and computational effort of the CME approximations with respect to the grids of Figure 5.5. l denotes the number of boundary layers which are included in the inner grid, $l=0$ corresponds to Figure 5.5a, $l=1$ to 5.5b, etc. For $l=8$ the inner grid equals the full one, so that this can be viewed as the mini element approximation.

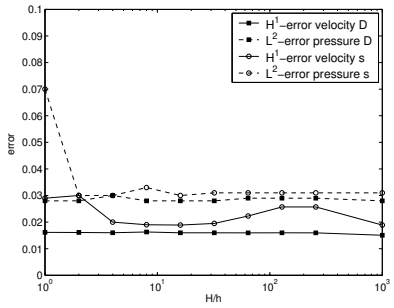

Figure 5.7: Dependence of the CME approximation error on the ratio $\frac{\mathsf{H}}{\mathsf{h}}$. Model problem $\mathcal{M}^{\mathrm{s}}(0.1,19,\mathbf{f})$, $\mathsf{H}=0.1$. The error decrease in the preasymptotic range is due to the fact that the domain boundary is not sufficiently resolved until a certain refinement level.

5.3 Convergence

After these tests for fixing the control parameters in the algorithm, we now investigate the convergence behavior of our method, especially in comparison to classical mini element methods. We use the Dirichlet model $\mathcal{M}^{\mathrm{D}}(0.001, 199, \mathbf{f})$ and the slip model $\mathcal{M}^{\mathrm{s}}(0.001, 199, \mathbf{f})$ according to the domain in Figure 5.1c.

We use two scale grids as depicted in Figure 5.5 for both, classical mini element (FEM) and composite mini element (CME) approximations. We choose the constant boundary grid size $\mathsf{h} = 2^{-10}$ and vary only the coarse grid parameter $\frac{1}{2} \geq \mathsf{H} \geq \mathsf{h}$. Additionally we compute mini element approximations on almost uniform triangulations as in Figure 1.2 (left side) which have a comparable computational effort as the composite mini element method but cannot resolve all the boundary details on coarse levels. This is equivalent to replacing the domain with the oscillating boundary by a simplified domain and then applying the standard mini element. We refer to this approach by FEM0. In the fourth method (FEM1) we use (almost) the same number of nodes as in FEM0 but a boundary concentrated node distribution to improve the boundary resolution. All approaches are summarized in Table 5.1. All grids satisfy the shape regularity condition (3.2) with a regularity constant $\rho > \frac{1}{2}$.

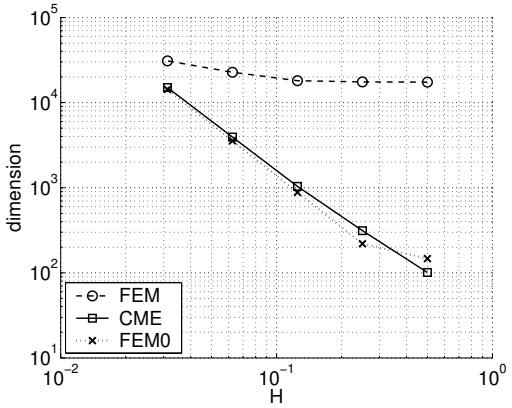

Figure 5.8: Dimension of the linear systems according to the different methods and their dependence on H.

Methods	H	h	Grids
FEM (Mini element)	2^{-1} $\mathbf{2^{-2}}$ 2^{-3} 2^{-4} 2^{-5}	2^{-10} $\mathbf{2^{-10}}$ 2^{-10} 2^{-10} 2^{-10}	$\rightarrow$ 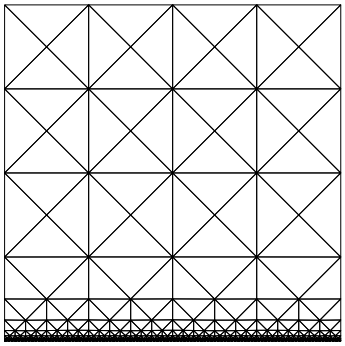
CME	2^{-1} $\mathbf{2^{-2}}$ 2^{-3} 2^{-4} 2^{-5}	2^{-10} $\mathbf{2^{-10}}$ 2^{-10} 2^{-10} 2^{-10}	$\rightarrow$ 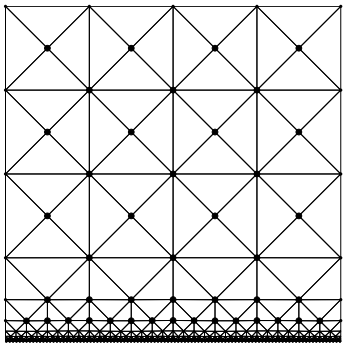
FEM0 (Mini element)	2^{-1} $\mathbf{2^{-2}}$ 2^{-3} 2^{-4} 2^{-5}	2^{-1} $\mathbf{2^{-2}}$ 2^{-3} 2^{-4} 2^{-5}	$\rightarrow$ 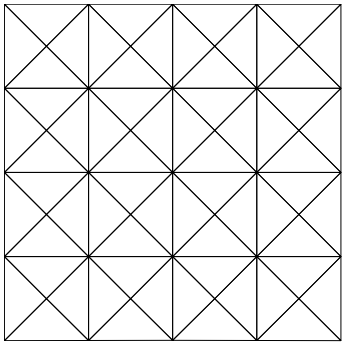
FEM1 (Mini element)	2^{-2} $\mathbf{2^{-2}}$ 2^{-3} 2^{-3} 2^{-4}	2^{-4} $\mathbf{2^{-5}}$ 2^{-6} 2^{-7} 2^{-10}	$\rightarrow$ 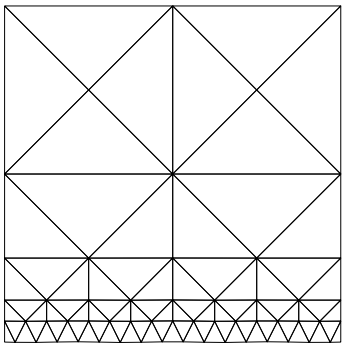

Table 5.1: The different approaches for the solution of the model problems $\mathcal{M}^{\mathrm{D}}(0.001, 199, \mathbf{f})$ and $\mathcal{M}^{\mathrm{s}}(0.001, 199, \mathbf{f})$.

5.3.1 The Dirichlet Model Problem

The results of our computations are visualized in Figure 5.9, where the dependence of the velocity and pressure errors on the mesh width and the system dimension are depicted. Since the maximal mesh width H decreases very slowly for FEM1 in comparison to the other methods, it makes no sense to visualize the H- dependence in the error of this approach. In the case of FEM, the dimension stays almost constant as H decreases (see Figure 5.8). Thus we only compare three methods at one time, either the three with equal maximal meshwidth (FEM, FEM0, CME) or the three with similar computational effort (FEM0, CME, FEM1) .

We make the following observations:

1. FEM and CME converge at the predicted optimal (linear) rate (cf. Figures 5.9a-d). The compressed method CME is only slightly worse than the full version FEM (cf. Figures 5.9a-b). Especially away from the rough boundary, differences cannot be recognized (cf. Figures 5.9c-d).

2. FEM0 produces comparable results as FEM and CME (cf. Figures 5.9a-d) although the boundary is not resolved by the underlying grids. In view of the resolution condition (2.47) this is not surprising. The amplitude of the perturbation is too small compared to the mesh width H to effect the approximations at least on the calculated coarse levels. That means the boundary resolution of FEM and CME is too fine compared to what is needed for the accuracy of the discretization in this situation. However, this does not increase the system dimension for CME. In the case of complicated inhomogeneous Dirichlet data, such a fine resolution might become necessary.

3. FEM1 is not competitive (cf. Figures 5.9e-h). Its errors are significantly larger than the errors arising from the other methods. This is not surprising because the theory predicts errors of order H which is larger in FEM1 than in the other approaches.

4. Due to to quasi uniform inner grids, the convergence of CME is also linear in the reciprocal of the system dimension which underpins the efficiency of our “fuzzy” treatment of the boundary conditions via CME.

5. If we neglect the effort for the generation of the system matrix, than CME is the most efficient method. Though FEM produces the best results it does not justify the much greater storage and computational effort (see Figure 5.8). Among the less costly methods, the composite mini element has the slightly smaller errors and particularly the higher degree of flexibility.

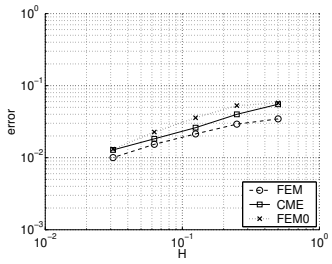

(a) $\mathbf{H}^1$-error of the velocity on Ω as a function of H.

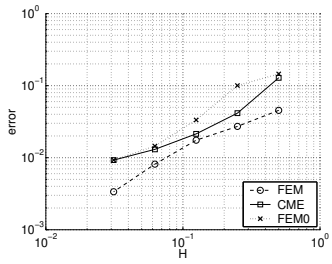

(b) L^2-error of the pressure on Ω as a function of H.

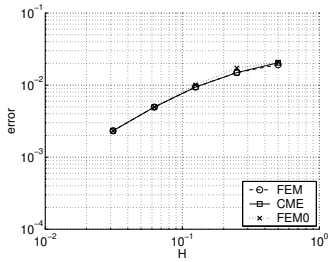

(c) $\mathbf{H}^1$-error of the velocity on $(0,1)\times(0.1,1)$ as a function of H.

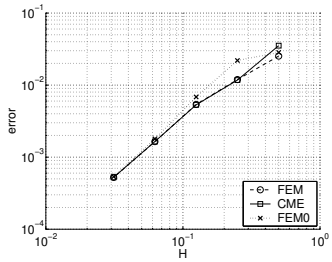

(d) L^2-error of the pressure on $(0,1)\times(0.1,1)$ as a function of H.

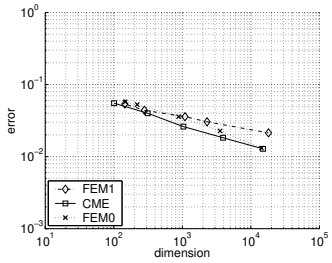

(e) $\mathbf{H}^1$-error of the velocity on Ω.

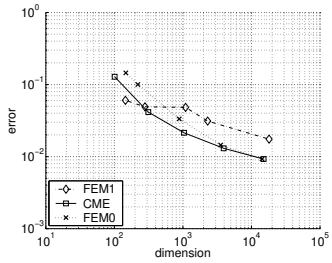

(f) L^2-error of the pressure on Ω.

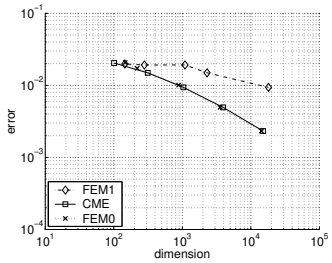

(g) $\mathbf{H}^1$-error of the velocity on $(0,1)\times(0.1,1)$.

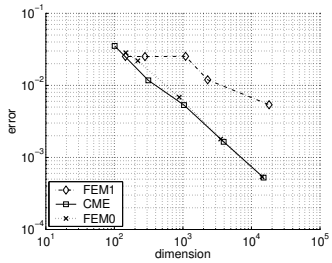

(h) L^2-error of the pressure on $(0,1)\times(0.1,1)$.

Figure 5.9: Convergence of the methods applied to the Dirichlet model $\mathcal{M}^{\mathrm{D}}(0.001, 199, \mathbf{f})$. The errors of velocity (left) and pressure (right) are plotted versus the maximal mesh width H (top) and the system dimension (bottom). In each case the errors are give with respect to the whole domain Ω and its subset $(0,1)\times(0.1,1)$.

5.3.2 The Slip Model Problem

The results of the slip model computations are depicted in Figure 5.10. We use the same presentation as in the previous section.

1. FEM and CME converge at the predicted optimal (linear) rate (cf. Figures 5.10a-d). The gap in between is slightly larger then for the Dirichlet model. This is based on the missing knowledge of the behavior of the tangential component of the solution velocity. The error of CME could be reduced by putting more degrees of freedom in the boundary zone. Note, that the error of the CME is larger than for the FEM in a near boundary zone. Away from the boundary the errors are almost equal, i.e. pollution effects can not be observed for this test case (cf. Figures 5.10c-d).

2. FEM0 is not competitive (cf. Figures 5.10a-d), since the resolution condition (2.51) is not satisfied for the values of H under consideration. The resolution of the other three methods cannot be weakened without increasing the errors.

3. Though FEM1 resolves the domain, it is not competitive away from the boundary (cf. Figures 5.10e-h).

4. As in the case of Dirichlet boundary, CME converges linearly in the reciprocal system dimension, so it combines the efficiency of a uniform approach with the requirements of boundary resolution.

5. CME is the most efficient method in this test case. Though FEM produces slightly smaller errors than CME, the resulting system dimension is up to 100 times bigger than for CME on the coarsest level (see Figure 5.8). In contrast to CME the other less costly methods FEM0 and FEM1 produce unsatisfying approximations.

To emphasize the results, we also visualize the velocity approximations of the methods FEM0, FEM1, and CME (cf. Figure 5.11) on different refinement levels. It is distinguishable where the flaccidities of the almost uniform approach FEM0 and the boundary concentrated version FEM1 are: FEM0 fails close to the boundary, while FEM1 cannot capture the behavior inside the domain. CME is able to calibrate the boundary adaption and a good approximation quality overall.

For the pressure, plotted in Figure 5.12, the behavior is similar. Since the pressure approximation is realized on a coarse grid, which is similar to the uniform grid of FEM0, the oscillating behavior of the solution cannot be captured by CME. However, as mentioned before, pollution effects cannot be observed.

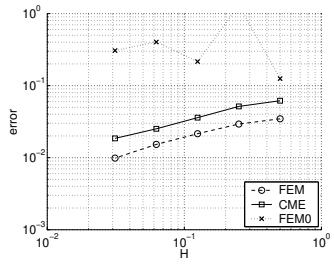

(a) $\mathbf{H}^1$-error of the velocity on Ω as a function of H.

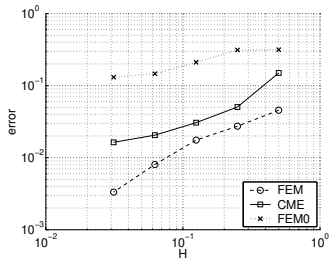

(b) L^2-error of the pressure on Ω as a function of H.

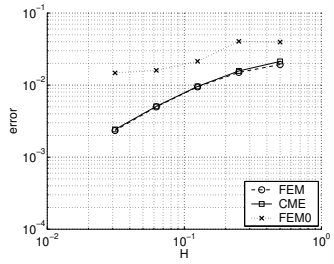

(c) $\mathbf{H}^1$-error of the velocity on $(0,1)\times(0.1,1)$ as a function of H.

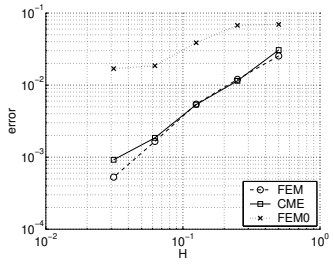

(d) L^2-error of the pressure on $(0,1)\times(0.1,1)$ as a function of H.

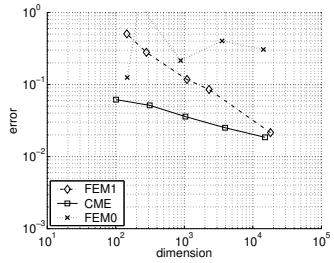

(e) $\mathbf{H}^1$-error of the velocity on Ω.

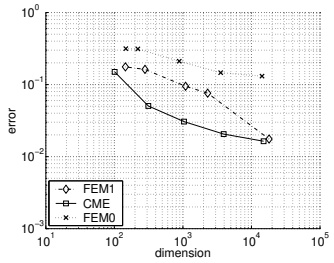

(f) L^2-error of the pressure on Ω.

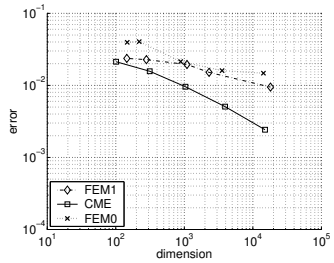

(g) $\mathbf{H}^1$-error of the velocity on $(0,1)\times(0.1,1)$.

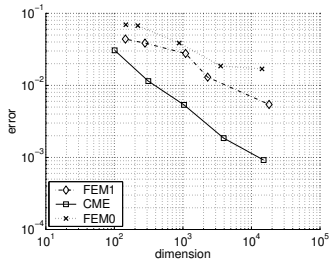

(h) L^2-error of the pressure on $(0,1)\times(0.1,1)$.

Figure 5.10: Convergence of the methods applied to the slip model $\mathcal{M}^{\mathrm{s}}(0.001, 199, \mathbf{f})$. The errors of velocity (left) and pressure (right) are plotted versus the maximal mesh width H (top) and the system dimension (bottom). In each case the errors are give with respect to the whole domain Ω and its subset $(0,1)\times(0.1,1)$.

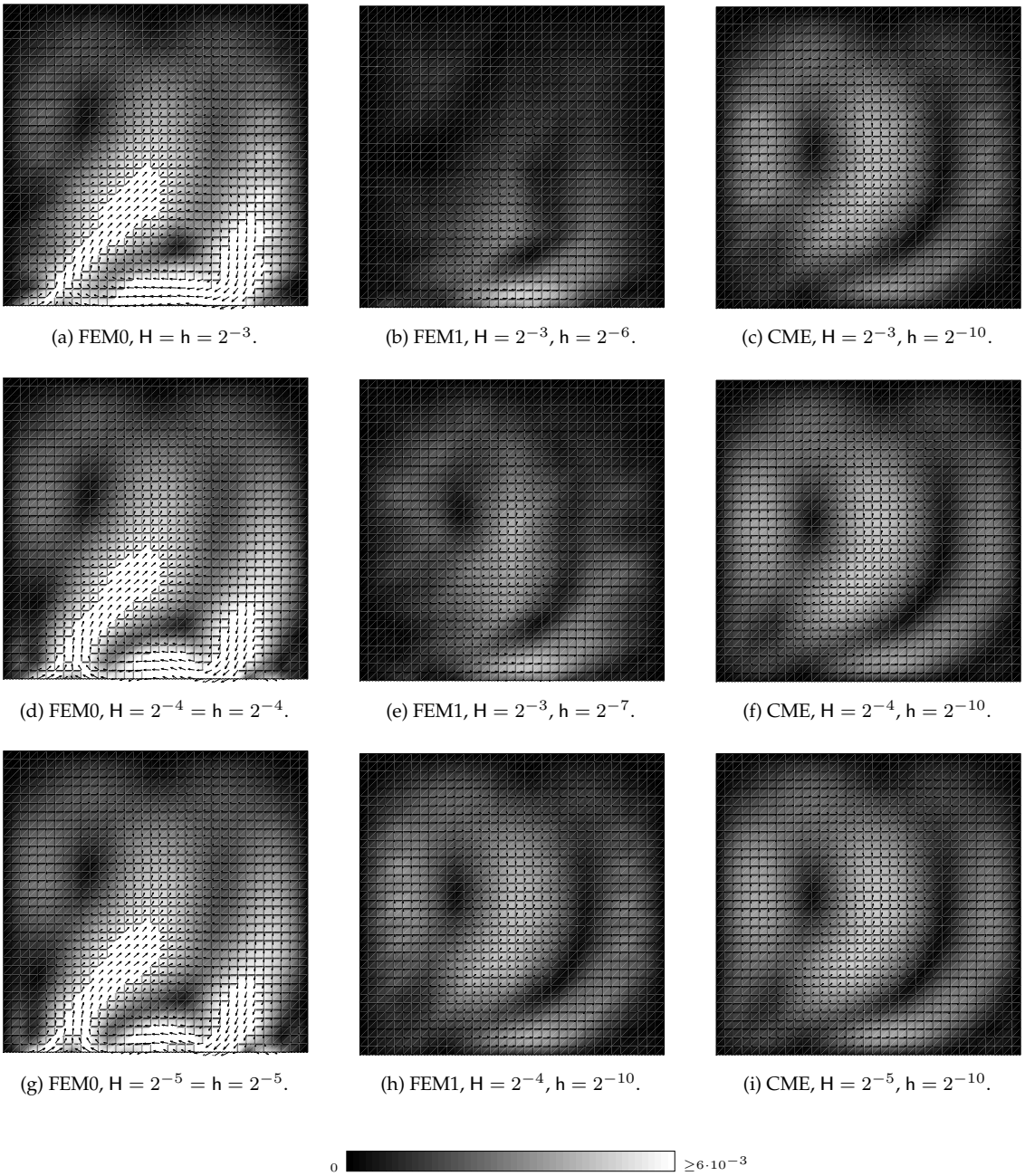

(a) FEM0, $\mathsf{H} = \mathsf{h} = 2^{-3}$. (b) FEM1, $\mathsf{H} = 2^{-3}$, $\mathsf{h} = 2^{-6}$. (c) CME, $\mathsf{H} = 2^{-3}$, $\mathsf{h} = 2^{-10}$.

(d) FEM0, $\mathsf{H} = 2^{-4} = \mathsf{h} = 2^{-4}$. (e) FEM1, $\mathsf{H} = 2^{-3}$, $\mathsf{h} = 2^{-7}$. (f) CME, $\mathsf{H} = 2^{-4}$, $\mathsf{h} = 2^{-10}$.

(g) FEM0, $\mathsf{H} = 2^{-5} = \mathsf{h} = 2^{-5}$. (h) FEM1, $\mathsf{H} = 2^{-4}$, $\mathsf{h} = 2^{-10}$. (i) CME, $\mathsf{H} = 2^{-5}$, $\mathsf{h} = 2^{-10}$.

Figure 5.11: Approximations to the model problem $\mathcal{M}^{\mathrm{s}}(0.001, 199, \mathbf{f})$: The velocity field computed by FEM0 (left), FEM1 (middle) and CME (right) on different levels of dimension 1000 (top row), 4000 (second row), and 10000 (bottom row).

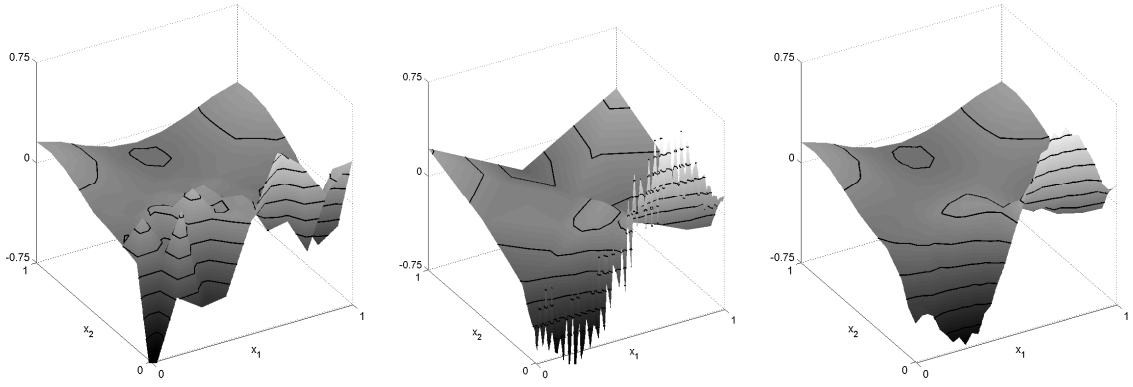

(a) FEM0, $\mathsf{H} = \mathsf{h} = 2^{-3}$. (b) FEM1, $\mathsf{H} = 2^{-3}$, $\mathsf{h} = 2^{-6}$. (c) CME, $\mathsf{H} = 2^{-32}$, $\mathsf{h} = 2^{-10}$.

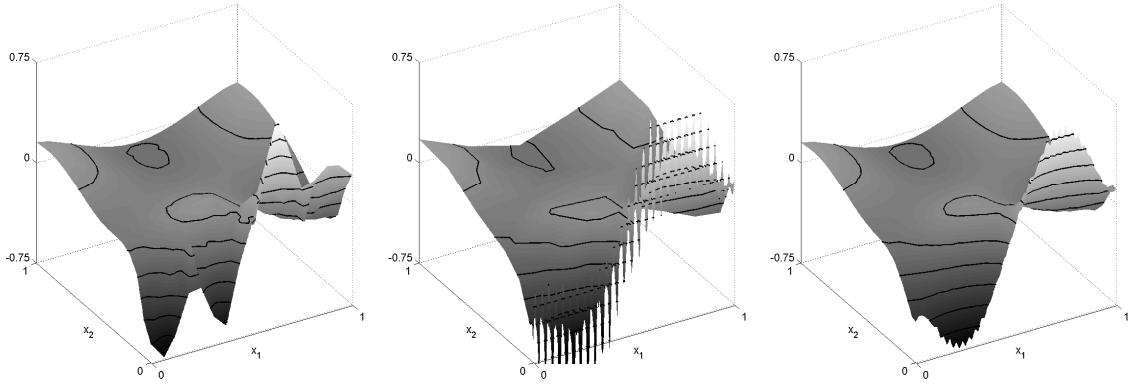

(d) FEM0, $\mathsf{H} = 2^{-4} = \mathsf{h} = 2^{-4}$. (e) FEM1, $\mathsf{H} = 2^{-3}$, $\mathsf{h} = 2^{-7}$. (f) CME, $\mathsf{H} = 2^{-4}$, $\mathsf{h} = 2^{-10}$.

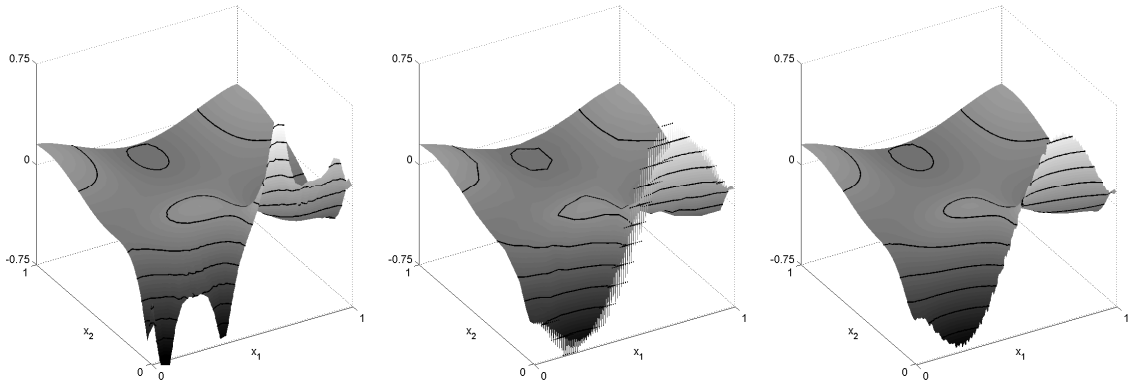

(g) FEM0, $\mathsf{H} = 2^{-5} = \mathsf{h} = 2^{-5}$. (h) FEM1, $\mathsf{H} = 2^{-4}$, $\mathsf{h} = 2^{-10}$. (i) CME, $\mathsf{H} = 2^{-5}$, $\mathsf{h} = 2^{-10}$.

Figure 5.12: Approximations to the model problem $\mathcal{M}^{\mathrm{s}}(0.001, 199, \mathbf{f})$: The pressure computed by FEM0 (left), FEM1 (middle) and CME (right) on different levels of dimension 1000 (top row), 4000 (second row), and 10000 (bottom row).

6

Conclusions

The presented new finite element method for the Stokes equations, the composite mini element, turns out to be a very efficient alternative to the use of finite elements on boundary concentrated grids that become necessary if the underlying domain contains a huge number of geometrical details. Especially, in the case of slipping flows, that are critically influenced by the shape of the domain boundary, the method produces significantly better results than standard approaches with comparable computational effort. The concept of employing slave nodes is sufficient to control errors due to unzureichend boundary resolution, enlarging the finite element space is not necessary.

We have tested the method for two dimensional problems, but in view of the full three dimensional analysis we expect the advantages to be even more significant in three dimensions because boundary resolution becomes much more expensive there.

Though we did not work this out in detail, the method can not only handle complicated boundaries but also complicated boundary data in an efficient way. We expect that the techniques of this thesis can also be applied to more general types of boundary conditions, especially to conditions including friction.

Future research will be focused on the generalization of the method for the solution of the non-stationary Stokes equations and the Navier-Stokes equations. In practical applications it is indispensable not only to approximate solutions but also to know about its errors. Suitable a posteriori error estimators will be developed which also takes into account the non-conformity in the boundary condition, i.e. which allows to decide whether more degrees of freedom are needed or introducing slave nodes is sufficient to fulfill a certain error bound. Error majorants with these properties have been developed in [Rech, 2006] for the Poisson problem and will be generalized to the case of the Stokes equations. We emphasize that the composite mini element method is a very good basis for an adaptive method, since it is able to produce expedient results at low costs.

Bibliography

Babuška, I. (1963). *The theory of small changes in the domain of existence in the theory of partial differential equations and its applications*. Academic Press, New York, New York.

Bänsch, E. and Deckelnick, K. (1999). Optimal error estimates for the stokes and Navier-Stokes equations with slip- boundary condition. *M2AN*, 33(5):923–938.

Brenner, S. and Scott, L. (1994). *The Mathematical Theory of Finite Element Methods*. SpringerVerlag.

Brezzi, F. and Fortin, M. (1991). *Mixed and Hybrid Finite Element Methods*. Springer-Verlag, New York.

Ciarlet, P. (1978). *The Finite Element Method for Elliptic Problems*. North Holland, Amsterdam.

Clément, P. (1975). Approximation by finite element functions using local regularization. *RAIRO Anal. Numer.*, R-2:77–84.

Duvaut, G. and Lions, J. L. (1976). *Inequalities in mechanics and physics*. Springer-Verlag, Berlin Heidelberg New York.

Girault, V. and Raviart, P.-A. (1979). *Finite Element Approximation of the Navier-Stokes Equations*. Springer-Verlag, Berlin Heidelberg New York.

Girault, V. and Raviart, P.-A. (1986). *Finite Element Methods for Navier-Stokes Equations*. Springer-Verlag, New York.

Hackbusch, W. and Sauter, S. A. (1997). Composite finite elements for the approximation of pdes on domains with complicated micro-structures. *Numer. Math.*, 75(4):447–472.

Knobloch, P. (2000). A finite element convergence analysis for 3d stokes equations in case of variational crimes. *Appl. Math.*, 45(2):99–129.

Navier, C. L. M. H. (1827). Sur les lois du mouvement des fluides. *Mem. Acad. R. Sci. Inst. Fr.*, 6:389–440.

Nitsche, J. A. (1981). On Korn's second inequality. *RAIRO Anal. Numér.*, 15:237–248.

Rech, M. (2006). *Composite finite elements: An adaptive two-scale approach to the non-conforming approximation of Dirichlet problems on complicated domains*. PhD thesis, Universität Zürich.

Rech, M., Sauter, S., and Smolianski, A. (2006). Two-scale composite finite element method for Dirichlet problems on complicated domains. *NUM-MATH*, 102(4):681–708.

Sauter, S. A. and Warnke, R. (1999). Extension operators and approximation on domains containing small geometric details. *East-West J. Numer. Math.*, 7(1):61–77.

Scott, L. R. and Zhang, S. (1990). Finite element interpolation of nonsmooth functions satisfying boundary conditions. *MATH-COMP*, 54(190):483–493.

Solonnikov, V. and Ščadilov, V. (1973). On a boundary value problem for a stationary system of the Navier-Stokes equations. *Proc. Steklov Inst. Math.*, 125:186–199.

Stein, E. M. (1970). *Singular Integrals and Differentiablity Properties of Function*. New York, Priceton Univ. Press.

Strang, G. and Fix, G. J. (1973). *An Analysis of the Finite Element Method*. Prentice–Hall, New York.

Temam, R. (1984). *Navier-Stokes Equations, Theory and Numerical Analysis*. North-Holland, Amsterdam.

Ullmann, P. (2006). Stokes-gleichungen auf komplizierten gebieten. Master's thesis, Universität Zürich.

Verfürth, R. (1985). Finite element approximation of steady Navier-Stokes equations with mixed boundary conditions. *M2AN*, 19(3):461–475.

Verfürth, R. (1987). Finite element approximation of incompressible Navier-Stokes equations with slip boundary condition. *Numer. Math.*, 50(6):697–721.

Verfürth, R. (1991). Finite element approximation of incompressible Navier-Stokes equations with slip boundary condition II. *Numer. Math.*, 59:615–636.

Verfürth, R. (1996). *A Review of a posteriori Error Estimation and adaptive Mesh-Refinement Techniques*. Teubner-Wiley, Stuttgart.

Verfürth, R. (1999). Interpolation error error estimates for some quasi-interpolation operators. *M2AN*, 33(4):695–713.

Curriculum vitae

Daniel Peterseim

Date of birth: May 22th, 1980, Germany
Nationality: German

August 1991 - June 1998 Comprehensive Secondary School: Staatliches Gymnasium Oberdorla (Germany), Abitur

October 1999 - May 2004 Graduation as Diplom-Mathematiker at the Technical University of Ilmenau, Germany

Mathematical focus: Numerical Mathematics and Computation, Functional Analysis

Minor subject: Informatics

October 2001: Intermediate Diploma

Diploma Thesis: *Numerische Analyse parameterabhängiger periodischer Orbits nichtlinearer dynamischer Systeme mittels Mehrzielmethode und effizienter Fortsetzungstechniken*

Since October 2004 Research Associate of the Department of Mathematics in the Working Group Computational Mathematics of Prof. Dr. Stefan A. Sauter at the University of Zurich
(partially financed by Swiss National Science Foundation, Grant 200020-113457/1)

Preparation of the present thesis

Supervision of master thesis: P. Ullmann *Stokes-Gleichungen auf komplizierten Gebieten*,
V. Künzle *The Composite Mini Element - A Computational Investigation* (under construction)